

FILTER MEDIA MODIFICATION IN RAPID SAND FILTRATION

A Dissertation

Presented to the Faculty of the Graduate School

of Cornell University

In Partial Fulfillment of the Requirements for the Degree of

Doctor of Philosophy

by

Po-Hsun Lin

May 2010

© 2010 Po-Hsun Lin

FILTER MEDIA MODIFICATION IN RAPID SAND FILTRATION

Po-Hsun Lin, Ph. D.

Cornell University 2010

The main objective of this research was to improve the filtration technologies to make them more sustainable and accessible. This study focused on developing improved operating methods for rapid sand filtration technology that would not require costly infrastructure upgrades to implement. Unlike previous filter media modifications conducted by other researchers, the filter media in this study was modified *in situ*. Process Controller software was used for automation of the test apparatus facilitating systematic variation of parameters and replication of results.

Several different coagulants at varying dosages were applied by either downflow or upflow to modify a sand filter medium. Initially coagulants were added in downflow mode to the top of a 7.5 cm deep sand column prior to challenging the filter with an otherwise untreated kaolin suspension. Three coagulants, alum ($\text{Al}_2(\text{SO}_4)_3 \cdot 14\text{H}_2\text{O}$), ferric chloride (FeCl_3), and polyaluminum chloride (PACl), were utilized separately to modify the sand filter medium. After modification of the filter medium, an initial particle removal of 96% was achieved by all coagulants versus 60% removal in the absence of pretreatment. Pretreatment with PACl and alum showed increasing particle removal with increasing dosage up to a maximum of 550 mmol Al/m² after which filter performance declined. Pretreatment with FeCl_3 increased particle removal over the entire range of dosages evaluated (70 to 2200 mmol Fe/m²) but headloss through FeCl_3 treated filters became prohibitive at the highest dosage.

Although downflow application of coagulant showed promise there was strong evidence that better performance and lower head loss would be possible if a more uniform application of the coagulant throughout the filter could be attained. Thus, a novel fluidized-bed pretreatment process was developed to modify the sand medium at the end of the backwash cycle of the filter. During backwash, a mixture of alum, base, and tap water were pumped into the filter upward from the bottom. The ensuing precipitation of $\text{Al}(\text{OH})_{3(\text{am})}$ in the filter pores enhanced the efficiency of turbidity removal from untreated raw water (up to 99.6%) without a substantial increase of head loss (≈ 14 cm). While pretreatment with $\text{Al}(\text{OH})_{3(\text{am})}$ was effective at enhancing particle removal, measurements of dissolved aluminum in the filter effluent showed that this process modification should only be considered for waters with circum-neutral pH. At pH of 8 a pretreatment dosage of 16 mol Al/m^3 resulted in effluent dissolved Al in excess of the EPA secondary drinking water standard of $0.05\sim 0.2 \text{ mg/L}$.

To clearly understand the fundamental aspects of the enhanced particle removal by fluidized-bed pretreatment with $\text{Al}(\text{OH})_{3(\text{am})}$, two alternative mechanisms were hypothesized: (1) $\text{Al}(\text{OH})_{3(\text{am})}$ coats the sand filter medium, and alters its porosity. (2) Precipitated $\text{Al}(\text{OH})_{3(\text{am})}$ embedded within the media pores acts as an additional filter medium that enhances the particle removal efficiency. Mathematical models for these two mechanisms were constructed and compared with experimental data for particle removal and head loss. Model predictions suggest that particle removal by the second mechanism, filtration through $\text{Al}(\text{OH})_{3(\text{am})}$ flocs, can account for the observed improvement of the filter performance.

BIOGRAPHICAL SKETCH

Po-Hsun Lin was born on February 29, 1980, in Tainan, Taiwan, which is a cultural and lovely city filled with historic monuments and delicious food. After he graduated from National Tainan First High School, he attended National Chung Hsin University, where he earned his Bachelor of Science in Environmental Engineering in 2002. After his college student life, he had served in the army for one and half years to learn fighting skills and experienced a totally different life which strengthened and matured his mind and will. Then he attended Cornell as a graduate student in the Civil and Environmental Engineering. He finished his master degree in 2006 and continued his Ph.D. degree under the guidance of Dr. Monroe Weber-Shirk and Dr. Leonard Lion in Cornell University.

Po-Hsun is a vivacious and optimistic person. He enjoyed outdoor activities around Ithaca and loves playing different ball sports. He also learned how to play Frisbee, downhill ski, and other interesting activities he never did in Taiwan. After he obtains his Ph.D., he will work as a post doc in Cornell.

Dedicated to my parents, Ching-Fu Lin and Chiou-Er Tsai

ACKNOWLEDGMENTS

First and foremost, I would like to thank my two advisers, Dr. Monroe Weber-Shirk and Professor Leonard Lion. Without their disciplined and systematic guidance and support, I could not have finished this research. It is truly an honor to be able to work with people who are so accomplished and enthusiastic in this field. Dr. Monroe Weber-Shirk has spent countless hours teaching and guiding me through the experimental processes and theories. Professor Lion has really helped shape and guide this research with his practical advice and experience. I would also like to thank my committee members, Professor Ruth Richardson for many helpful discussions and support that have been invaluable; and Professor Abraham Stroock who served a great source of knowledge and who introduced me to the world of heat and mass transfer.

I am grateful to my lab mates and officemates, Kwok Loon, Matt, Ian, Brian, Annie, Cloelle, Iman, Gabi, Wan, and Gretchen, for helping and sharing your upbeat experiences with me. As an international student, I am so glad for being friends with you. In addition, I am also grateful my Taiwanese friends, James Co, Potato, Norah, CP Co, Holly, Kai-Wen, Jason Co, Jon, Lillian, Jeffrey, Vicky, Joyce, and Brad for your help and giving me a great time during these years.

I would like to thank my parents for their support, encouragement and for always being there. To my sisters, thank you for your experiences in the U.S. And Hsin-Yi, you've always been there to support and encourage me. Thank you for sharing your laugh with me everyday. Finally, I am grateful to Uncle Lai's family. You treat me like I were your son. I feel so warm to be a member in your family.

Funding for this project was provided by the U.S. National Science Foundation under Grant CBET-0604566 and by Sanjuan Foundation.

REFERENCES	51
CHAPTER 4 Enhanced Filter Performance by Fluidized-Bed Pretreatment with Al(OH)_{3(am)}: Observations and Model Simulation *	53
4.1 Abstract.....	53
4.2 Nomenclature	53
4.3 Introduction	55
4.4 Materials and Methods	56
4.4.1. Filtration apparatus.....	56
4.4.2. Fluidized-bed pretreatment of filter media.....	57
4.4.3. Filter operation	58
4.5 Results	59
4.5.1. Turbidity removal efficiency and head loss profile for alternative fluidized-bed pretreatments	59
4.5.2. Measurement of the settled volume of Al(OH) _{3(am)}	62
4.6 Alternative Models for the Effect of Fluidized-Bed Pretreatment on Filter Performance	63
4.6.1. Model predictions of head loss and filter performance assuming Al(OH) _{3(am)} coating	64
4.6.1.1 Head loss	64
4.6.1.2. Particle removal (pC*)	66
4.6.2. Model predictions of head loss and filter performance assuming Al(OH) _{3(am)} filtration.....	67
4.6.2.1. Head loss	70
4.6.2.2. Particle removal (pC*)	71
4.7 Conclusion.....	73
4.8 Acknowledgements	73
REFERENCES	74
CHAPTER 5 Conclusions and Recommendations for Future Work	75
5.1 Conclusions	75
5.2 Future Work.....	76
APPENDIX A	78
A.1 Calculation of the detection limit of particle capture efficiency	78
A.2 Comparison of FeCl ₃ and alum in long term experiments	79
A.2.1 Introduction	79
A.2.2 Results	79
A.3 Distribution of aluminum in the filter column	82
A.3.1 Aluminum distribution in short (7.5 cm) sand column	82
A.3.2 Aluminum distribution in long (60 cm) sand column	85
A.4 Deterioration of performance in pretreated filters.....	86
A.4.1 Colloid capacity.....	86
A.4.2 Negative charge capacity.....	89

LIST OF FIGURES

Figure 2-1.	Schematic of the filter test apparatus showing the valve and pump configuration for pretreatment with aluminum sulfate.	10
Figure 2-2.	Effluent Al concentrations after pretreatment with alum at three surface loadings during 20 minute challenge.	17
Figure 2-3.	Alum pretreatment. Clay removal (pC*) over time by the filter as a function of different pretreatment surface loadings (mmol/m ²) of Al. ...	18
Figure 2-4.	Clay removal (pC*) by the filter as a function of different surface loadings of three coagulants.....	19
Figure 2-5.	Head loss during pretreatment as a function of the surface loading of three different coagulants applied to the filter.	20
Figure 2-6.	Clay removal (pC*) by the filter as a function of predicted head loss of the three coagulants tested.....	21
Figure 2-7.	Head loss during the kaolin challenge to the filter as a function of run time after pretreatment with three different coagulants..	23
Figure 3-1.	Dissolved Al concentration in equilibrium with precipitated alum and PACl in deionized water at 25°C.....	30
Figure 3-2.	Schematic of the experimental filtration apparatus.....	32
Figure 3-3.	Al(OH) _{3(am)} fluidized-bed pretreatment. Effect of humic acid in the influent to a rapid sand filter on particle removal (pH = 8)..	38
Figure 3-4.	Al(OH) _{3(am)} fluidized-bed pretreatment. Particle removal (pC*) over time by a sand filter as a function of different pretreatment dose (mol Al/m ³).	39
Figure 3-5.	pC* as a function of different pretreatment dose (mol Al/m ³).....	40
Figure 3-6.	Two hypothesized mechanisms by which Al(OH) _{3(am)} improves filter performance.....	41
Figure 3-7.	Total head loss of the alum-pretreated filter as a function of pretreatment dose.....	42

Figure 3-8. Particle removal (pC^*) over time by the filter using different pretreatment methods..	44
Figure 3-9. Head loss during 48 hour challenge of the four different experiments...	46
Figure 3-10. Effluent Al concentrations during challenge at pH of 6 and 7.....	47
Figure 3-11. Particle removal (pC^*) over time as a function of pH.....	48
Figure 4-1. Schematic of experimental apparatus.....	57
Figure 4-2. Alum fluidized-bed pretreatment. Particle removal (pC^*) over time by a sand filter as a function of the pretreatment dose (mol Al/m^3)..	60
Figure 4-3. pC^* as a function of different pretreatment dose (mol Al/m^3).....	61
Figure 4-4. Total head loss of the alum-pretreated filter as a function of pretreatment dose. 62	
Figure 4-5. Alternative hypothesized mechanisms by which $\text{Al(OH)}_{3(\text{am})}$ may act to improve filter performance.....	64
Figure 4-6. Comparison of model predicted and experimental head loss by the alum-pretreated filter as a function of pretreatment dose.....	65
Figure 4-7. Comparison of predicted and measured particle removal by the alum-pretreated filter as a function of pretreatment dose.....	67
Figure 4-8. $\text{Al(OH)}_{3(\text{am})}$ floc porosity as a function of diameter.....	70
Figure 4-9. Comparison of model predicted and experimental head loss by the alum-pretreated filter as a function of pretreatment dose.....	71
Figure 4-10. Comparison of model predicted and observed particle removal by the alum-pretreated filter as a function of pretreatment dose..	72
Figure A-1. Detection limit (pC^*) as a function of raw water turbidity.	78
Figure A-2. Alum downflow pretreatment. Particle removal (pC^*) over time by the filter using different pretreatment methods.....	80
Figure A-3. FeCl_3 downflow pretreatment. Particle removal (pC^*) over time by the filter using different pretreatment methods.....	81

Figure A-4. Comparison of using alum and FeCl_3 for combining pretreatment and contact filtration.	82
Figure A-5. Schematic diagram of the new filter column.	83
Figure A-6. Head loss during pretreatment as a function of the surface loading of each pressure sensor.	84
Figure A-7. Head loss per unit depth during pretreatment as a function of the surface loading.	85
Figure A-8. Head loss per unit depth during pretreatment as a function of the surface loading.	86
Figure A-9. Alum fluidized-bed pretreatment. Particle removal (pC^*) over time by a sand filter as a function of the clay concentration.	87
Figure A-10. Particle removal (pC^*) as a function of cumulative removed clay (NTU) over 12 hours of operation.	88
Figure A-11. Effluent turbidity as a function of cumulative removed clay (NTU) over 12 hours of operation.	89
Figure A-12. Alum fluidized-bed pretreatment. Particle removal (pC^*) over time by a sand filter as a function of the HA concentration.	90

LIST OF TABLES

Table 2-1. Stock and feed concentrations of the reagents used.....	12
Table 2-2. Process Controller States.	14
Table 2-3. Fraction of applied Al and Fe retained in the sand medium during pretreatment	16

CHAPTER 1

INTRODUCTION

1.1 Porous Media Filtration

Filtration is a fundamental unit process that is commonly used to help remove: particles present in surface water, precipitated hardness from lime-softened water, microorganisms (bacteria, viruses, and protozoan cysts), precipitates of aluminum and iron used in coagulation, and precipitated iron and manganese present in many well water supplies (Weber 1972; Letterman 1999).

Filters may be broadly classified as “rapid” or “slow” based on the rate at which they operate. A slow sand filter is a filter operated at very low filtration rates (usually 0.1~0.2 m/hr) without coagulation in pretreatment (Casey 1997). Rapid sand filtration was introduced in the United States in the 1880s and has been widely accepted for municipal application because of its high productivity and flexibility in treating waters of different turbidities (Letterman 1999). In drinking water treatment, the function of rapid sand filters is to remove particulate matter in the influent suspension and provide significant pathogen removal. In contrast to slow sand filters, rapid sand filters are operated at a much higher filtration rates (5~10 m/hr) and are frequently used in water treatment following pretreatment of the raw water by chemical coagulation, flocculation, and sedimentation.

Models for predicting the single-collector contact efficiency in physicochemical particle filtration in saturated porous media have been presented in many studies (Yao et al. 1971; O'Melia 1980; Elimelech and O'Melia 1990; Tufenkji and Elimelech 2004). The particle removal efficiency of a conventional rapid sand filter (particle diameter: 1

μm , filtration velocity: 5 m/hr, sand grain diameter: 0.5 mm, sand depth: 60 cm, attachment efficiency: 0.8, and porosity: 0.4) is about 60% based on the model derived from Tufenkji and Elimelech (2004). The filter performance in the Cornell Water Filtration Plant is around 90%, and this good performance could be due to the pretreatment of the raw water with polyaluminum chloride (PACl) which would modify the surface charge on the colloidal particles improving their attachment efficiency, and also acting to create larger particle sizes through flocculation.

1.2 Research Objectives

This research tests the hypothesis that a particle removal efficiency better than 95% can be achieved through modification of sand filter media even without pretreatment of the raw water with coagulants. Filter media modification will be achieved by applying coagulants that will act to modify the negative surface charge of the sand media and also act to augment the filter medium by introducing a Al or Fe hydroxide precipitate. Previous studies have shown that the addition of small amounts of precipitated aluminum to slow sand filters can greatly improve removal of *E. coli* (Weber-Shirk and Chan 2007). In rapid sand filters, back wash water augmented with low concentrations of alum and/or polymer have been shown by Yapijakis (1982) and Cranston and Amirtharajah (1987) to improve the initial performance.

Experiments were performed using two automated filtration test apparatus with short (7.5 cm) and long (60 cm) sand columns, respectively. Automation was achieved using Process Controller software developed by Weber-Shirk (2008). Tests with systematic variation of pretreatment conditions were carried out to optimize rapid sand filtration performance. The main experimental objectives included:

1. Evaluation of the effect on filter performance of addition of different coagulants at varying dosages by either downflow or upflow prior to challenging a filter (referred to here as pretreatment).
2. Investigation of the spatial distribution of Al or Fe hydroxide precipitates in the filter.
3. Measurement of effluent Al or Fe during filter operation to ensure their concentrations were below EPA secondary MCL.
4. Development of a fundamental understanding of the dominant particle removal mechanisms in pretreated rapid sand filters.

1.3 Organization of Dissertation

This dissertation is organized in a manner reflecting the course of the author's investigation of enhanced filter performance of a rapid sand filter. The following chapters present different research investigations related to the enhanced performance of a rapid sand filter.

The comparison of the ability of three coagulants to improve filter performance is described in Chapter 2. Alum, ferric chloride, and polyaluminum chloride (PACl), were separately applied by downflow mode to a 7.5 cm deep sand column to modify the sand filter medium. Particle capture efficiency (pC^*), head loss development, and metal concentrations in the effluent during filter pretreatment and operation are evaluated.

Chapter 3 presents an evaluation of the limitations of PACl and alum application to pretreat a filter medium. The effect of raw water pH and natural organic matter to the alum-pretreated filters are also discussed.

Observations and model simulations of enhanced filter performance by fluidized-bed pretreatment with $\text{Al}(\text{OH})_{3(\text{am})}$ are the subject of Chapter 4. Two alternative mechanisms for improved performance are hypothesized, and mathematical models for these two mechanisms are compared with experimental results for particle capture efficiency and head loss.

Finally, conclusions based on this research and recommendations for future work are provided in Chapter 5.

REFERENCES

- Casey, T. J. (1997). *Unit Treatment Processes in Water and Wastewater Engineering*.
- Cranston, K. O. and A. Amirtharajah (1987). Improving the Initial Effluent Quality of a Dual-Media Filter by Coagulants in Backwash. *Journal / American Water Works Association* 79(12), 50-63.
- Elimelech, M. and C. R. O'Melia (1990). Kinetics of deposition of colloidal particles in porous media. *Environ. Sci. Technol.* 24(10), 1528-1536.
- Letterman, R. D. (1999). *Water Quality and Treatment*, American Water Works Association.
- O'Melia, C. (1980). ES&T Features: Aquasols: the behavior of small particles in aquatic systems. *Environ. Sci. Technol.* 14(9), 1052-1060.
- Tufenkji, N. and M. Elimelech (2004). Correlation Equation for Predicting Single-Collector Efficiency in Physicochemical Filtration in Saturated Porous Media. *Environ. Sci. Technol.* 38(2), 529-536.
- Weber-Shirk, M. (2008). An Automated Method for Testing Process Parameters from <https://confluence.cornell.edu/display/AGUACLARA/Process+Controller>.
- Weber-Shirk, M. L. and K. L. Chan (2007). The role of aluminum in slow sand filtration. *Water Research* 41(6), 1350-1354.
- Weber, W. J. (1972). *Physicochemical Processes for Water Quality Control*
- Yao, K.-M., M. T. Habibian and C. R. O'Melia (1971). Water and waste water filtration. Concepts and applications. *Environ. Sci. Technol.* 5(11), 1105-1112.
- Yapijakis, C. (1982). Direct Filtration: Polymer in Backwash Serves Dual Purpose. *Journal / American Water Works Association* 74(8), 426-428.

CHAPTER 2

Comparison of the Ability of Three Coagulants to Enhance Filter Performance *

2.1 Abstract

In the operation of porous media filtration systems, poor initial performance is often observed in which particle removal is less than desired. Alum ($\text{Al}_2(\text{SO}_4)_3 \cdot 14\text{H}_2\text{O}$), ferric chloride (FeCl_3), and polyaluminum chloride (PACl) are often used in drinking water treatment to modify the surface properties of the particles being filtered and enhance their removal by filters; however modification of the filter medium is not a common practice. In the research described in this chapter, these three coagulants were utilized to artificially modify a sand medium before challenging the filter with an otherwise untreated kaolin suspension. After modification of the filter medium, high particle removal efficiencies were achieved using a short (7.5 cm) sand column with relatively large grained sand ($\cong 1$ mm in diameter). The best observed particle removal (96%) using alum and PACl occurred at the surface loading of 550 mmol Al/m^2 , but the filter performance deteriorated at higher surface loadings. Fractional colloid removal increased with increased ferric chloride surface loading over the entire range of dosages tested (up to 97.5% at 2200 mmol Fe/m^2). The experimental results suggest that pretreatment of filter media by coating with Fe or Al hydroxides can eliminate the poor performance.

Keywords: Filter ripening, enhanced filtration, coagulants

* The contents of this chapter have been submitted for publication with co-authors L. Lion and M. Weber-Shirk.

2.2 Introduction

Filtration through porous media is a commonly used method for removal of solids present in surface waters, precipitated hardness from lime-softened water, and precipitated iron and manganese present in many well water supplies (Weber 1972). The removal of suspended particles within a filter is considered to involve at least two sequential steps: transport and attachment. In the first step, the particles are transported from the bulk fluid to the immediate vicinity of solid-liquid interface presented by the filter (i.e., to a grain of the media or to another particle previously retained in the filter bed). The transport of particles to the filter medium may occur through three mechanisms: Brownian diffusion (molecular effects), interception (contact as a result of fluid flow near the surface of the porous media), and sedimentation (gravity effects). Particle attachment to the media surface is dominated by electrical and chemical interactions such as electrostatic attraction or repulsion within the electrical double layer and van der Waals attractive forces that act between particles and surfaces at short distances (Yao et al. 1971; O'Melia 1980; Elimelech & O'Melia 1990).

Sand media is a key, if not the sole, component of most filters. However, sand media may not be efficient in the removal of fine or sub-micron particles including mineral colloids, bacteria, and viruses because of electrostatic repulsion arising from the fact that both the particles and sand media are negatively charged at circumneutral pH values. As a result, Fe and Al are commonly added as coagulants to destabilize particles (Weber 1972; Tchobanoglous et al. 2003) and improve particle removal. Destabilization involving adsorption of Al or Fe monomers is referred to as charge neutralization; coagulation of colloidal particles in the presence of $\text{Al}(\text{OH})_{3(\text{am})}$ and $\text{Fe}(\text{OH})_{3(\text{am})}$ is termed enmeshment or sweep floc (Van Benschoten & Edzwald 1990).

Polyaluminum chloride (PACl) has recently been reported to be superior to alum in removal of particles with advantages of reduced alkalinity consumption, less sludge production, decreased temperature and pH dependence, and reduction of cost (Hu et al. 2006).

In some cases iron and aluminum hydroxides have been used to modify filtration media to improve the particle removal efficiency (Edwards & Benjamin 1989; Lukasik et al. 1999; Ahammed & Meera 2006). In these studies Fe and Al surface modification was achieved by soaking the sand medium in aluminum chloride or ferric chloride solutions followed by treatment with an ammonium hydroxide solution. The pretreatment improved particle capture, but the treatment method required removing the sand from the filter and thus would not be easily applied to operating filtration systems.

In the research described in this paper, three common coagulants, alum, ferric chloride, and PACl were chosen to modify a sand filter medium prior to challenging the filter with a colloidal suspension of kaolin. The resulting modification of the filter could include coating the sand surface with precipitated aluminum or iron hydroxides, or deposition of Al or Fe precipitates in the pore space of the filter medium, or some combination of these two processes. The point of zero charge (PZC) of aluminum hydroxide and ferric hydroxide are 9.6 (Scholtz et al. 1985) and 8.5 (Benjamin 2002), respectively. Thus, at neutral pH, the modified sand media is expected to be positively charged and to have an enhanced ability to capture negative colloidal particles. In this study, a process was used for in situ modification of the sand before challenging the filter. The resulting particle removal efficiencies are compared as a function of Al and

Fe surface loading. Head loss was also monitored during pretreatment and during the challenge to the filter.

2.3 Materials and Methods

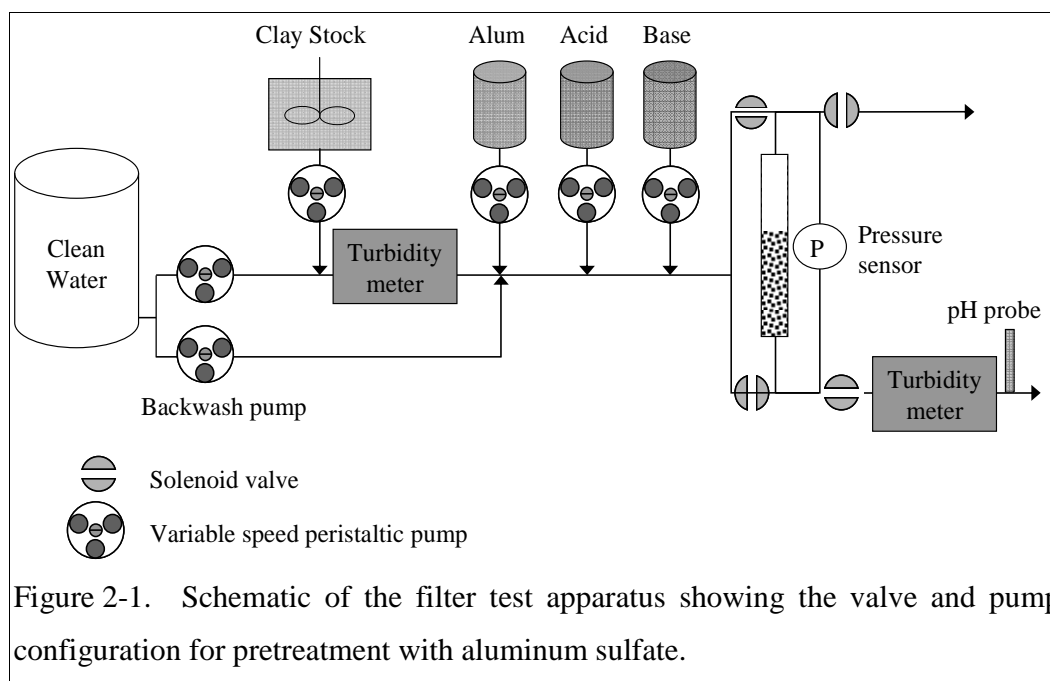
Measurement of effluent Al and Fe concentrations. Retention of applied Al or Fe precipitates in the filter medium was assessed by measuring aluminum and iron concentrations in the effluent during pretreatment at the highest (2200 mmol/m²) and lowest (70 mmol/m²) surface loading used in experiments. In addition, the Al concentration in the effluent was measured during challenge at the alum surface loadings of 70, 550, and 2200 mmol Al/m².

A colorimetric assay, the modified Eriochrome Cyanine R Method, was selected for Al analysis, in which the volume of reagents and samples were scaled down to fit into 4.5 mL cuvettes. (Standard Methods for the Examination of Water and Wastewater, 1998). The assay can detect aluminum at concentrations above 20 µg/L (i.e., 7.4 µmol/L). All glassware used was first acid washed for 24 hours with 10% nitric acid (reagent grade) made with distilled deionized (DDI) water followed by a 24 hour wash in 10% nitric acid (trace metal grade). The glassware was rinsed with DDI water 6 times in between the 24 hour wash steps. Aluminum chloride (AlCl₃•6H₂O, Fisher Scientific) was used to prepare Al standard curves.

Atomic absorption spectrometry was utilized for the determination of iron in the effluent water during pretreatment (Standard Methods for the Examination of Water and Wastewater, 1998). An air-acetylene flame was used. The assay can detect iron at concentrations above 20 µg/L (7.4 µmol/L). All glassware was acid washed as

described above. Iron standards were made by dilution of iron stock (1000 mg/L, Fisher Scientific). The measurements were carried out in triplicate.

Apparatus. An automated filtration test apparatus described by Weber-Shirk (Weber-Shirk 2008) was used to conduct parametric tests of the use of alum, ferric chloride (Fisher Scientific), and polyaluminum chloride, PACl (PCH-180, Al-5.5%, Cl-12.1%, SO₄-1.8%, basicity-69%, Holland Company Inc.) to modify (artificially ripen) the medium in a sand filter. A schematic of the apparatus is shown in Figure 2-1.



In all tests 22°C Cornell University tap water (pH \approx 7.6, total organic carbon \approx 2.0 mg/L, hardness \approx 150 mg/L as CaCO₃, alkalinity: \approx 110 mg/L as CaCO₃, chlorine residual \approx 0.7 mg/L) was used as the raw water source. Kaolin clay (R.T. Vanderbilt Company, Inc., Connecticut) was added to distilled water as a concentrated stock (350 mg/L, pH = 4.3) and then diluted with tap water to achieve an influent turbidity of 55~60 NTU and pH of 7.5. At this pH the zeta potential of the clay was determined to be -18 ± 2 mV by laser Doppler electrophoresis (Malvern Zetasizer Nano-ZS). The zeta

potential of most particles in surface waters at neutral pH is in the range of -15 to -30 mV (Ongerth and Pecoraro 1996). Aquatic fulvic acid, a major form of natural organic matter (NOM), usually has a total negative surface potential 30 times more than that of clay particles (Pernitsky & Edzwald 2006). The clay particle size was approximately 1 μm as measured by dynamic light scattering (Malvern Zetasizer Nano-ZS).

Many sand filters are operated with an influent turbidity of less than 5 NTU. We chose to use a higher influent turbidity of ~60 NTU in the experiments reported here to ensure that significant differences in particle concentration could be accurately measured and so that we could use a shorter run time and still obtain significant particle loading in the filter. Results from experiments at two different clay concentrations (~5 and ~60 NTU) show that a ~10 fold variation in turbidity did not cause significant difference in the performance of an alum-pretreated filter (see Figure A-9 in Appendix A.4.1) and an untreated filter (data not shown). The concentration of the stock solutions, clay suspension and the coagulant doses used are given in Table 2-1.

Table 2-1. Stock and feed concentrations of the reagents used.

Chemical name	Concentration of the stock solution	Dilution factor	Concentration at filter influent
Kaolin clay	350 (mg/L)	7	50 (mg/L)
Aluminum sulfate	3.4 (mmole/L as Al)	13.6	250 (μ mole/L as Al)
Polyaluminum Chloride (PACl)	3.4 (mmole/L as Al)	13.6	250 (μ mole/L as Al)
Ferric Chloride	3.4 (mmole/L as Fe)	13.6	250 (μ mole/L as Fe)
Sodium bicarbonate	12 (mmole/L as HCO_3^{-1})	40.8	300 (μ mole/L as HCO_3^{-1})
Hydrochloric acid	0.1 (mole/L as H^+)	1	0.1 (mole/L as H^+)

The alum, PACl, and ferric chloride concentrations at the filter influent were equivalent to 74 mg/L as alum, 6.7 mg/L PACl as Al, and 67 mg/L as FeCl_3 , respectively. The filter column was 2.5 cm in diameter and contained 7.5 cm of 0.8 to 1 mm in diameter filter sand (U.S. Filter, New Jersey). In effect, the shallow filter column and test conditions provide an experimental model of the top 7.5 cm of a rapid sand filter.

Coagulants were mixed with base (sodium bicarbonate) and tap water to maintain the pH at 6.8 for alum, 7.1 for PACl, and 6.6 for FeCl_3 and then applied to the top of the filter column to treat the filter medium prior to challenging the filter with the clay suspension. We report the amount of coagulant applied to the filter as a surface

loading with units of mmol/m^2 where the area is the cross sectional area of the filter. Filter cross sectional area is used to express dosage rather than filter volume because the $\text{Al(OH)}_{3(\text{am})}$ accumulates in the top few centimeters of the filter bed. Presenting the dose as a surface loading facilitates generalization of the experimental results to other filter sizes. The total surface loading of coagulant, Γ , is a function of the coagulant flow rate, Q , filter surface area, A , influent concentration, C , and application time, t , as described by equation 1.

$$\Gamma = \frac{QCt}{A} \quad (1)$$

Experiments were performed over a wide range of surface loadings (0 as a control, 70, 140, 280, 550, 1100, and 2200 mmol/m^2) to explore the dose-dependence of particle capture efficiency. The filtration rate was held constant at 5 m/hr in all experiments. While the experimental results may be affected to some extent by scale (the column diameter/sand size ratio was $\cong 30$), these variables were systematically retained for all experiments and therefore trends in our results are expected to be valid. Backwash and an acid wash (0.1 M HCl) were used between each experiment to remove residual clay and metal hydroxide precipitates. Duplicate control experiments with no coagulant addition were conducted at the start of each series of experiments and after the experiment with the highest surface loading to confirm the ability of the filter washing steps to restore the sand to its original (untreated) condition.

Process Control software (Weber-Shirk 2008) for the automated filtration apparatus cycled through states shown in Table 2-2 for each test. The hydraulic retention time from the clay stock pump to the effluent turbidity meter was 3.8 minutes based on the filtration rate of 5 m/hr. In the filter column, the volume of water above the sand was

35 cm³, and the hydraulic retention time from top of filter to the bottom of filter was 1.2 minutes (porosity = 0.4).

Table 2-2. Process Controller States.

State Name	Purpose	Duration
Backwash filter-1	Clean the filter	4 minutes
Acid wash	Wash out the coagulant	2 minutes
Backwash filter-2	Clean the filter	4 minutes
Wash turbidity meters	Wash the turbidity meters	4 minutes
Pretreatment	Ripen the filter	variable
Downflow	Challenge the filter	20 minutes

The concentration of the applied coagulants was approximately the same during the pretreatment state, but the pretreatment state duration was varied to achieve different surface loadings.

During the particle challenge state, the filter was operated at a constant flow rate of 5 m/hr (40.8 mL/min) for 20 minutes and the filter performance was measured by inline turbidimeters (Figure 2-1). The turbidimeters were chosen because they have small volume sample cells (30 mL) that make it possible to achieve reasonable response times at the flow rates used in this research. The 20 minute challenge with an influent turbidity of 60 NTU made it possible obtain significant particle loadings for each pretreatment condition and to cycle over a wide range of coagulant dosages in a reasonable length of time. The hydraulic residence time from the inlet of the influent turbidimeter to the outlet of the effluent turbidimeter at a flow rate that corresponds to

a filtration velocity of 5 m/hr was 4 min. We do not report the data from the first 1.5 hydraulic residence times (i.e., about 6.5 minutes) at the beginning of each the particle challenge since that data show an artificially high particle removal caused by the clean pore water that is still exiting the filter into the effluent turbidimeter and being displaced from the tubing and turbidimeter sample vial.

Particle capture efficiency is expressed here as pC^* where C^* is the turbidity of the effluent water normalized by the turbidity of the influent water and p is the $-\log$ function (base 10) (i.e. $pC^* = -\log(C_{\text{effluent}}/C_{\text{influent}})$).

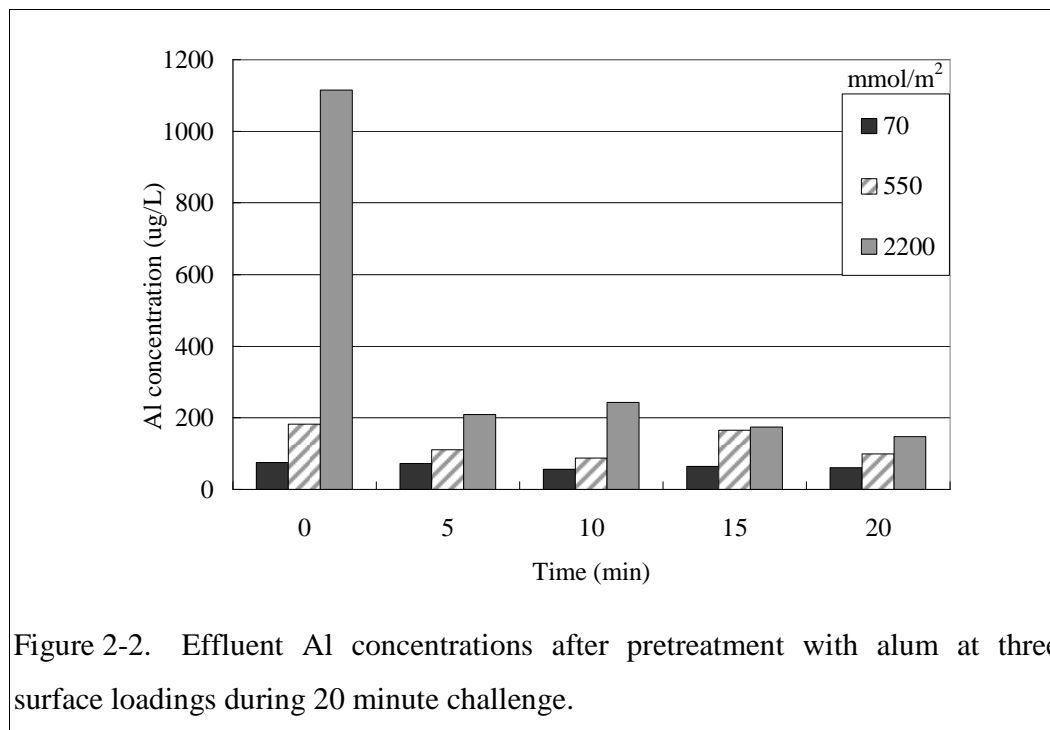
2.4 Results and Discussion

Aluminum and iron concentration in the effluent. All effluent during pretreatment was collected and measured for Al or Fe concentration. Mass balance showed that $\geq 78\%$ of applied Al or Fe was retained in the filter at a surface loading of 70 mmol/m^2 and $\geq 82\%$ of Al or Fe remained in the filter at a surface loading of 2200 mmol/m^2 (Table 2-3). The two applied dosages are used as maximum and minimum surface loadings in the following discussion and comparison of results so that the retained Al or Fe concentrations for other dosages between this range can be estimated.

Table 2-3. Fraction of applied Al and Fe retained in the sand medium during pretreatment

Sample Name	Surface Loading (mmol/m²-Al or Fe)	Al or Fe fraction retained in filter (%)
Low Alum	70	78
High Alum	2200	82
Low PACl	70	92
High PACl	2200	87
Low FeCl ₃	70	93
High FeCl ₃	2200	97

Effluent Al concentrations for alum application at the surface loading of 70, 550, and 2200 mmol/m² during challenge are presented in Figure 2-2. At loadings of 70 and 550 mmol/m² the Al concentrations were below the maximum EPA secondary drinking water standards (200 µg/L). For the surface loading of 2200 mmol/m² the Al concentration at 0th minute exceeded the predicted solubility of amorphous Al(OH)_{3(s)} (i.e. 170 µg/L at pH of 7.5). The high Al concentrations were likely due to an initial washout of precipitated Al from the column. Subsequent Al concentrations were slightly higher than the Al(OH)_{3(am)} solubility limit and may also have been caused by the release of small amounts of precipitated Al. The effluent Al concentration increased with increasing surface loadings. We did not measure Al and Fe concentration for PACl and ferric chloride during challenge because the solubility at pH of 7.5 for both metal hydroxide precipitates were much less than that of alum (i.e. 54 µg/L as Al determined by experiments for PACl (Van Benschoten & Edzwald 1990) and 0.002 µg/L as Fe based on the solubility of amorphous Fe(OH)_{3(s)} (Snoeyink & Jenkins 1980)).



Improvement of filter performance. Three coagulants, alum, ferric chloride, and polyaluminum chloride (PACl), were applied to the sand filter. Figure 2-3 shows representative results from the experiments with alum. The correspondence of duplicate pre and post control experiments (i.e. without application of alum) shows that the cleaning procedure was effective. The untreated sand achieved a baseline particle removal of $\cong 60\%$. Figure 3 also shows clay removal (pC^*) as a function of different aluminum surface loadings. The agreement of filter performance at replicate dosages was excellent. Clay removal increased as a function of Al surface loading up to a dose of 550 mmol/m^2 and then declined. Similar results were obtained with PACl with best particle removal obtained at loadings of 550 mmol/m^2 of aluminum (data not shown). Readers are cautioned that the value of the maximum effective alum and PACl surface loading applies to the conditions used in these experiments and is expected to be a function of the application method used to pretreat the sand medium, the size distribution of the sand, solution conditions (e.g., pH and natural organic

matter concentration) and type of colloidal particle. Particle removal using iron increased with increasing surface loading over the entire range of ferric chloride dosages (data not shown).

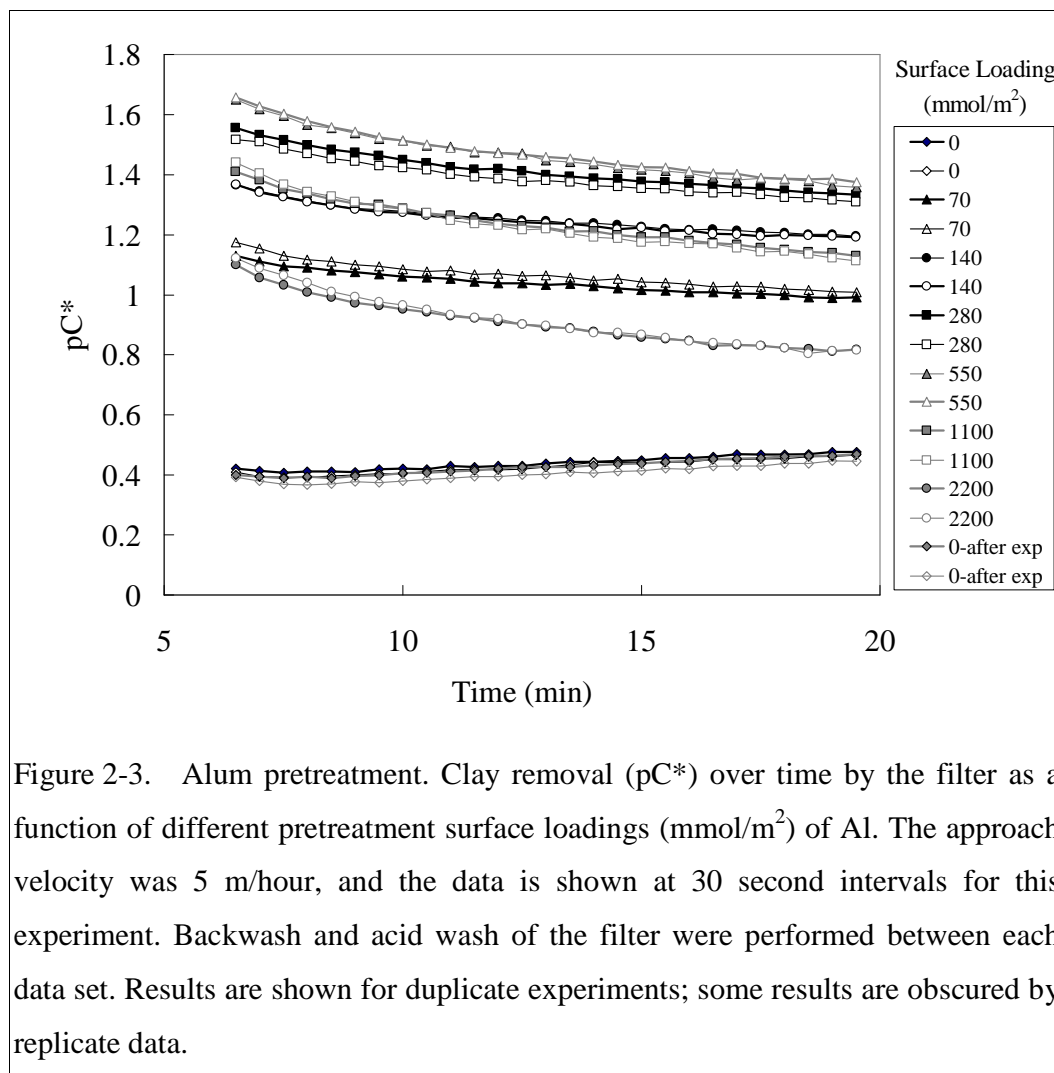


Figure 2-3. Alum pretreatment. Clay removal (pC^*) over time by the filter as a function of different pretreatment surface loadings (mmol/m^2) of Al. The approach velocity was 5 m/hour, and the data is shown at 30 second intervals for this experiment. Backwash and acid wash of the filter were performed between each data set. Results are shown for duplicate experiments; some results are obscured by replicate data.

The performance, pC^* , of the filter for each coagulant is shown in Figure 2-4 as a function of surface loading. Performance values shown are for a 5 minute average for the effluent data centered at the 15th minute (i.e. average the data from 12.5 to 17.5 minutes) and then averaged with the results of the replicate experiment. As noted

above, maximum clay removal occurred at 550 mmol/m² of aluminum, and the performance deteriorated at higher alum and PACl doses.

The performance using ferric chloride is slightly better than alum and PACl when all treatments are compared at a surface loading of 550 mmol/m². There is a larger difference for pC* between iron and Al at surface loadings of 1100 mmol/m² and 2200 mmol/m² because of the deterioration of performance of using alum and PACl at the higher surface loadings.

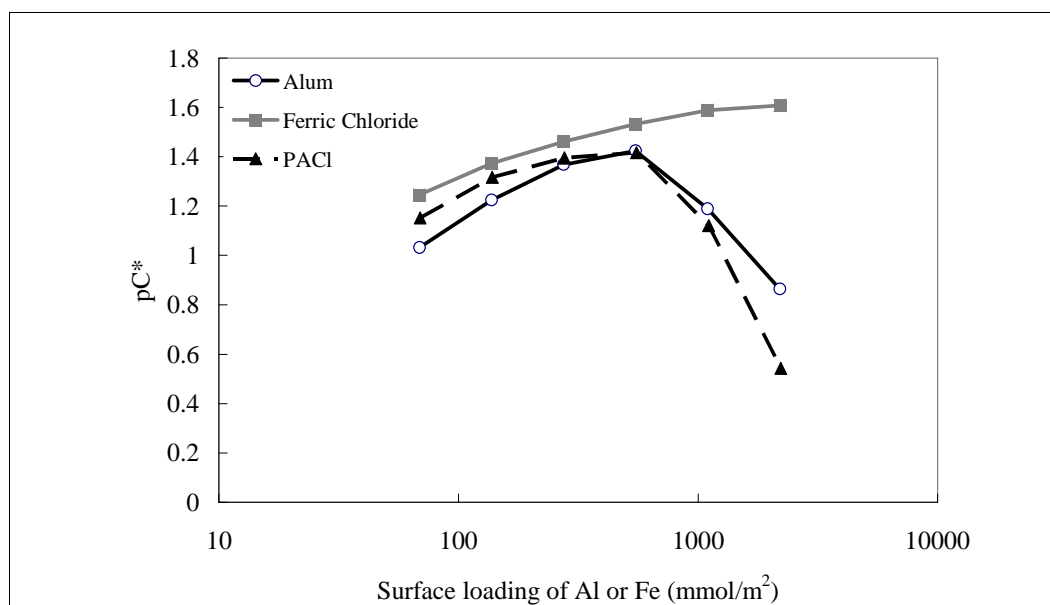
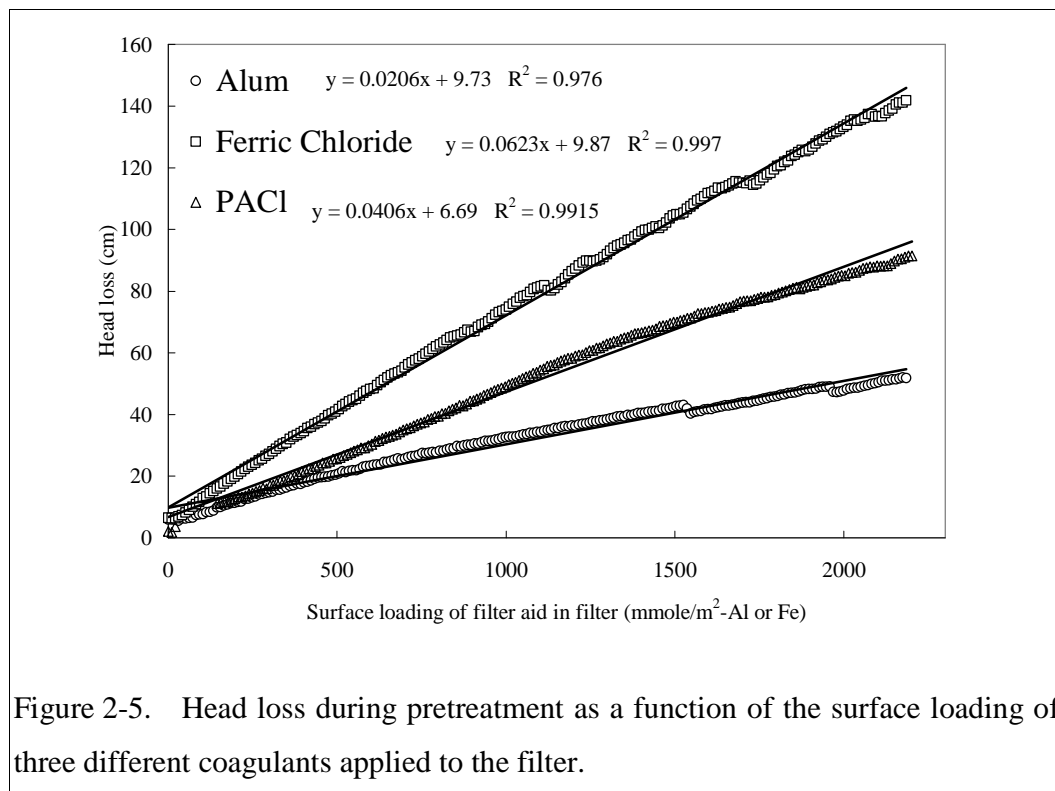


Figure 2-4. Clay removal (pC*) by the filter as a function of different surface loadings of three coagulants. pC* values were taken a 5 minute average for the data centered at the 15th minute of each experiment (average the data from 12.5 to 17.5 minutes), and then averaged with those for the replicate experiment.

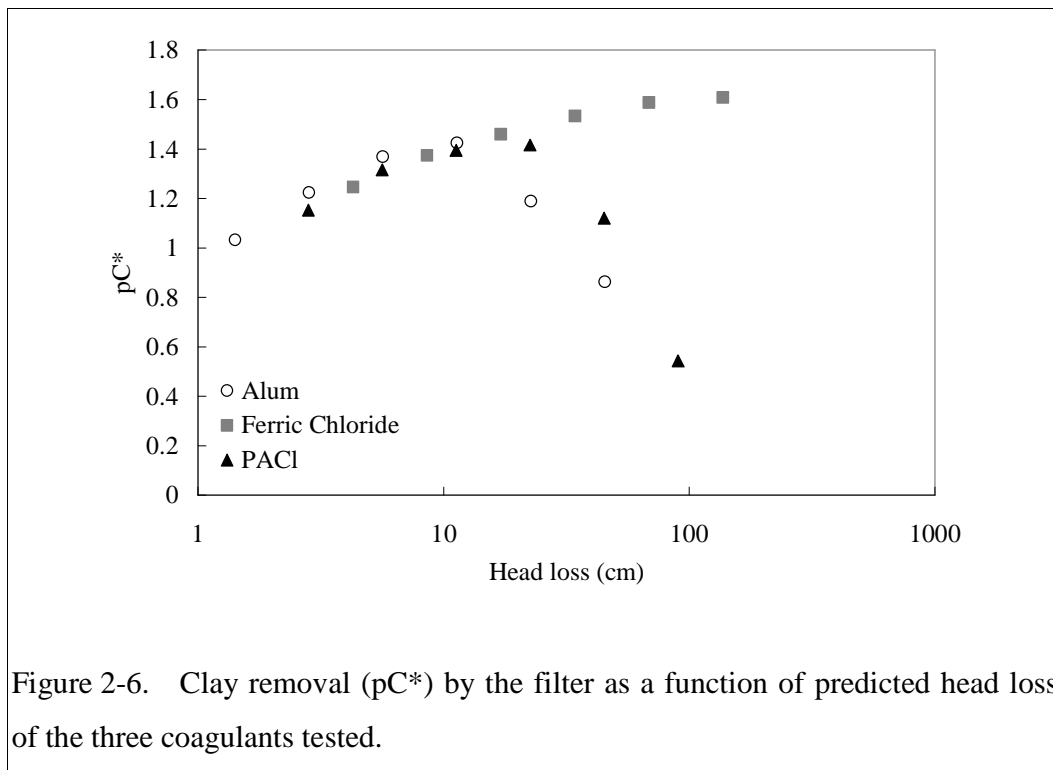
Head loss profiles. Addition of the three coagulants caused increased head loss during the pretreatment stage. Figure 2-5 shows head loss as a function of surface loading of alum, ferric chloride, and PACl. In each case the rate of head loss increase was

directly proportional to the surface loading. Ferric chloride had the largest head loss per mmol/m^2 applied, followed by PACl, and then alum. The difference in head loss between alum and PACl suggests that the precipitates formed from these two different sources of Al are distinct, and for the same surface loading PACl occupied a greater void volume in the filter bed. Some researchers have shown that the polymeric structure within the PACl precipitate remains intact, and the PACl precipitate often appears as small ($< 25 \mu\text{m}$) spheres, clusters of small spheres and even chain-like structures; while alum flocs are reported to consist of an amorphous solid that usually appears as fluffy, porous structures, ranging in size from 25 to $100 \mu\text{m}$ (Van Benschoten & Edzwald 1990).



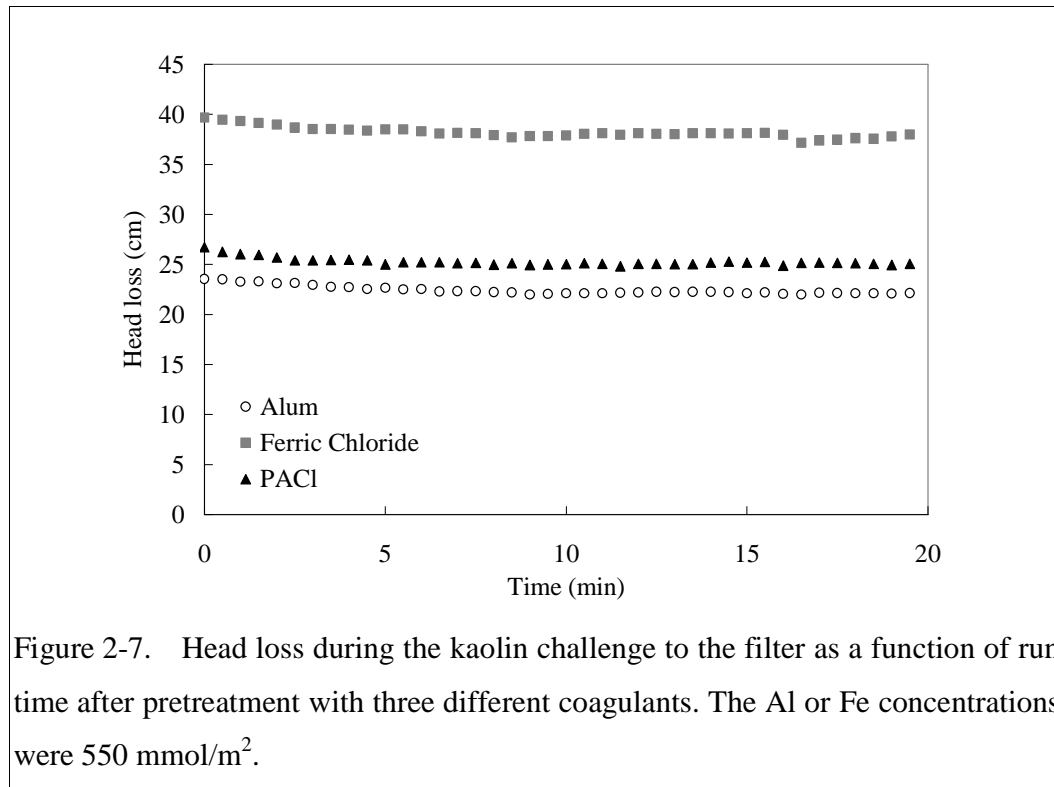
Lines were fit to the data in Figure 2-5 by least squares regression and the slopes were used to predict head loss for pretreatment at the surface loading values shown in

Figure 2-4. These calculated head loss values are compared in Figure 2-6 to the observed clay removal in the subsequent challenge (pC* data from Figure 2-4). At head loss ≤ 25 cm, the relationship between the clay removals and the head losses for the three coagulants were almost identical. As noted below (see Figure 2-7 and discussion) negligible additional head loss accumulation occurred during the clay challenge to the pretreated filter media. Given that the volume that metal hydroxide precipitate occupied in the pores caused the head loss and not the captured clay, then the correlation between pC* and head loss for head loss ≤ 25 cm suggests that the Al and Fe precipitates had the same clay removal because they were distributed similarly in the filter medium. With repetitive experimental use of the filter column, destructive testing of the filter medium was not desirable. Thus, the hypothesis that Fe and Al were similarly distributed was not confirmed. However, alternative explanations for the correlation between pC* and head loss (at head loss below 25 cm) are not apparent.



Precipitation of aluminum and iron hydroxides would both act to decrease void space in the porous medium. It is possible that the molar volumes of the Al and Fe precipitates are different. The higher head losses experienced with Fe vs. Al suggest that, if volume differences exist, Fe occupies a greater pore volume on a molar basis (see Figure 2-5). Analysis of the distribution head loss caused by Al hydroxide precipitate in the filter (see Appendix A.3) indicated that, at high Al loadings (1100 and 2200 mmol Al/m²), the void space near the top of the filter bed was sufficiently reduced so that the resulting shear stress inhibited clay deposition. As a result, performance deteriorated. For ferric chloride, the best clay removal was at the highest surface loading of iron. The better colloid removal by Fe despite higher head loss (see Figure 2-6) suggests that the strength of clay-ferric hydroxide interactions was strong enough to resist the higher shear stress.

Figure 2-7 presents the head loss as a function of time during the kaolin suspension challenge to the filter when the applied surface loading of Al or Fe was 550 mmol/m². The control head loss was about 7 cm during the filter run (data not shown). The small head loss change during filter operation (Figure 2-7) relative to the head loss change during filter pretreatment (Figure 2-5) suggests that the space the metal hydroxide precipitates occupied in the pores was much larger than the volume of clay particles that accumulated during the challenge.



2.5 Conclusions

The addition of alum, ferric chloride, or PACl as a pretreatment to a sand filter resulted in greatly enhanced removal of clay relative to the untreated sand medium. Relatively low surface loadings of 140 mmol/m² produced significant improvement in performance without causing excessive head loss. The maximum observed particle removal using alum and PACl occurred at the surface loading of 550 mmol Al/m² and at this loading for alum application the Al concentrations in the filtered effluent were below the EPA secondary MCL. Fractional removal of clay increased with increased ferric chloride over the entire range of dosages tested (maximum = 2200 mmol Fe/m²). However, high surface Fe loadings might not be practical in application because of the associated high head loss. For alum and PACl, the filter performance deteriorated when the surface loading was higher than 550 mmol Al/m². At the same surface

loading on a molar basis, pretreating with ferric chloride achieved better particle removal efficiency than the other two coagulants. However, all coagulants achieved the same clay removal when compared based on the head loss associated with their application at head loss ≤ 25 cm.

In this study, high particle removal efficiencies were achieved using a very shallow sand column with relatively large sand. All three pretreatment agents tested show good potential to reduce the interval required for ripening sand filters. Real natural waters, however, contain different sizes and types of particulates and natural organic matter (NOM) such as humic and fulvic acids. At circumneutral pH, NOM is negatively charged and can adsorb onto the surface of clay and other suspended particles, further increasing their negative charge (Pernitsky & Edzwald 2006). The presence of NOM in influent of the coagulant-pretreated filter is expected to result in a lower particle removal efficiency. Prior to using these pretreatment techniques on municipal sand filters further research will be required to account for the effect of the NOM and the diverse types of particulate matter in the raw water, and to ensure that our experimental results from a small diameter column apply at full scale.

REFERENCES

- Ahamed, M. M. & Meera, V. 2006 Iron hydroxide-coated sand filter for household drinking water from roof-harvested rainwater. *Journal of Water Supply: Research and Technology* **55**(7-8), 493-498.
- Benjamin, M. M. 2002 *Water Chemistry*. New York, NY.
- Edwards, M. & Benjamin, M. M. 1989 Adsorptive filtration using coated sand: a new approach for treatment of metal-bearing wastes. *J. Water Pollut. Fed.* **61**(9), 1523-1533.
- Elimelech, M. & O'Melia, C. R. 1990 Kinetics of deposition of colloidal particles in porous media. *Environ. Sci. Technol.* **24**(10), 1528-1536.
- Hu, C., Liu, H., Qu, J., Wang, D. & Ru, J. 2006 Coagulation Behavior of Aluminum Salts in Eutrophic Water: Significance of Al₁₃ Species and pH Control. *Environ. Sci. Technol.* **40**(1), 325-331.
- Lukasik, J., Cheng, Y.-F., Lu, F., Tamplin, M. & Farrah, S. R. 1999 Removal of microorganisms from water by columns containing sand coated with ferric and aluminum hydroxides. *Water Research* **33**(3), 769-777.
- O'Melia, C. 1980 ES&T Features: Aquasols: the behavior of small particles in aquatic systems. *Environ. Sci. Technol.* **14**(9), 1052-1060.
- Ongerth, J. E. and J. P. Pecoraro (1996). Electrophoretic Mobility of Cryptosporidium Oocysts and Giardia Cysts. *Journal of Environmental Engineering* **122**(3), 228-231.
- Pernitsky, D. J. & Edzwald, J. K. 2006 Selection of alum and polyaluminum coagulants: principles and applications. *Journal of Water Supply: Research and Technology* **55**(2), 121-141
- Scholtz, E. C., Feldkamp, J. R., White, J. L. & Hem, S. L. 1985 Point of zero charge of amorphous aluminum hydroxide as a function of adsorbed carbonate. *Journal of Pharmaceutical Sciences* **74**(4), 478-481.
- Snoeyink, V. L. & Jenkins, D. 1980 *Water Chemistry*. John Wiley & Sons, Inc.
- Standard Methods for the Examination of Water and Wastewater 1998 17th edition., American Public Health Association/American Water Works Association/Water Environment Federation, Washington DC
- Tchobanoglous, G., Burton, F. L. & Stensel, H. D. 2003 *Wastewater Engineering Treatment and Reuse*.

Van Benschoten, J. E. & Edzwald, J. K. 1990 Chemical aspects of coagulation using aluminum salts--I. Hydrolytic reactions of alum and polyaluminum chloride. *Water Research* **24**(12), 1519-1526.

Weber-Shirk, M. (2008). "An Automated Method for Testing Process Parameters"
<https://confluence.cornell.edu/display/AGUACLARA/Process+Controller>

Weber, W. J. 1972 *Physicochemical Processes for Water Quality Control*

Yao, K.-M., Habibian, M. T. & O'Melia, C. R. 1971 Water and waste water filtration. Concepts and applications. *Environ. Sci. Technol.* **5**(11), 1105-1112.

CHAPTER 3

Enhanced Particle Capture through Aluminum Hydroxide Addition to Pores in Sand Media *

3.1 Abstract

In this study, precipitation of $\text{Al}(\text{OH})_{3(\text{am})}$ was used to modify a sand filter medium by fluidized-bed pretreatment. A mixture of alum, sodium hydroxide, and tap water was applied to the filter bed in the last stage of the backwash cycle. The placement of $\text{Al}(\text{OH})_{3(\text{am})}$ in the filter pores was evaluated for both an alum treated raw water (contact filtration) and as an alternative treatment technique in which the raw water was untreated prior to filtration. A filter that was pretreated with $\text{Al}(\text{OH})_{3(\text{am})}$ achieved better than 99.98% removal of an untreated clay suspension with the effluent turbidity below the detection limit of 0.01 NTU. $\text{Al}(\text{OH})_{3(\text{am})}$ pretreated filters that were challenged with clay and humic acid achieved $\geq 99.8\%$ turbidity removal efficiency for 14 hours of operation in the contact filtration mode. Pretreatment with $\text{Al}(\text{OH})_{3(\text{am})}$ also enhanced turbidity removal efficiency (up to 99.8%) when challenged with clay and humic acid even when the raw water was not coagulated. The head loss from filtration of a clay and humic acid suspension that was not coagulated was 36 cm after 48 hours while the head loss by contact filtration was 160 cm. The Al concentration in the effluent of an $\text{Al}(\text{OH})_{3(\text{am})}$ pretreated filter was below the maximum EPA secondary drinking water MCL (i.e., 200 $\mu\text{g/L}$ for Al) when the raw water pH was between 6 and 7, and the pretreated filter had the best performance at pH 6.

* The contents of this chapter have been submitted for publication with co-authors L. Lion and M. Weber-Shirk.

Keywords: Rapid sand filter, fluidized-bed pretreatment, $\text{Al}(\text{OH})_{3(\text{am})}$, contact filtration

3.2 Introduction

Filtration is a fundamental unit process that is commonly used to remove particulate matter in treatment of drinking water. Rapid sand filtration was introduced in the United States in the 1880s and has been widely used following treatment of source waters by chemical coagulation, flocculation, and sedimentation processes.

During the operational cycle of conventional rapid filtration, which typically ranges from 12 to 96 hours, three distinct phases can be distinguished: (1) A ripening stage, at the beginning of the filter run, characterized by low head loss and low particle removal. The duration of the ripening period in rapid sand filters with properly pretreated water ranges from 5 to 10 minutes (McGhee 1991). (2) A working stage during which the filter performance is optimal and the head loss gradually increases. A particle removal efficiency of ~90% is typical during this stage (personal communication, based on data provided by Mr. Chris Bordlemay, Manager of the Cornell Water Filtration Plant). (3) A breakthrough stage during which turbidity removal slowly deteriorates and the head loss rapidly accumulates. Typically the maximum head loss is in the range 2.5 to 3 meters (Letterman 1999; Gitis, Adin et al. 2002).

Several researchers have studied the addition of coagulants to the backwash water to reduce the magnitude and duration of the filter ripening. Studies conducted by Yapijakis (1982) have shown that adding small amount of nonionic polymer (0.05~0.15 mg/L) to backwash water reduced the initial turbidity from 0.8 to 0.32 NTU. Cranston and Amirtharajah (1987) evaluated the effects of low concentrations

of alum (0~58 mg/L as alum) and polymer (0~3 mg/L as polymer) that were added to backwash water. These treatments resulted in a 75% reduction in effluent turbidity during the initial 20 minutes.

In the research described in this paper, we develop a fluidized-bed pretreatment process, by the addition of concentrated $\text{Al}(\text{OH})_{3(\text{am})}$ (3.3~10 g/L as alum; i.e., ~170 times higher than concentrations used in the studies described above), to artificially modify a sand filter medium. Pretreatment is performed during the end of backwash cycle while the sand bed is still fluidized. Unlike the pretreatment techniques developed previously that improved performance during the first few minutes of operation, the application is shown below to significantly improve the particle capture efficiency for several hours

Alum ($\text{Al}_2(\text{SO}_4)_3 \cdot 14\text{H}_2\text{O}$) and polyaluminum chloride (PACl) are both widely used coagulants in water treatment. PACl has been reported to be superior to alum in removal of particles with advantages of reduced alkalinity consumption, less sludge production, decreased temperature and pH dependence, and reduction of cost (Hu et al. 2006). We selected alum, however, as the pretreatment agent because the solubility of dissolved aluminum (Al) for alum is less than that of PACl (Van Benschoten and Edzwald 1990). Figure 3-1 shows the reported concentration of dissolved Al in equilibrium with precipitated alum and PACl in deionized water at 25°C. Alum has a broader range of pH values (5.5~7.5) over which the EPA secondary drinking water standard can be met.

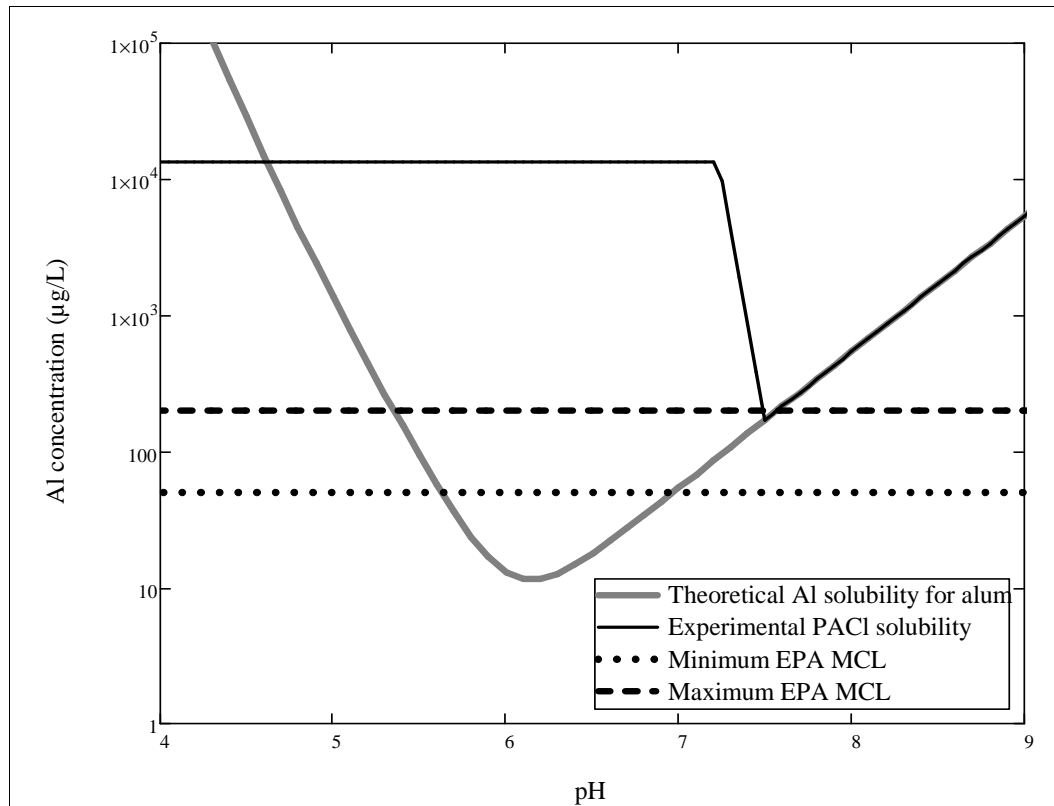


Figure 3-1. Dissolved Al concentration in equilibrium with precipitated alum and PACl in deionized water at 25°C (Van Benschoten and Edzwald 1990). The two horizontal lines present the minimum and maximum EPA secondary drinking water MCL (i.e. 50~200 µg/L) for Al.

Humic substances are reported to reduce particle capture by porous media filters (Franchi and O'Melia 2003). Humic substances constitute a major fraction (40~60%) of dissolved organic matter in natural aquatic systems (Gjessing 1976). In addition to their detrimental effect on filtration, humic substances are undesirable in a potable water supply for a number of reasons, ranging from aesthetics to the fact that they are precursors of potentially carcinogenic disinfection byproducts (trihalomethanes) (Suffet and MacCarthy 1989). Humic substances have properties of anionic polyelectrolytes and carry weakly acidic functional groups, including carboxylic and phenolic groups (Gjessing 1976). Dissolved aquatic humic substances, which are

negatively charged macromolecules because of the ionization of those acidic functional groups, can adsorb onto the surface of clay and other natural particles, further increasing their negative charge (Pernitsky and Edzwald 2006). In this research we utilized commercial humic acid (HA) as a surrogate to represent humic substances in the synthetic raw water and evaluated the effect of HA on particle removal by an untreated and $\text{Al}(\text{OH})_{3(\text{am})}$ -pretreated sand filter.

3.3 Materials and Methods

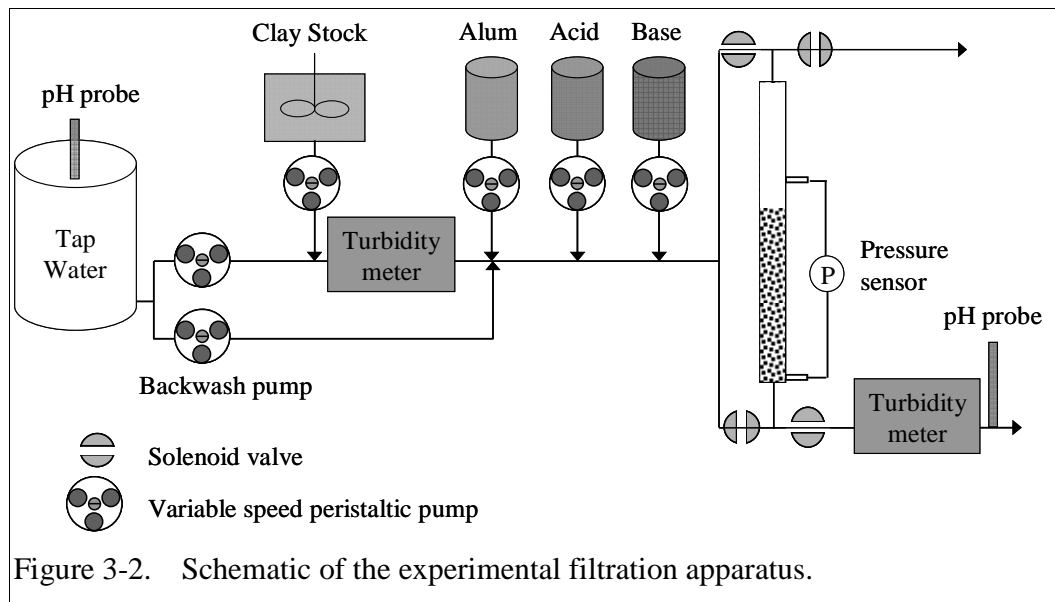
3.3.1. Filtration apparatus

A schematic of the research apparatus used is presented in Figure 3-2. Process Controller software for automation of test apparatus and experiments (Weber-Shirk 2008) was used to conduct parametric tests. All chemical reagents and synthetic raw waters were introduced into the filter by computer controlled digital peristaltic pumps (Masterflex, Cole-Parmer, USA). The filter column, 1.2 m long and 2.5 cm inside diameter, contained 60 cm of 0.45 to 0.55 mm diameter sand with a uniformity coefficient of 1.65 and porosity of 0.4 (Ricci Bros. Sand Company Inc, New Jersey, USA). The filter was precisely leveled to ensure uniform flow through the bed during backwash and operated at a constant flow rate of 1.4 mm/s (0.68 mL/s) when in downward flow. Head loss was measured with a differential pressure sensor connected to the top and bottom of the filter. Tap water pH and the effluent pH were monitored as well.

The filter performance was monitored by inline turbidimeters (Micro TOL, HF Scientific, Inc.) (Figure 3-2). The turbidimeters were chosen because they have small volume sample cells (30 mL) that make it possible to achieve reasonable response times at the flow rates used in this research. We do not report the data from the first

1.5 hydraulic residence times (i.e., about 20 minutes) at the beginning of each the particle challenge since those data show an artificially high particle removal caused by the clean pore water that is still exiting the filter into the effluent turbidimeter and being displaced from the tubing and turbidimeter sample vial.

All data including turbidity, head loss, and pH were logged at 5 second intervals. Particle capture efficiency is expressed here as pC^* where C^* is the turbidity of the effluent water in Nephelometric Turbidity Units (NTU) normalized by the turbidity of the influent water and p is the negative logarithm (base 10) (i.e., $pC^* = -\log(C_{\text{effluent}}/C_{\text{influent}})$). pC^* is the negative logarithm of the fraction of influent turbidity remaining in the effluent and is identical to what is often referred to as the log “removal” in some filtration research.



3.3.2. Fluidized-bed pretreatment of filter media

Prior to challenging the filter with a suspension of colloidal particles, 60 g/L alum (Fisher Scientific), 0.55 mole/L of sodium hydroxide solution (Fisher Scientific), and Cornell University tap water (22°C, pH ≈ 8, total organic carbon ≈ 2.0 mg/L, hardness

≈ 150 mg/L as CaCO_3 , alkalinity: ≈ 110 mg/L as CaCO_3 , chlorine residual ≈ 0.7 mg/L) were rapidly mixed in the tubing to generate amorphous Al hydroxide precipitate at a neutral pH of 7.5 and pumped upward through the filter. The pretreatment flow rate was 7.5 mL/s and occurred at the end of backwash cycle while the sand bed was fluidized. The corresponding upflow velocity was 15 mm/s and the bed was expanded 50%. The volume ratio of alum and NaOH was 1 to 1, and the alum and base pump flow rates were varied to achieve different pretreatment doses. The pretreatment time was set to 14 seconds so that all the $\text{Al}(\text{OH})_{3(\text{am})}$ remained within the fluidized sand (i.e., no floc breakthrough occurred above the sand bed). The hydraulic residence time between the alum and sodium hydroxide injection points and the bottom of the filter column was 3 seconds. Thus $\text{Al}(\text{OH})_{3(\text{am})}$ was pumped into the filter for 11 seconds at 15 mm/s. Retention of the alum input within the fluidized bed was verified visually using a dyed alum feed stock. Three different dosages of Al (8, 15, and 23 mol Al/m³ of pore volume) were applied to the filter. Expressing the dose in these units facilitates generalization of the experimental results to other filter bed sizes. The Al concentrations in the pretreatment feed before injecting into the filter were 11, 22, and 33 mol Al/m³ (corresponding to 3.3, 6.7, and 10 g/L as alum). The difference in these two alternative concentrations is caused by fact that the pretreatment volume was approximately 70% of the filter pore volume. Al dosages expressed below are on a per pore volume basis.

After pretreatment, the test filter bed was compacted by a vibrator to ensure a uniform filter height for each test, and clean tap water was passed through the filter in a downward flow for two hydraulic retention times of the sand bed (i.e., 2 x 3 minutes) to remove dissolved aluminum species and unattached precipitated $\text{Al}(\text{OH})_{3(\text{am})}$ from the filter.

3.3.3. Filter operation

In all filtration studies Cornell University tap water was used as the raw water source. Kaolin clay (R.T. Vanderbilt Company, Inc., Connecticut), was used as a source for turbidity, and a commercial humic acid sodium salt (molecular weight: 2000~500,000, chemical formula: $C_9H_8Na_2O_4$, Aldrich Chemical Company, Inc.) was selected as a surrogate for natural organic matter (NOM). The properties of commercial humic materials are expected to differ from those of any individual source of natural dissolved organic matter (Suffet and MacCarthy 1989); however, use of commercial humic acid was adopted to facilitate the ability to reproduce our experiments. The humic acid and clay were mixed with distilled water as a 7x concentrated stock (pH = 4.3) and then diluted with tap water to achieve a desired influent turbidity and humic acid concentration. The pH of this synthetic raw water was similar to the pH of the tap water. The clay particle size was heterodisperse with diameters ranging from approximately 1 to 3 μm as measured by dynamic light scattering (Malvern Zetasizer Nano-ZS) and by light microscopy. Process Controller (Weber-Shirk 2008) was used to control the tap water pH by metering a stock solution of 0.5 mole/L of nitric acid (trace metal grade, Fisher Scientific). The pH of filter effluent was similar to that of the raw water because the pH of the combined alum and sodium hydroxide feeds were set to be close to the desired raw water pH. The filtration rate was held constant at 1.4 mm/s in all experiments. Between each test, the sand medium was backwashed with approximately 60% volumetric expansion for 8 minutes at an upflow velocity of 22 mm/s, followed by an 2.5 mm/s downflow acid wash (0.1 M HCl) for 6 minutes to dissolve and remove $Al(OH)_{3(am)}$, followed by another 8 minute backwash to remove acid and any residual clay.

3.3.4. Measurement of Al concentrations in the effluent water during challenge

Al concentrations in the effluent were measured during a 12 hour challenge with the highest pretreatment dose of 23 mol Al/m³ (injected concentration = 10 g/L as alum) at pH 6, 7, and 8. The effluent was sampled every 5 minutes for the first half hour and then was sampled at 2 hour intervals.

A colorimetric assay, the modified Eriochrome Cyanine R Method (Standard Methods for the Examination of Water and Wastewater, 1998), was selected for Al analysis. The volume of reagents and samples were scaled to fit into 4.5 mL cuvettes. The assay can detect aluminum at concentrations above 20 µg/L. All glassware used was first acid washed for 24 hours with 10% nitric acid (Reagent grade, Fisher Scientific) made with distilled deionized (DDI) water followed by a 24 hour wash in 10% nitric acid (trace metal grade, Fisher Scientific). The glassware was rinsed with DDI water 6 times in between the 24 hour wash steps. An aluminum standard (1,000 ppm, Ricca Chemical Company) was used to prepare Al standard curves.

3.3.5. Wall and thickness effects

The cylindrical container used to hold a packing of particles will induce a local area of order at the container wall in an otherwise random packing. This will make both micro- and macro-structural properties of particles near the wall different from those away from the wall. This is known as the “wall effect” and usually is characterized by a change in porosity (Zou and Yu 1995). Generally, the wall effect consists of two components, namely the effect of the side wall and the effect of the top and/or bottom filter boundaries. The latter is dependent on the height of the packed media and is referred to as the thickness effect (Zou and Yu 1995).

Because of wall effects, the porosity (ϵ) will be dependent on not only the ratio of the particle diameter (d) to the container diameter (D), but also the ratio of the particle diameter to the media depth (H). In this study, the sand and filter column diameter were 0.5 and 25 mm, respectively (i.e. $d/D = 0.02$), and the depth of sand media was 600 mm (i.e. $d/H = 8.3 \times 10^{-4}$). At these ratios the porosity for both loose and dense packing is almost the same as the original porosity (Zou and Yu 1995). Thus, wall and thickness effects did not significantly affect the porosity in our filtration studies.

3.4 Results and Discussion

3.4.1. Effect of humic acid on performance of an untreated and $\text{Al}(\text{OH})_{3(\text{am})}$ -pretreated filter

A kaolin clay suspension (~60 NTU) without and with HA (0.5 mg/L as mass of organic matter) was used as raw water ($\text{pH} = 8 \pm 0.2$) to challenge the untreated and $\text{Al}(\text{OH})_{3(\text{am})}$ -pretreated filters. In initial experiments, a relatively high influent turbidity of ~60 NTU was used to ensure that significant differences in particle concentration could be accurately measured and so that we could use a shorter run time and still obtain substantial particle loading in the filter. Results from experiments at two different clay concentrations (~5 and ~60 NTU) showed that a ~10 fold variation in turbidity did not cause significant difference in the performance of an alum-pretreated filter (see Figure A-9 in Appendix A.4.1) and an untreated filter (data not shown). No raw water pretreatment such as coagulation, flocculation and sedimentation was employed before filtration. As a result, the experimental conditions differ from conventional water treatment practice. Thus, the initial experimental results show the effect of modifying porous media properties on an inorganic colloid that has not had its properties altered by coagulants. Experimental results also evaluate the impact on head loss that can be achieved by pretreating a filter during the backwash cycle. Below

we also report results using low influent turbidity (~5 NTU) to simulate the influent concentrations more commonly encountered in conventional water treatment plants.

Figure 3-3 shows the particle removal over time by the pretreated and untreated filter in the presence and absence of 0.5 mg/L humic acid. The pretreatment Al dose was 23 mol Al/m³ (injected concentration = 10 g/L as alum). Particle removals as high as 97 to 99% (pC* from 1.5 to 2) and 99.98% (pC* = 3.7) for untreated (gray squares) and pretreated filter (gray triangles), respectively, were attained in the absence of HA. The particle removal for the untreated filter (gray squares) increased over time. It is likely that accumulation of captured clay was responsible for a slight change in pore geometry or that captured particles acted as collectors themselves. However, filter performance (as pC*) was reduced by more than 1 for both types of filters in the case where the influent contained HA. The effluent turbidity for the pretreated filter challenged with clay in the absence of HA was below the detection limit of the turbidimeter (0.01 NTU) during the entire filter run except at a few sample times when gas bubbles in the effluent are thought to have registered as turbidity spikes. Effluent turbidity below detection was assumed to be the detection limit (0.01 NTU) to permit calculation of a minimum achieved value of pC*. A considerable deterioration of particle removal efficiency resulted from the presence of 0.5 mg/L HA. The effect of HA on particle capture is assumed to be caused by adsorption of negatively charged HA on both suspended particles and the filter media resulting in electrostatic and steric contributions of HA to the repulsive interaction energy (Franchi and O'Melia 2003).

The experimental results show that particle removal was significantly improved in the pretreated filter compared to the untreated filter and that the agreement of filter performance in replicate experiments was excellent. Close replication of results also

indicates that the filter medium was not influenced by irreversible retention of remnant particles after backwash, a phenomenon that can impact filter performance. In subsequent experiments described below, clay suspensions with humic acid were used as raw water.

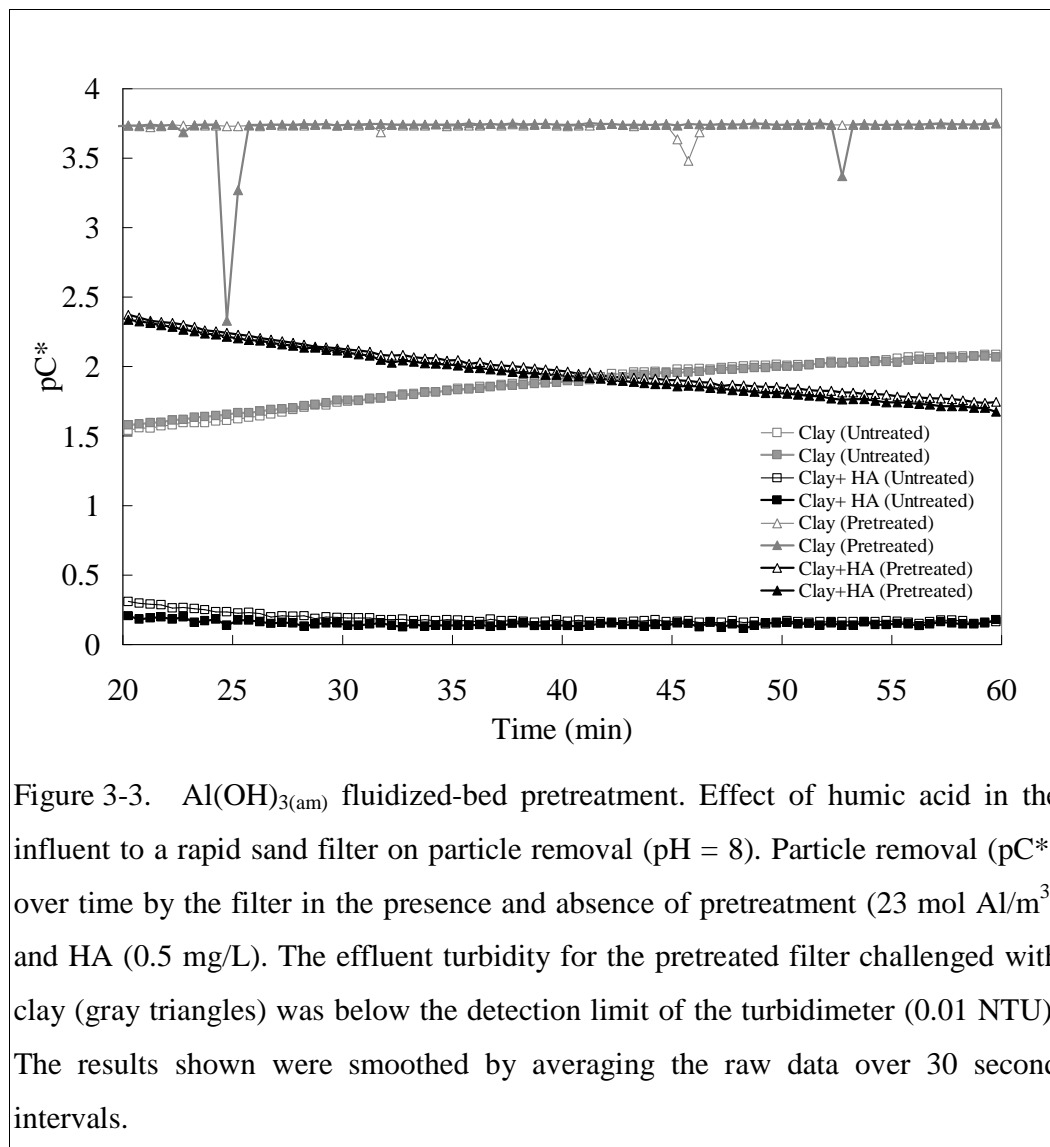


Figure 3-3. $\text{Al}(\text{OH})_{3(\text{am})}$ fluidized-bed pretreatment. Effect of humic acid in the influent to a rapid sand filter on particle removal (pH = 8). Particle removal (pC^*) over time by the filter in the presence and absence of pretreatment (23 mol Al/m^3) and HA (0.5 mg/L). The effluent turbidity for the pretreated filter challenged with clay (gray triangles) was below the detection limit of the turbidimeter (0.01 NTU). The results shown were smoothed by averaging the raw data over 30 second intervals.

3.4.2. Turbidity removal efficiency and head loss profile for alternative fluidized-bed pretreatments

Turbidity removal (pC^*) over time as a function of different pretreatment Al doses is shown in Figure 3-4. The influent synthetic raw water used contained turbidity of ~ 60

NTU, 0.5 mg/L of HA, and pH was 8. Each pretreatment dosage was replicated except the control experiment (0 mol Al/m³). Removal efficiency increased with increasing pretreatment dosage and the highest pretreatment dose resulted in excellent particle removal (99.6 to 98% during a one hour filter run) compared to the untreated filter (36% removal). While it may appear that turbidity removal could increase at even higher pretreatment doses, an Al dose of 24 mol/m³ (injected concentration = 10.4 g/L as alum) resulted in the generation of gelatinous aluminum hydroxide that caused our laboratory-scale filter clog. Thus, the maximum pretreatment dose was 23 mol Al/m³ (injected concentration = 10 g/L as alum).

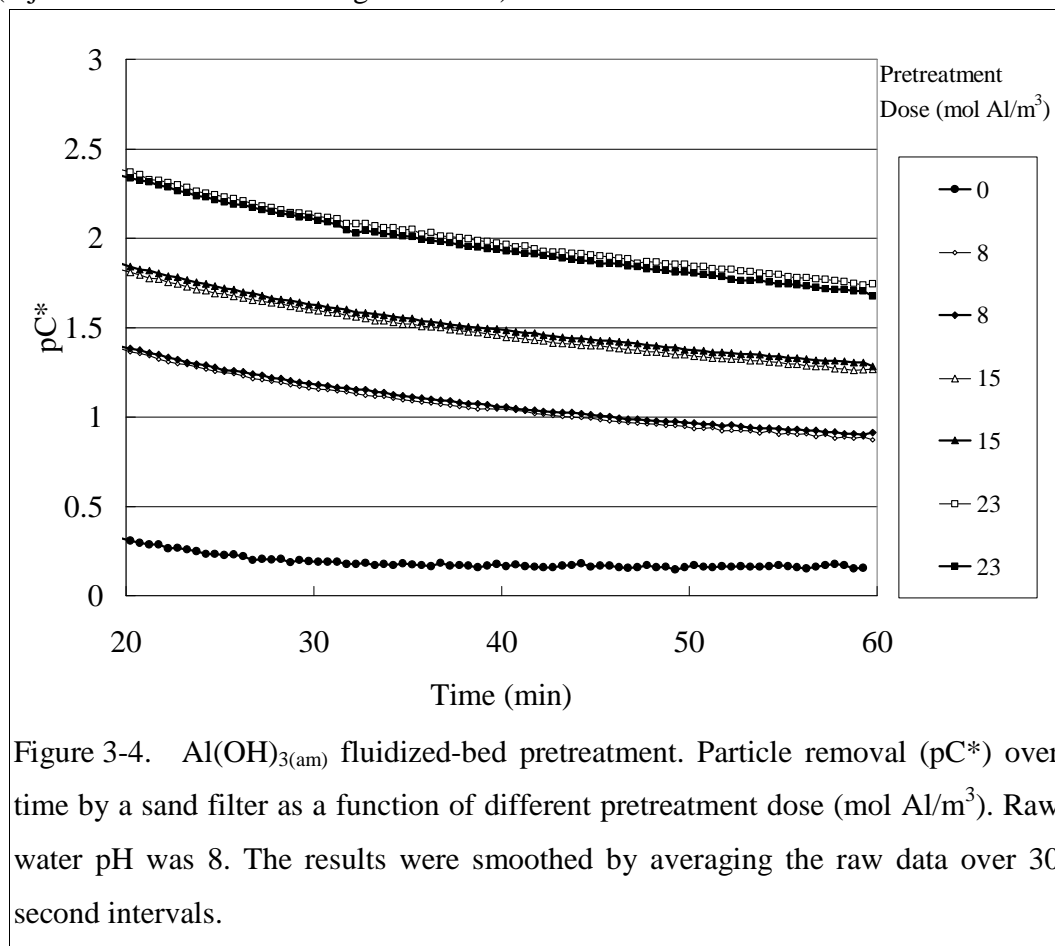
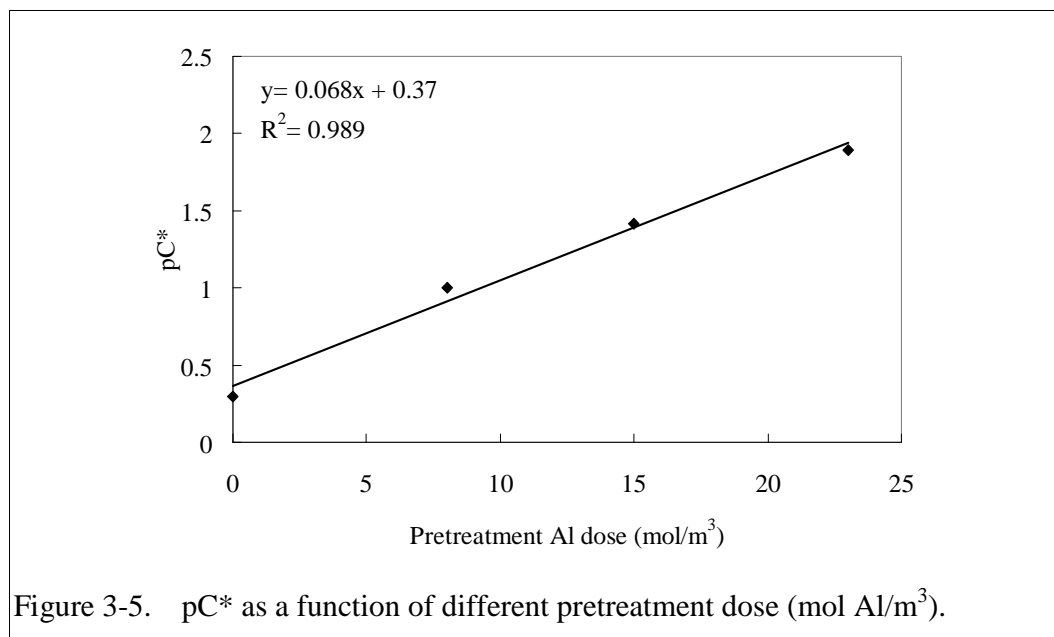


Figure 3-5 presents the performance, pC*, as a function of pretreatment dose in which pC* values shown are for a 10 minute average centered at the 45th minute (i.e.,

average of the data from 40 to 50 minutes) and then averaged with the result of the replicate experiment. The improvement in pC^* was directly proportional to pretreatment Al doses. Two mechanisms are hypothesized to explain the linear improvement in the filter efficiency with Al dose: (1) Positively charged or circumneutral $Al(OH)_{3(am)}$ attached to the negatively charged sand grains may enhance the particle-grain attachment efficiency by reducing Coulombic repulsion of negatively charged colloidal clay (Figure 3-6 (a)). The point of zero charge (PZC) of amorphous aluminum hydroxide is 9.6 (Scholtz, Feldkamp et al. 1985) and the isoelectric point (i.e.p.) in the presence of sulfate is reported to be close to 8 (Van Benschoten and Edzwald 1990). (2) $Al(OH)_{3(am)}$ flocs embedded within the filter pores acted as filters to increase the particle capture efficiency (Figure 3-6 (b)). It is also possible that a combination of both mechanisms was involved.



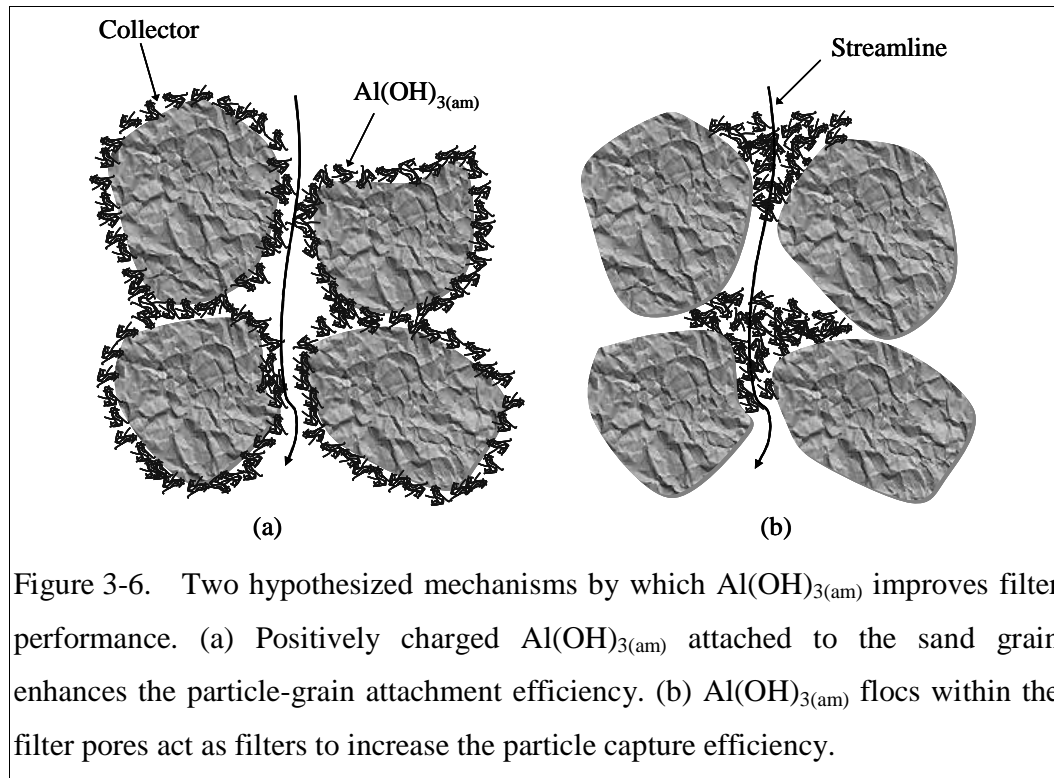
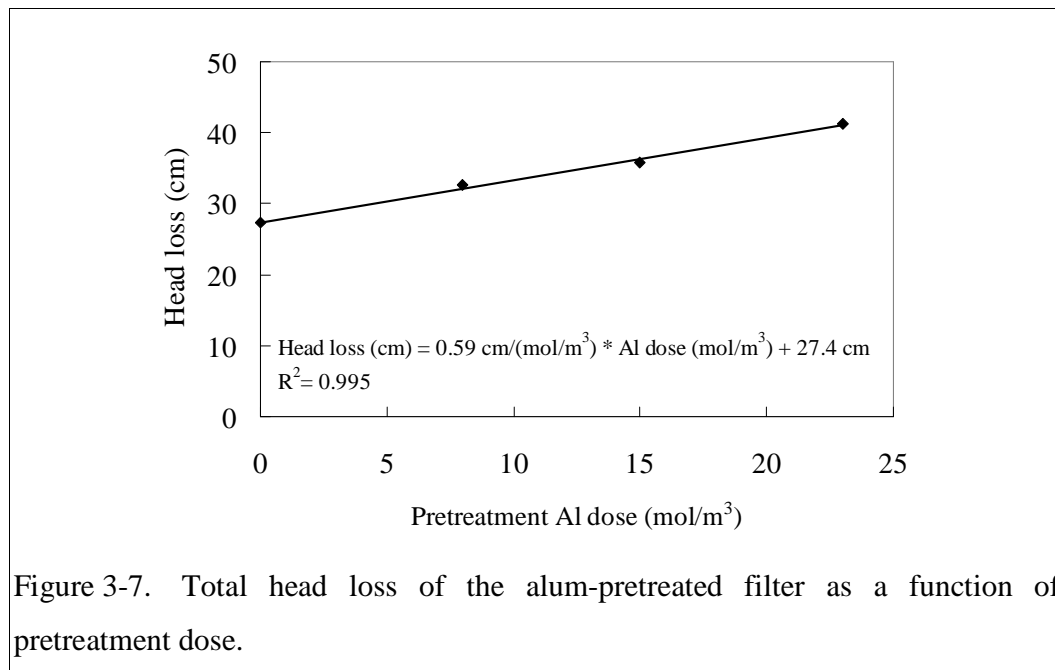


Figure 3-6. Two hypothesized mechanisms by which $\text{Al(OH)}_{3(\text{am})}$ improves filter performance. (a) Positively charged $\text{Al(OH)}_{3(\text{am})}$ attached to the sand grain enhances the particle-grain attachment efficiency. (b) $\text{Al(OH)}_{3(\text{am})}$ flocs within the filter pores act as filters to increase the particle capture efficiency.

Pressure measurement across the filter bed was used to monitor changes in head loss during experiments. Addition of alum into the filter during pretreatment resulted in increased head loss during the challenge. The head loss after fluidized-bed pretreatment is plotted against the corresponding pretreatment Al dose (Figure 3-7). The values shown are for a 10 minute average centered at the 45th minute and then averaged with the result of the replicate experiment (i.e., same data analysis and time period as Figure 3-5). The magnitude of head loss accumulation was proportional to the pretreatment dose. At the highest applied Al dose (i.e., 23 mol/m³) the head loss increase relative to untreated sand was ≈ 14 cm or 0.025 m head loss/(mol Al/m² of filter bed area). In prior experiments using downflow pretreatment with alum, $\text{Al(OH)}_{3(\text{am})}$ accumulated at the top of the filter media and caused 0.21 m head loss/(mol Al/m² of filter bed area) (see Chapter 2). Thus upflow application reduced the head loss due to accumulation of $\text{Al(OH)}_{3(\text{am})}$ by a factor of 8. These results

indicate that fluidized-bed pretreatment can enhance filter performance while adding only a small additional head loss that is very unlikely to interfere with operation in full-scale plants. After upflow pretreatment only a small increase (<1 cm) in head loss was observed after 1 hour of treatment of a raw water with ~60 NTU. Assuming head loss reflects filling of pores in the sand media, this result indicates that the space occupied by the Al hydroxide precipitate in the filter pores was much larger than the volume of clay particles that accumulated.



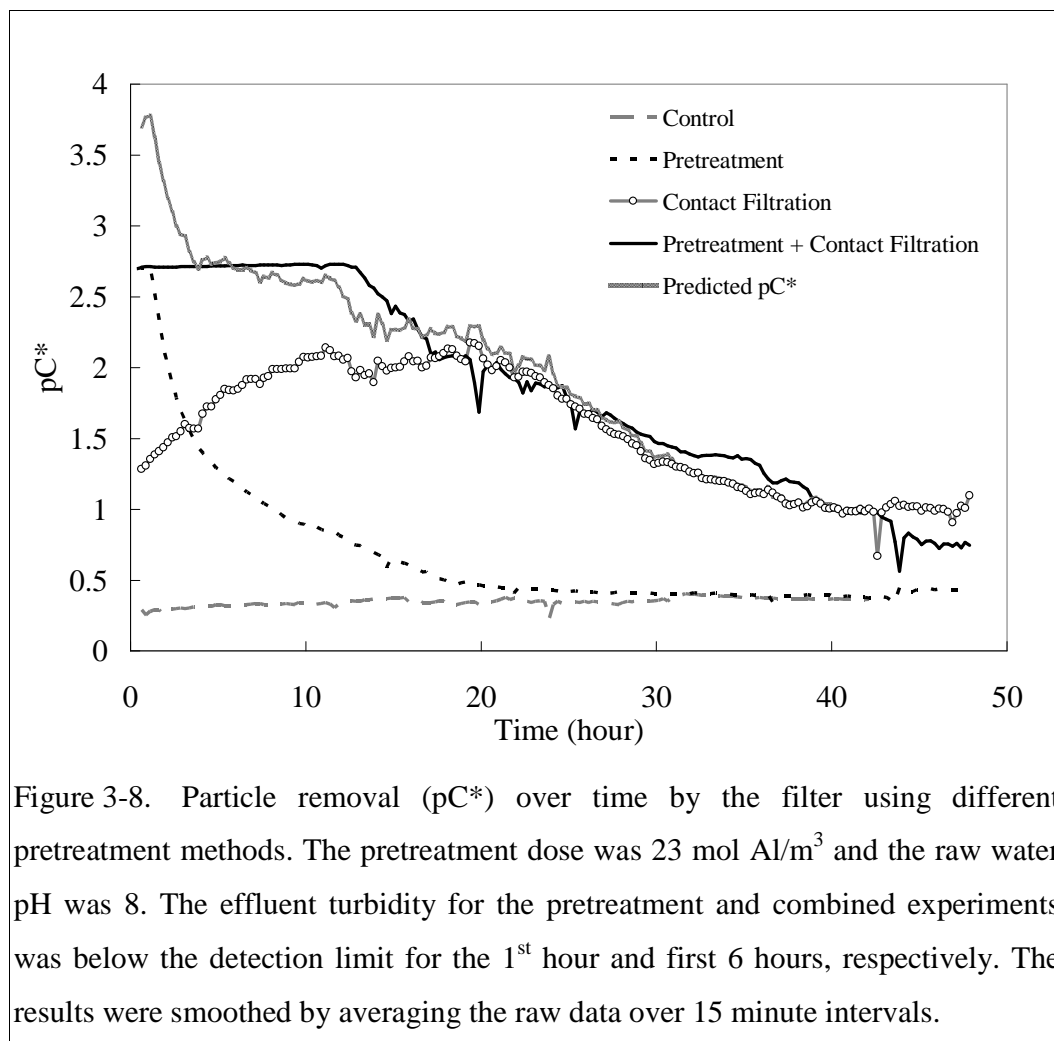
3.4.3. Long term experiments

In full-scale water treatment plants the influent turbidity of rapid sand filters is typically less than 5 NTU, and the operation time ranges from 1 to 4 days. To better simulate these conditions a ~5 NTU clay suspension with 0.5 mg/L of HA was used as the raw water and the experimental filter was challenged for 48 hours. Four experiments were conducted: (1) Filtration without pretreatment (control); (2) Fluidized-bed pretreatment with 23 mol Al/m³; (3) Contact filtration of alum treated clay by an untreated filter bed. The alum (7 mg/L as alum during coagulation) was

mixed with the raw water prior to filtration, and the total alum applied was equal to the 23 mol Al/m³ dose applied in fluidized-bed pretreatment. The reader is cautioned that 7 mg/L as alum was not the optimal dose for contact filtration; the selected dosage was used to match the total mass of aluminum used in the pretreatment experiment. Filtration of alum treated clay is what is typically practiced in conventional water treatment. (4) Combination of pretreatment and contact filtration (total Al dose applied was 46 mol/m³).

Figure 3-8 shows particle removal over 48 hours by the filter using four test conditions. The control experiment (gray dashed line) had a pC* of 0.3 (50% removal) which provided a baseline for filtration without pretreatment. The effluent turbidity after Al(OH)_{3(am)} pretreatment of the filter (black dashed line) was below detection during the 1st hour of operation. A turbidity equal to the detection limit of 0.01 NTU (i.e., equal to 99.8% removal) was assumed for purposes of calculating a low estimate of pC* during this time interval. Performance of the Al(OH)_{3(am)}-pretreated filter started to decline after 1.5 hour and reached the base line (control) at the 30th hour. In contact filtration of alum treated clay (circles) the removal efficiency started at 95%, improved to 99% after 20 hours of operation and then deteriorated. A pC* of 1 was observed after 48 hour operation (effluent turbidity ≈ 0.6 NTU). Comparing these two experiments, the pretreatment experiment had better particle removal for the first 4 hours of operation than contact filtration. This result indicates that pretreating the filter with Al(OH)_{3(am)} helped eliminate the poor performance during the initial period in contact filtration. Combining pretreatment with contact filtration (black solid line) we obtained 99.8% removal efficiency for 14 hours (the effluent turbidity was below the detection limit for the first 6 hours). This result indicates that combining fluidized-bed pretreatment with conventional treatment can substantially improve particle capture

efficiency. Figure 3-8 also illustrates the predicted pC^* curve obtained by adding pC^* of pretreatment and contact filtration and then subtracting one control value. The predicted curve agrees well with the observations for the combined experiment except during the first 6 hours where the detection limit of the turbidimeter limited observations. This result suggests that the performance measured as pC^* for pretreatment of the sand media and for treatment of the raw water are additive.



Head loss during the above four experiments is presented in Figure 3-9. Head loss development in the control was negligible. Head loss decreased over time in the pretreatment experiment because of slow dissolution of applied Al hydroxide

precipitate (further discussion is provided below). The head loss in the contact filtration and combined experiment after 48 hours was 160 and 180 cm, respectively, and the head loss generation rate was linear and proportional to the applied alum during contact filtration. When the filter was operated in contact filtration mode, the coagulated particles and Al hydroxide precipitates deposited on the top layer of filter bed and consequently a high head loss developed. A predicted head loss for the combined experiment was obtained by adding head loss of pretreatment and contact filtration and then subtracting one control value. The predicted head loss was slightly lower than that observed after 10 hours. This decrease is associated with the decreasing head loss observed during the pretreatment experiment which is hypothesized to result from dissolution of precipitated $\text{Al}(\text{OH})_{3(\text{am})}$ in the pore space. In the combined experiment, the top of filter received an input of dissolved Al which was at a concentration dictated by equilibrium with $\text{Al}(\text{OH})_{3(\text{am})}$. As a result dissolution of the $\text{Al}(\text{OH})_{3(\text{am})}$ present from pretreatment was inhibited, resulting in a higher head loss than that predicted.

The combination of fluidized-bed pretreatment and contact filtration resulted in a greater particle removal for the first 14 hours of operation than is typical for rapid sand filters. The experimental results suggest that the filter should have been backwashed with additional pretreatment after 30 hours of operation to maintain the quality of the effluent. Under the conditions of this study the filter was able to remove >96% of influent particles for the first 30 hours. The effluent turbidity increased to 0.18 NTU and the observed head loss reached 1.1 m after 30 hours. These values would be practical for most filtration plants. For a filter run of 14 hours the effluent turbidity was less than 0.01 NTU and the observed head loss was only 70 cm.

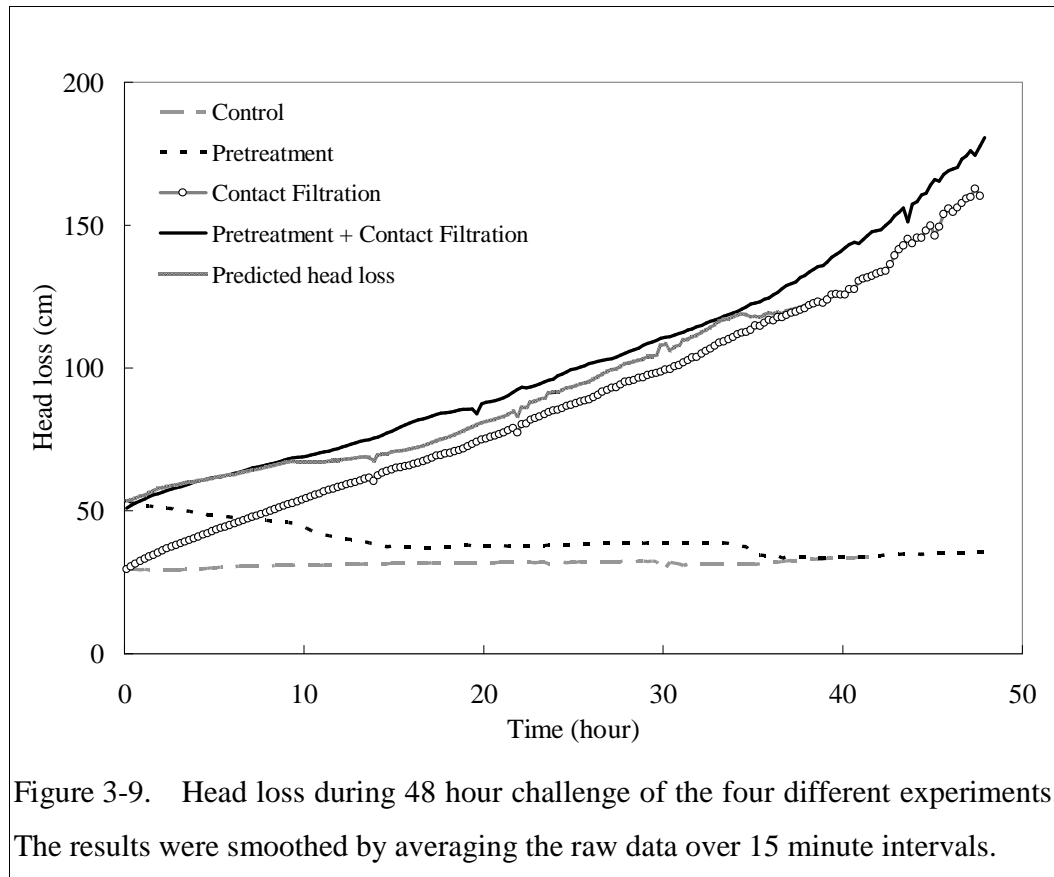


Figure 3-9. Head loss during 48 hour challenge of the four different experiments. The results were smoothed by averaging the raw data over 15 minute intervals.

3.4.4. Aluminum concentrations in the filtered effluent

It is important to ensure that Al concentrations in the effluent from the $\text{Al(OH)}_{3(\text{am})}$ -pretreated filter are below the EPA secondary MCL (i.e., 50–200 $\mu\text{g/L}$ for Al). The effluent was sampled at the beginning of several experiments at 5 minute intervals for $\frac{1}{2}$ hour, and then at 2 hour intervals up to 12 hours with influent pH values of 6, 7, and 8. At pH 8, Al concentrations in all samples were above the maximum secondary MCL (12-hour averaged concentration: 660 $\mu\text{g/L}$, data not shown), while Al concentrations were below 200 $\mu\text{g/L}$ in most samples at pH 6 and 7 (Figure 3-10). The averaged Al concentrations of these samples (except for 0th minute) were 30 and 90 $\mu\text{g/L}$ for pH 6 and 7, respectively. These values are higher than the theoretical dissolved Al concentration in equilibrium with $\text{Al(OH)}_{3(\text{am})}$ (i.e., 13 and 54 $\mu\text{g/L}$ for pH 6 and 7). Therefore it is likely that Al hydroxide precipitates were flushed out of

the column especially early in a filter run. Release of particulate $\text{Al}(\text{OH})_{3(\text{am})}$ could also explain the high initial Al concentration at 0th minute sample at pH 7. Although these experiments were terminated after 12 hours, the decreasing trend of Al concentrations over time at both pH 6 and 7 suggest that the Al concentration after 12 hours will remain under the EPA secondary drinking water standard.

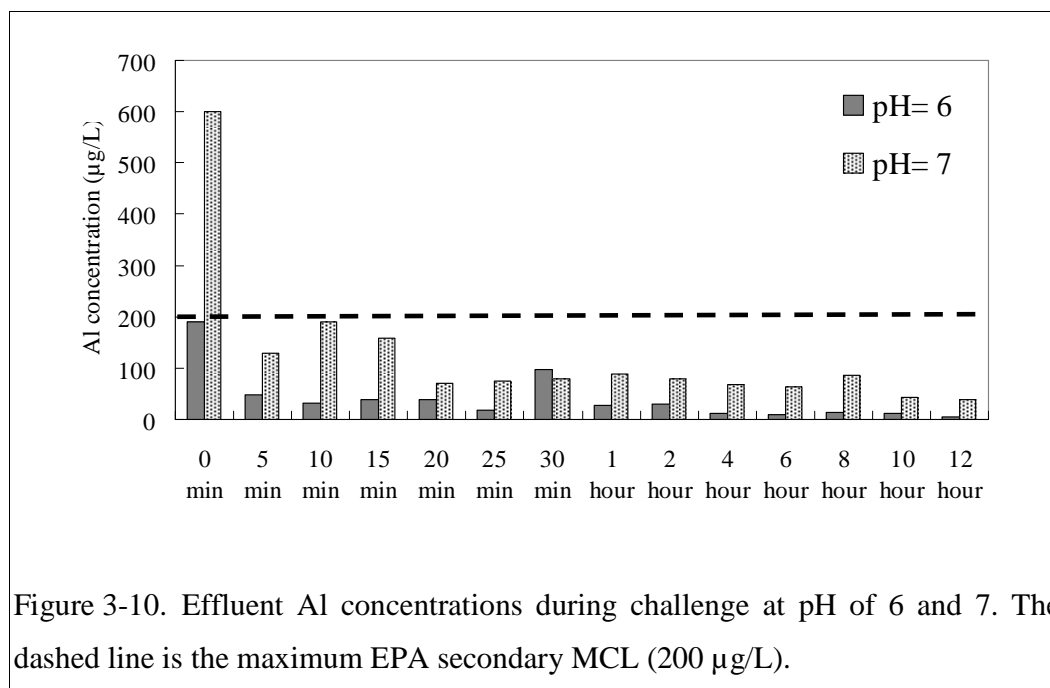


Figure 3-10. Effluent Al concentrations during challenge at pH of 6 and 7. The dashed line is the maximum EPA secondary MCL (200 µg/L).

3.4.5. Effect of influent pH on $\text{Al}(\text{OH})_{3(\text{am})}$ -pretreated filters

Al solubility is pH-dependent and the pretreated filters also appear to have lost $\text{Al}(\text{OH})_{3(\text{am})}$ during operation, particularly at pH 8. Figure 3-11 shows the particle removal by an $\text{Al}(\text{OH})_{3(\text{am})}$ -pretreated filter over 12 hours as a function of influent pH. The raw water contained ~5 NTU turbidity and 0.5 mg/L of HA. The pretreatment dose was 23 mol Al/m^3 . The pretreated filter had the best removal at pH of 6 and followed by 7 and 8. At pH of 6 the effluent turbidity was below the detection limit during the first 3 hours. For the filter operating at pH 7, the effluent turbidity was below the detection limit during the first 2.5 hours. At both pH 6 and 7, the particle removal efficiency was $\geq 94\%$ ($\text{pC}^* \approx 1.2$; effluent turbidity ≈ 0.3 NTU) for 12 hours.

When the influent pH was 8, the effluent turbidity was below the detection limit during the first hour, and the removal efficiency was 85% at the end of filter run. The disparity in particle removal at these pH conditions likely reflected pH dependent solubility of $\text{Al(OH)}_{3(\text{am})}$ (see Figure 3-1). Solubility is highest at pH 8 which corresponds to the poorest observed particle removal. This suggests that the dissolution of $\text{Al(OH)}_{3(\text{am})}$ during challenge may have been one of the mechanisms that caused deterioration of filter performance. At pH 8, 25% of the applied aluminum was calculated to be lost during the 12 hour experiment based on the aluminum solubility. The dissolution of aluminum potentially resulted in the release of clay that had been previously captured by the filter. The decrease of positive charge on $\text{Al(OH)}_{3(\text{am})}$ with increasing pH also may have contributed to poorer performance at higher pH.

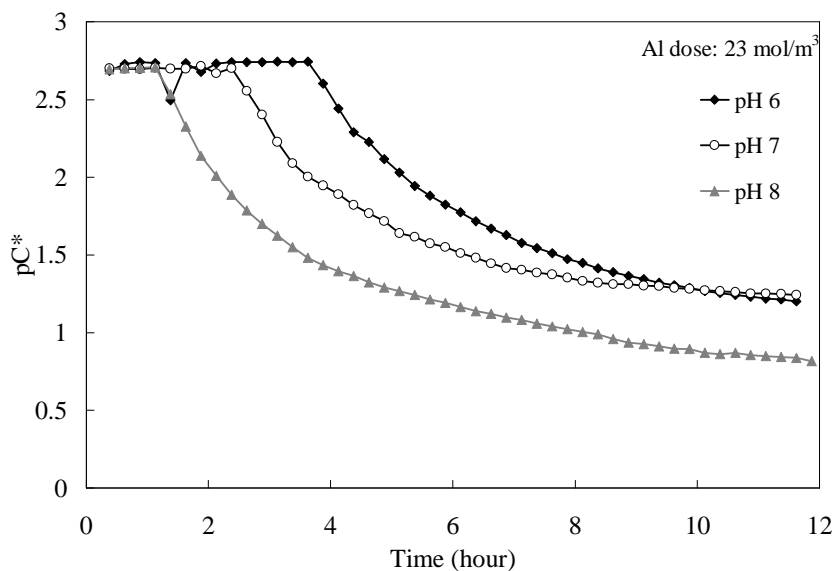


Figure 3-11. Particle removal (pC^*) over time as a function of pH. The pretreatment dose was 23 mol Al/m^3 . The results were smoothed by averaging the raw data over 15 minute intervals.

3.5 Conclusions

An $\text{Al}(\text{OH})_{3(\text{am})}$ -pretreated filter achieved better than 99.98% removal of an untreated clay suspension (~60 NTU) with the effluent turbidity below the detection limit of 0.01 NTU. Consistent with prior observations of the effect of dissolved organic matter on particle removal in filters, the presence of humic acid in the influent decreased particle removal efficiency in both untreated and alum-pretreated filters. The adsorption of humic acid to clay particles and media sand grains is thought to increase the electrostatic repulsion. The fluidized-bed pretreatment substantially improved particle removal efficiency (more than 99% removal) even when the raw water contained 0.5 mg/L humic acid.

Head loss development was directly proportional to the pretreatment Al dose, and at the highest dose of alum (23 mol Al/m^3) fluidized-bed pretreatment only added ≈ 14 cm head loss which is expected to be compatible with application in full-scale conventional water treatment plants. Filter performance measured as pC^* was also directly proportional to the pretreatment Al dose.

The results from the 48 hour filtration experiments showed that $\text{Al}(\text{OH})_{3(\text{am})}$ pretreatment eliminated the initial poor performance compared with an otherwise untreated filter in contact filtration. Moreover, the combination of fluidized-bed pretreatment and contact filtration significantly improved particle removal with greater than 99.8% removal for the first 14 hours and greater than 96% removal for the first 30 hours.

Aluminum solubility is pH-sensitive and influent pH plays an important role in the applicability of fluidized-bed pretreatment. At pH of 8, the Al in the filtered effluent

exceeded the maximum secondary MCL, and the loss of Al during operation at pH 8 or differences in $\text{Al(OH)}_{3(\text{am})}$ surface charge reduced performance relative to that observed at pH of 6 and 7. At pH 6 and 7 Al concentrations in the effluent were below the EPA secondary standard except for the initial sample taken at pH 7. Particle removal at pH 6 was better than that at pH 7 as expected based on the lower solubility of $\text{Al(OH)}_{3(\text{am})}$ at pH of 6. Some of the results of this research (Figure 3-3, Figure 3-4, and Figure 3-8) were obtained at pH 8. Based on the pH dependence of performance presented in Figure 3-11, higher removals in those experiments would be obtained for influents with pH below 8.

3.6 Acknowledgements

The research described in this paper was supported by the U.S. National Science Foundation under Grant CBET-0604566 and by Sanjuan Foundation.

REFERENCES

Cranston, K. O. and A. Amirtharajah (1987). Improving the Initial Effluent Quality of a Dual-Media Filter by Coagulants in Backwash. *Journal / American Water Works Association* 79(12), 50-63.

Franchi, A. and C. R. O'Melia (2003). Effects of Natural Organic Matter and Solution Chemistry on the Deposition and Reentrainment of Colloids in Porous Media. *Environmental Science & Technology* 37(6), 1122-1129.

Gitis, V., A. Adin, A. Nasser, J. Gun and O. Lev (2002). Fluorescent Dye Labeled Bacteriophages--a New Tracer for the Investigation of Viral Transport in Porous Media: 2. Studies of Deep-bed Filtration. *Water Research* 36(17), 4235-4242.

Gjessing, E. T. (1976). *Physical and Chemical Characteristics of Aquatic Humus*. Ann Arbor, Ann Arbor Science.

Hu, C., H. Liu, J. Qu, D. Wang and J. Ru (2006). Coagulation Behavior of Aluminum Salts in Eutrophic Water: Significance of Al_{13} Species and pH Control. *Environ. Sci. Technol.* 40(1), 325-331.

Letterman, R. D. (1999). *Water Quality and Treatment*, American Water Works Association.

McGhee, T. J. (1991). *Water Supply and Sewerage*, McGraw-Hill.

Pernitsky, D. J. and J. K. Edzwald (2006). Selection of alum and polyaluminum coagulants: principles and applications. *Journal of Water Supply: Research and Technology* 55(2), 121-141

Scholtz, E. C., J. R. Feldkamp, J. L. White and S. L. Hem (1985). Point of zero charge of amorphous aluminum hydroxide as a function of adsorbed carbonate. *Journal of Pharmaceutical Sciences* 74(4), 478-481.

Standard Methods for the Examination of Water and Wastewater, 20th ed, 1998 Washington DC American Public Health Association/American Water Works Association/Water Environment Federation.

Suffet, I. H. and P. MacCarthy. *Aquatic Humic Substances*. 1989, American Chemical Society. 131-157.

Van Benschoten, J. E. and J. K. Edzwald (1990). Chemical Aspects of Coagulation Using Aluminum Salts--I. Hydrolytic Reactions of Alum and Polyaluminum Chloride. *Water Research* 24(12), 1519-1526.

Weber-Shirk, M. (2008). An Automated Method for Testing Process Parameters. <https://confluence.cornell.edu/display/AGUACLARA/Process+Controller>.

Yapijakis, C. (1982). Direct Filtration: Polymer in Backwash Serves Dual Purpose. *Journal / American Water Works Association* 74(8), 426-428.

Zou, R. P. and A. B. Yu (1995). The Packing of Spheres in a Cylindrical Container: the Thickness Effect. *Chemical Engineering Science* 50(9), 1504-1507.

CHAPTER 4

Enhanced Filter Performance by Fluidized-Bed Pretreatment with $\text{Al}(\text{OH})_{3(\text{am})}$: Observations and Model Simulation *

4.1 Abstract

Fluidized-bed pretreatment with alum ($\text{Al}_2(\text{SO}_4)_3 \cdot 14\text{H}_2\text{O}$) of a rapid sand filter has been shown to significantly improve performance during the initial portion of filter operation. Two alternative mechanisms are hypothesized by which alum pretreatment acts to improve particle removal: (1) $\text{Al}(\text{OH})_{3(\text{am})}$ coats the sand filter medium, and alters its porosity. (2) Precipitated $\text{Al}(\text{OH})_{3(\text{am})}$ embedded within the media pores acts as an additional filter medium that increases the particle capture efficiency. Conceptual models for these two mechanisms are developed and compared with experimental data for particle removal and head loss. Model predictions indicate that particle removal by filtration through $\text{Al}(\text{OH})_{3(\text{am})}$ flocs is likely the mechanism that significantly enhances the filter performance.

Keywords: Fluidized-bed pretreatment, alum, rapid sand filter, ripening

4.2 Nomenclature

Symbols

- A_{filter} the total cross sectional area of the filter
 A_{pore} the total cross sectional area of pores
 As porosity-dependent parameter
 C_{dose} the Al concentration in the pretreatment feed

* The contents of this chapter have been submitted for publication with co-authors L. Lion and M. Weber-Shirk.

$d_{Al(OH)_3(am)}$	diameter of $Al(OH)_3(am)$ floc
d_c	diameter of collector
d_p	diameter of particle
f_v	floc volume per mole ratio
g	acceleration due to gravity
h	head loss
k	Kozeny's constant
L	filter medium packed depth
L_{clean}	filter bed depth without $Al(OH)_3(am)$ deposition
$L_{settled}$	the total depth that $Al(OH)_3(am)$ deposited in the filter pores
pC^*	Particle capture efficiency, $-\log(C_{effluent}/C_{influent})$
V_a	filtration rate
V_{dose}	the total volume of the mixture of alum, NaOH, and tap water pumped into the filter
V_{pore}	total void volume for the experimental sand medium
$V_{settled}$	settled $Al(OH)_3(am)$ volume

Greek Letters

α	attachment efficiency
ϵ_0	porosity of a clean-bed filter
ϵ	porosity of a alum-pretreated filter
$\epsilon_{Al(OH)_3(am)}$	porosity of $Al(OH)_3(am)$ floc
γ	$(1-\epsilon_0)^{1/3}$
Π_{Br}	dimensionless grouping for Brownian motion transport
Π_g	dimensionless grouping for gravitational transport
Π_R	dimensionless grouping for geometry
ρ_p	particle density

- ρ_w water density
 ν kinematic viscosity of water

4.3 Introduction

Transport and deposition are the mechanisms controlling removal of particulate matter in deep-bed filtration, a commonly used method for water and wastewater treatment and industrial separations (Tufenkji and Elimelech 2004). Transport of suspended particles from the bulk fluid to the immediate vicinity of solid-liquid interface presented by the filter (i.e., to a grain of the media or to another particle previously retained in the filter bed) can occur through Brownian motion, interception, and sedimentation. Smaller particles are most susceptible to the thermal buffeting of water molecules and the resulting Brownian motion can cause colloidal particles to contact a collector. Transport of particles by interception occurs when a particle following a flow streamline comes into contact with a collector by virtue of the particle's size. If the density of the particle is greater than that of the fluid, gravitational forces will influence the particle's trajectory and can create contact with a collector through sedimentation. Particle attachment to the media surface is dominated by electrical and chemical interactions such as electrostatic attraction or repulsion within the electrical double layer and short range van der Waals attractive forces (Yao et al. 1971; O'Melia 1980; Elimelech and O'Melia 1990; Tufenkji and Elimelech 2004).

In previous filtration studies by the authors of this paper, a fluidized-bed pretreatment process with alum ($\text{Al}_2(\text{SO}_4)_3 \cdot 14\text{H}_2\text{O}$), was shown to improve particle capture by a sand filter medium. Pretreatment was performed during the end of backwash cycle while the sand bed was still fluidized. This filtration process modification was shown to be capable of eliminating the ripening stage during the initial portion of operation of

a rapid sand filter and enhanced the efficiency of turbidity removal (up to 99.6%) for untreated raw water without a substantial increase of head loss (Lin et al. 2009, submitted).

In this paper, two mechanisms are hypothesized by which alum pretreatment acts to enhance particle removal in a sand filter. Conceptual representations based on the TE filtration model (Tufenkji and Elimelech 2004) and Carman-Kozeny equation (Carman 1937) are developed, and compared with the experimental observations of particle removal and head loss.

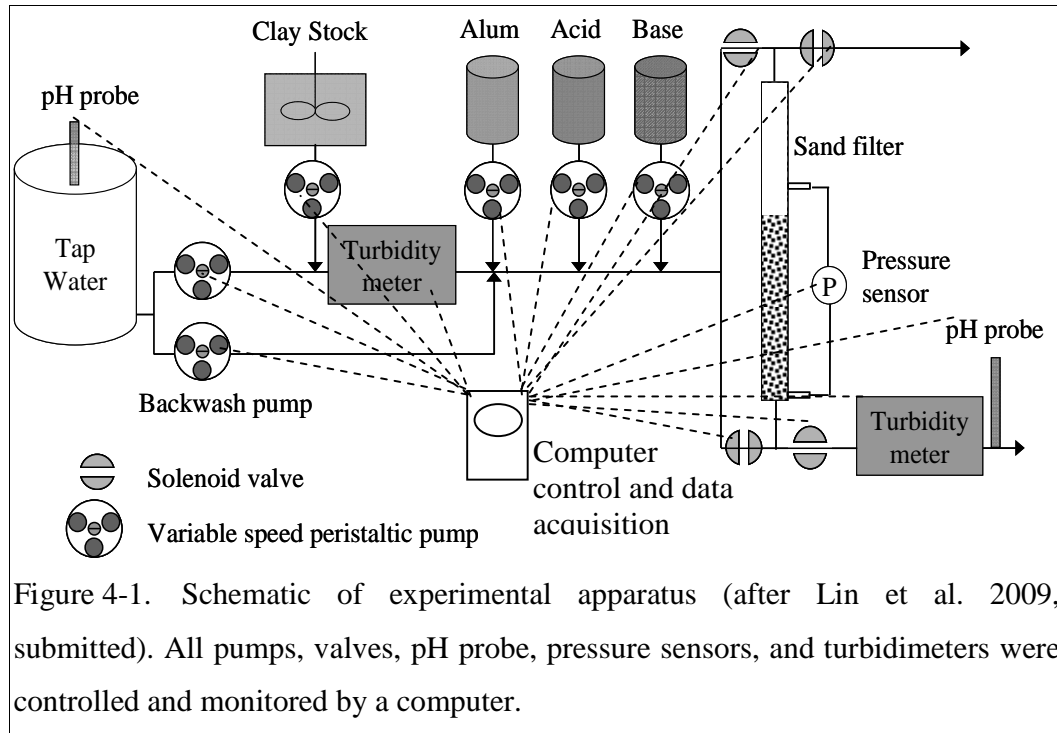
4.4 Materials and Methods

4.4.1. Filtration apparatus

A schematic of the research apparatus used is presented in Figure 4-1. Process Controller software for automation of test apparatus and experiments (Weber-Shirk 2008) was used to conduct parametric tests. All chemical reagents and synthetic raw waters were introduced into the filter by digital peristaltic pumps under computer control (Masterflex, Cole-Parmer, USA). The filter column, 1.2 m long and 2.5 cm inside diameter, contained 60 cm of 0.45 to 0.55 mm diameter sand with a uniformity coefficient of 1.65 and porosity of 0.4 (Ricci Bros. Sand Company Inc, New Jersey, USA). The filter was precisely leveled and operated at a constant flow rate of 5 m/hr (40.8 mL/min) when in downward flow. Head loss was measured with a differential pressure sensor connected to the top and bottom of the filter. Tap water pH and the effluent pH were also monitored.

Filter performance was monitored by inline turbidimeters (Micro TOL, HF Scientific, Inc.) on the untreated raw water and filtered effluent (Figure 4-1). All data including

turbidity, head loss, and pH were logged at 5 second intervals. Particle capture efficiency is expressed here as pC^* where C^* is the turbidity of the effluent water in Nephelometric Turbidity Units (NTU) normalized by the turbidity of the influent water and p is the negative logarithm (base 10) (i.e., $pC^* = -\log(C_{effluent}/C_{influent})$).



4.4.2. Fluidized-bed pretreatment of filter media

Prior to challenging the filter, 60 g/L alum (Fisher Scientific), 0.55 M NaOH (Fisher Scientific), and Cornell University tap water were blended to generate amorphous Al hydroxide precipitate at a neutral pH of 7.5 and pumped upward through the filter. The pretreatment flow rate was 450 mL/min and occurred at the end of backwash cycle while the sand bed was fluidized. The corresponding upflow velocity was 55 m/hr and the bed was expanded 50%. The volume ratio of alum and NaOH was always 1 to 1, and the ratio of chemical feed flow rates to tap water flow rate was varied to achieve different pretreatment doses. The pretreatment time was set to 14 seconds so that all the $Al(OH)_{3(am)}$ remained within the fluidized sand (i.e., no floc

breakthrough occurred above the sand bed). Retention of the alum input within the fluidized bed was verified visually using a dyed alum feed stock. Different dosages of Al (0, 0.15, 0.23, 0.8, 1.5, 2.3, 5, 8, 11, 14, 17.5, 20.5 and 23.5 mol Al/m³ of pore volume) were applied to the filter. Expressing the dose in units of mol Al/m³ of pore volume facilitates generalization of the experimental results to other filter bed sizes. The Al concentrations in the mixed pretreatment feed before injecting into the filter were 0, 0.22, 0.33, 1.1, 2.2, 3.3, 7.2, 11.7, 16.2, 20.7, 25.1, 29.6 and 33.7 mol Al/m³. The difference in these concentrations and those given above is because the pretreatment volume was approximately 70% of the filter pore volume. All subsequent Al dosages in this paper are expressed on a per pore volume basis.

After pretreatment, the clean tap water was passed through the filter in a downward flow for two hydraulic retention times of the sand bed (i.e., 6 minutes) to remove dissolved aluminum species and unattached precipitated Al(OH)_{3(am)} from the filter.

4.4.3. Filter operation

In all filtration studies Cornell University tap water was used as the raw water source (22°C, pH ≈ 8, total organic carbon ≈ 2.0 mg/L, hardness ≈ 150 mg/L as CaCO₃, alkalinity: ≈ 110 mg/L as CaCO₃, chlorine residual ≈ 0.7 mg/L). It was acidified with nitric acid (trace metal grade, Fisher Scientific) to achieve desired pH value of 7. Kaolin clay (R.T. Vanderbilt Company, Inc., Connecticut), was used as a source for turbidity, and a commercial humic acid sodium salt (Aldrich Chemical Company, Inc.) was selected as a surrogate for natural organic matter (NOM). The humic acid (HA) and clay were mixed with distilled water as a 7x concentrated stock (pH = 4.3) and then diluted with tap water to achieve a desired influent turbidity (~55 NTU) and humic acid concentration (0.5 mg/L). No raw water pretreatment such as coagulation, flocculation and sedimentation was employed before filtration. The clay particle size

was heterodisperse with diameters ranging from approximately 1 to 3 μm as measured by dynamic light scattering (Malvern Zetasizer Nano-ZS) and by light microscopy. The filtration rate was held constant at 5 m/hr in all experiments. Between each test, the sand medium was backwashed with approximately 60% volumetric expansion for 8 minutes at an upflow velocity of 80 m/hr, followed by an 9 m/hr down-flow acid wash (0.1 M HCl) for 6 minutes to dissolve and remove $\text{Al}(\text{OH})_{3(\text{am})}$, followed by another 8 minute backwash to remove acid and any residual clay.

4.5 Results

4.5.1. Turbidity removal efficiency and head loss profile for alternative fluidized-bed pretreatments

Turbidity removal over time as a function of the 7 highest pretreatment Al doses is shown in Figure 4-2. These results obtained at pH =7 differ from those reported by Lin et al. (2009, submitted) at higher and lower pH values. Data from the first 1.5 hydraulic residence times (i.e., about 20 minutes) at the beginning of each the filter challenge are not reported since those data show an artificially high particle removal caused by the clean pore water that was exiting the filter into the effluent turbidimeter and being displaced from the tubing and turbidimeter sample cell. Each pretreatment dosage was replicated and, with the exception of the 23.5 mol/m^3 Al dose where effluent turbidity levels were often below detection (i.e., ≤ 0.01 NTU), the agreement of filter performance at replicate dosages was excellent. A turbidity of 0.01 NTU was assumed for purposes of calculating pC^* when the effluent was below the detection limit. Removal efficiency increased with increasing pretreatment dosage and the highest pretreatment dose of 23.5 mol/m^3 resulted in excellent particle removal (≥ 99.9 % during a one hour filter run) compared to the untreated filter (68 % removal). These results confirm that fluidized-bed pretreatment eliminates the initial poor effluent quality and enhances filter performance. While it may appear that turbidity

removal could increase at even higher pretreatment doses, an Al dose above 23.5 mol/m³ resulted in the generation of gelatinous aluminum hydroxide that caused our laboratory-scale filter to clog. Thus, the maximum pretreatment dose was 23.5 mol Al/m³.

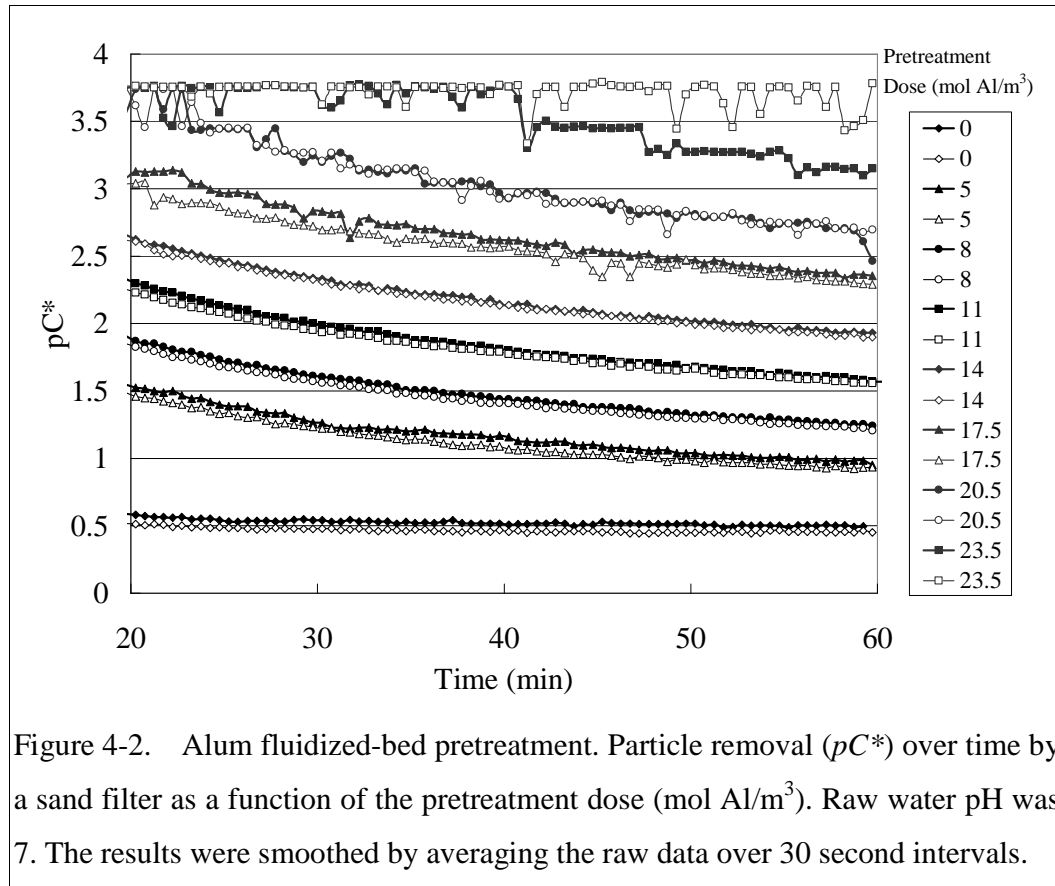


Figure 4-3 presents the performance, pC^* , as a function of the pretreatment dose. The pC^* values shown are for a 10 minute average centered at the 25th minute (i.e., average values from 20 to 30 minutes) and then averaged with the result of the replicate experiment. The improvement in pC^* was directly proportional to the pretreatment Al dose. The pretreatment dose of 23.5 mol/m³, the hollow diamond data point, was not fit by the least-squares-regression line because it assumes undetected turbidity was equal to the detection limit of the turbidimeter.

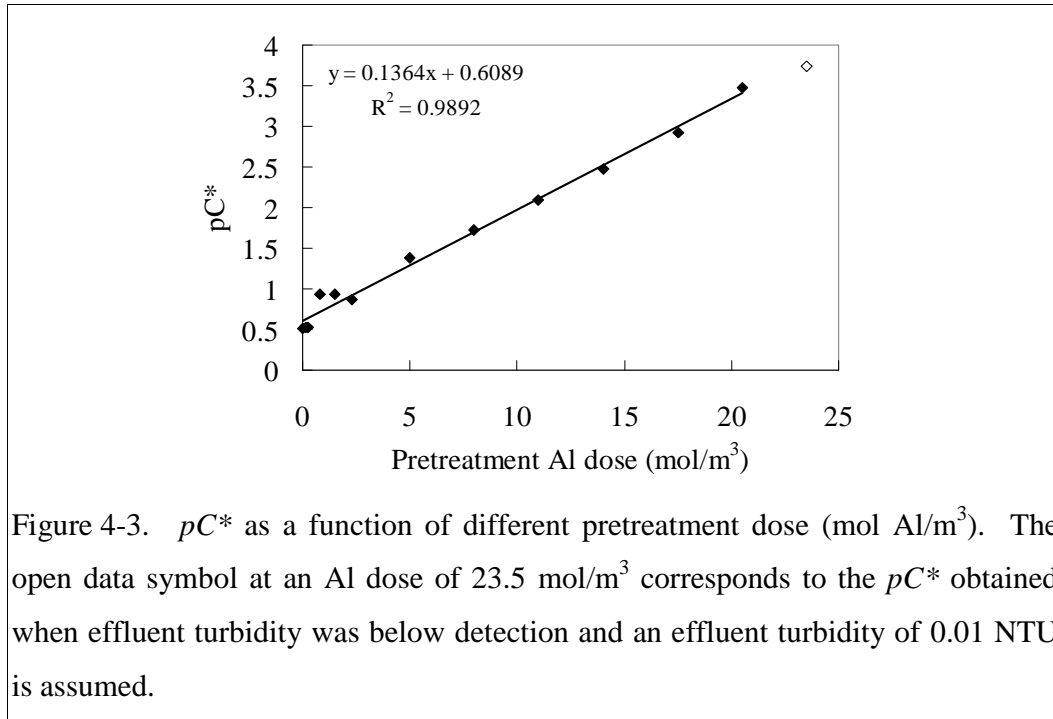
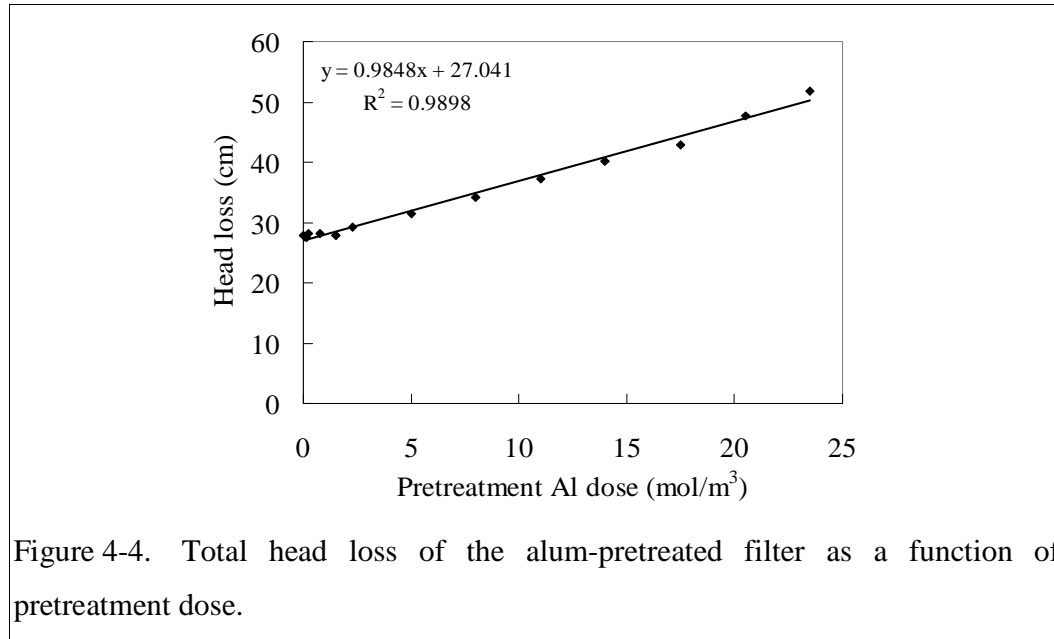


Figure 4-3. pC^* as a function of different pretreatment dose (mol Al/m³). The open data symbol at an Al dose of 23.5 mol/m³ corresponds to the pC^* obtained when effluent turbidity was below detection and an effluent turbidity of 0.01 NTU is assumed.

Differential pressure measurements across the filter bed were used to monitor head loss during experiments. Addition of alum into the filter during pretreatment resulted in increased head loss. The averaged head loss after fluidized-bed pretreatment is plotted against the corresponding pretreatment Al dose (Figure 4-4). These head loss values were obtained by averaging a 10 minute interval centered at the 25th minute (i.e., average values from 20 to 30 minutes) and then averaging with the result of the replicate experiment. The magnitude of head loss accumulation was proportional to the pretreatment dose. At the highest applied Al dose (i.e., 23.5 mol/m³) the head loss increase relative to untreated sand was ≈ 23 cm. These results indicate that fluidized-bed pretreatment can enhance filter performance while adding a small additional head loss that is unlikely to interfere with operation in full-scale plants.



4.5.2. Measurement of the settled volume of $\text{Al}(\text{OH})_{3(\text{am})}$

The pore volume occupied by $\text{Al}(\text{OH})_{3(\text{am})}$ was a required constant in the model simulations described below. 130 mL of solution at the maximum Al pretreatment concentration (i.e., 33.7 mol Al/m^3 used to produce the pretreatment dose of 23.5 mol Al/m^3 of pore volume) in combination with NaOH, and tap water was allowed to settle in a graduated cylinder that did not contain sand media (cross sectional area = 10.5 cm^2). After the settled volume was stable (1 month), the flocs occupied a volume of 50 mL giving a floc volume per mole ratio, f_v , of 0.011 m^3 (mole $\text{Al})^{-1}$. It is possible that the shear stress generated by the fluidized sand bed during backwash prevented the formation of large flocs, and thus the flocs in the graduated cylinder may have been larger than those in the filter column. Given that large flocs are less dense, it is possible that the measured molar volume was larger than that in the filter column. Assuming the settled floc volume is linearly proportional to the alum dose, the pore volume (mL) occupied by a given Al dose was calculated as:

$$V_{\text{settled}} = f_v \cdot C_{\text{dose}} \cdot V_{\text{dose}} \quad (4.1)$$

Where $V_{settled}$ is settled $\text{Al(OH)}_{3(am)}$ volume, C_{dose} is the Al concentration in the pretreatment feed before injecting into the filter, and V_{dose} is the total volume of the mixture of alum, NaOH, and tap water pumped into the filter.

4.6 Alternative Models for the Effect of Fluidized-Bed Pretreatment on Filter Performance

Two alternative mechanisms are examined here to explain the linear improvement in the filter efficiency and head loss increase with pretreatment Al dose: (1) $\text{Al(OH)}_{3(am)}$ coated the sand filter medium and altered the porosity (Figure 4-5 (a)). This mechanism is referred to here as “ $\text{Al(OH)}_{3(am)}$ coating.” For this mechanism, changes in performance and head loss are caused exclusively by the change in porosity. (2) $\text{Al(OH)}_{3(am)}$ flocs embedded within the filter pores acted as filters to increase the particle capture efficiency (Figure 4-5 (b)). This mechanism is referred to here as “ $\text{Al(OH)}_{3(am)}$ filtration”. For this mechanism, changes in performance and head loss are caused exclusively by the additional filter bed composed of $\text{Al(OH)}_{3(am)}$ flocs.

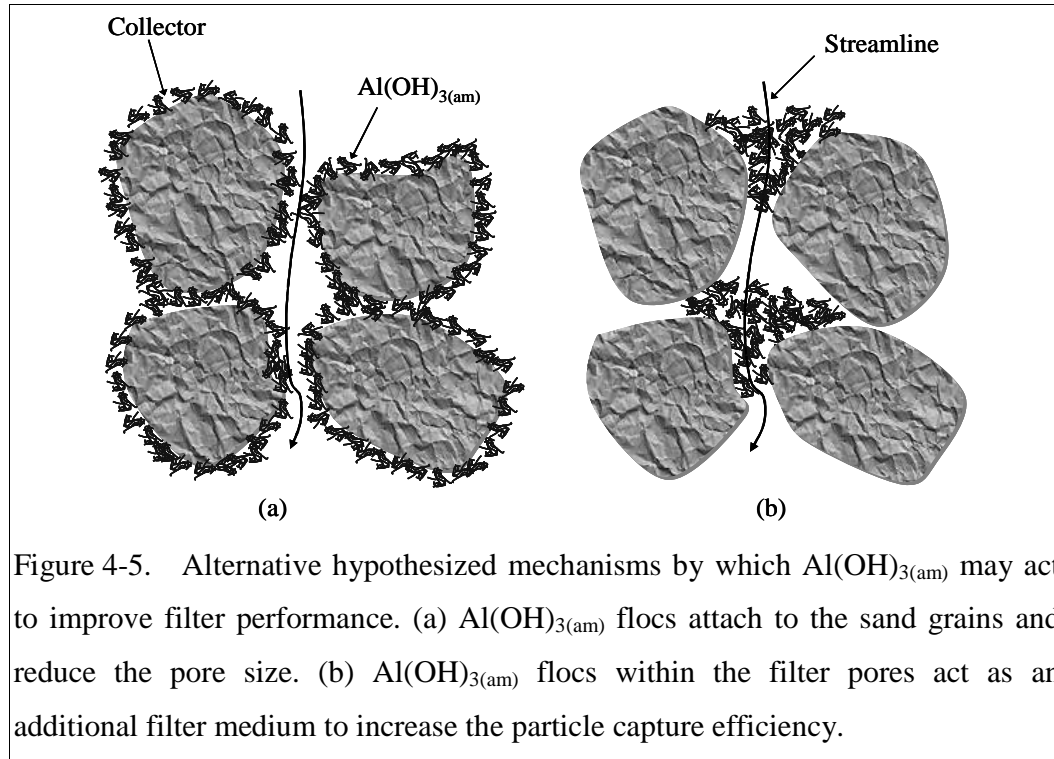


Figure 4-5. Alternative hypothesized mechanisms by which Al(OH)_{3(am)} may act to improve filter performance. (a) Al(OH)_{3(am)} floes attach to the sand grains and reduce the pore size. (b) Al(OH)_{3(am)} floes within the filter pores act as an additional filter medium to increase the particle capture efficiency.

4.6.1. Model predictions of head loss and filter performance assuming Al(OH)_{3(am)} coating

4.6.1.1 Head loss

The Carman-Kozeny equation (Carman 1937) was used to predict head loss increase with different pretreatment Al doses as described in equation 4.2.

$$\frac{h}{L} = 36k \frac{(1-\varepsilon)^2}{\varepsilon^3} \frac{\nu V_a}{g d_c^2} \quad (4.2)$$

where h is total head loss through the filter bed, L is the depth of filter medium, k is Kozeny's constant ($k \approx 5$ for common filter media), ν is kinematic viscosity of the fluid, V_a is filtration rate, g is acceleration of gravity, and d_c is diameter of collector (i.e., a sand grain). The porosity (ε) in equation 4.2 is the porosity after alum pretreatment, dependent on the voids occupied by the pretreatment Al dose (see eq. 4.1) and may be determined from equation 4.3,

$$\varepsilon = \varepsilon_0 \left(1 - f_v \frac{C_{dose} V_{dose}}{V_{pore}} \right) \quad (4.3)$$

where ε_0 is porosity of the clean-bed filter, and V_{pore} , the total void volume for the experimental sand medium, was 120 mL. It was assumed that the molar volume (f_v) was the same in the measurement of the settled volume of $\text{Al}(\text{OH})_{3(\text{am})}$ as in the filter column. In addition, the flow of water through $\text{Al}(\text{OH})_{3(\text{am})}$ flocs attached to the sand grains was assumed to be insignificant for both head loss and particle capture predictions. Figure 4-6 shows the comparison of predicted and observed head loss as a function of pretreatment Al dose. The predicted head loss of the untreated bed (0 mol Al/m^3) agrees well with the observed head loss; however the predicted head loss after pretreatment does not match the experimental data.

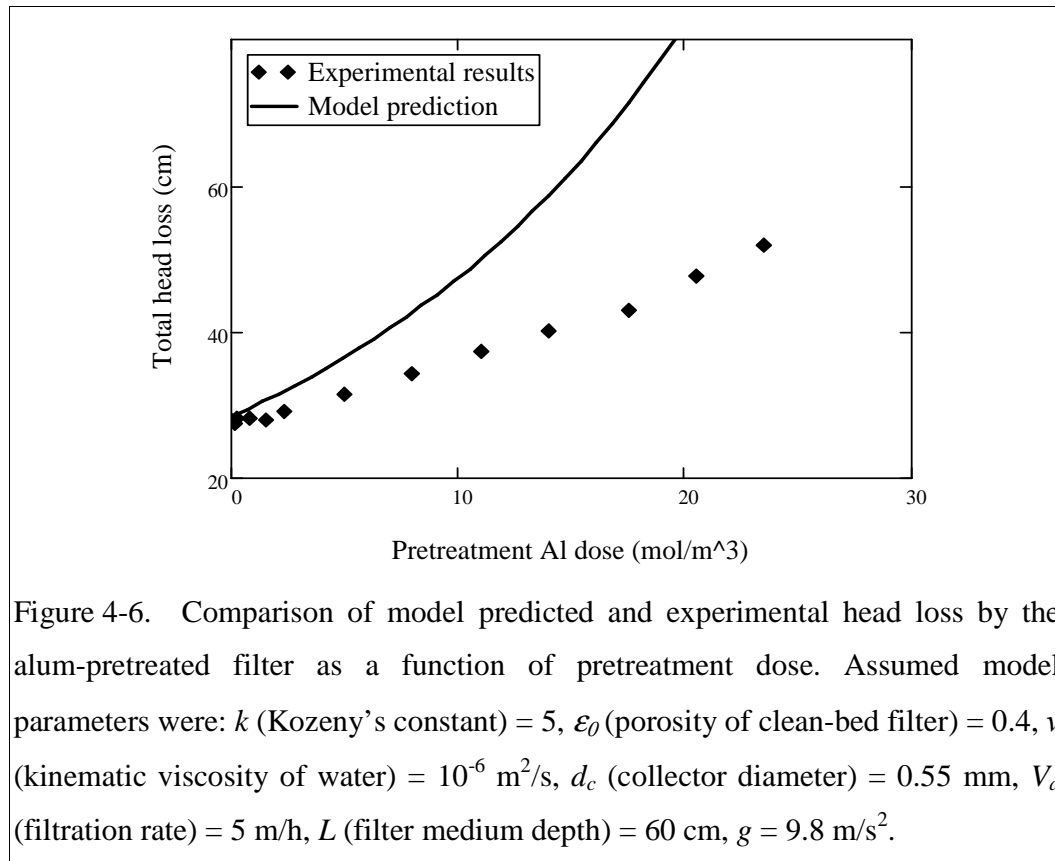


Figure 4-6. Comparison of model predicted and experimental head loss by the alum-pretreated filter as a function of pretreatment dose. Assumed model parameters were: k (Kozeny's constant) = 5, ε_0 (porosity of clean-bed filter) = 0.4, ν (kinematic viscosity of water) = 10^{-6} m^2/s , d_c (collector diameter) = 0.55 mm, V_a (filtration rate) = 5 m/h, L (filter medium depth) = 60 cm, $g = 9.8 \text{ m/s}^2$.

4.6.1.2. Particle removal (pC^*)

The porosities after pretreatment (ε in equation 4.3) were applied using Yao et al.'s model (1971) as modified by Tufenkji and Elimelech (the TE model) (2004) to predict particle removal (pC^*). The TE model for particle removal is shown in equation 4.4,

$$pC^* = \frac{3 \cdot (1 - \varepsilon)}{2 \cdot \ln(10)} \cdot \left(\frac{L}{d_c} \right) \cdot \alpha \cdot \left(0.75 \cdot A_s^{\frac{1}{3}} \cdot \Pi_R^{\frac{1}{6}} \cdot \Pi_{Br}^{\frac{2}{3}} + 0.047 \cdot A_s \cdot \Pi_R^{1.425} + 0.31 \cdot \Pi_g \right) \quad (4.4)$$

where α is attachment efficiency, A_s is a porosity-dependent parameter, and Π_R , Π_{Br} , and Π_g , dimensionless grouping for geometry, Brownian motion, and gravitational transport, respectively. These parameters are shown in equation 4.5, 4.6, 4.7, and 4.8.

$$A_s = \frac{2(1 - \gamma^5)}{2 - 3\gamma + 3\gamma^5 - 2\gamma^6} \quad (4.5)$$

Where $\gamma = (1 - \varepsilon_0)^{1/3}$.

$$\Pi_R = \frac{d_p}{d_c} \quad (4.6)$$

Where d_p is particle diameter.

$$\Pi_{Br} = \frac{k_b T}{3\pi d_p V_a d_c} \quad (4.7)$$

Where k_b is Boltzmann constant and T is fluid absolute temperature.

$$\Pi_g = \frac{d_p^2 (\rho_p - \rho_w) g}{18\mu V_a} \quad (4.8)$$

Where ρ_p is the particle density, ρ_w is water density and μ is the absolute water viscosity. In the model prediction it was assumed that the whole filter bed was uniformly pretreated with $\text{Al}(\text{OH})_{3(\text{am})}$. The predicted performance with different clay particle sizes (1, 2, and 3 μm) by the alum-pretreated filter is compared with the measured particle removal as a function of pretreatment Al dose in Figure 4-7. The removal of untreated filter (0 mol Al/m^3) agrees well with model prediction assuming

the particle diameter was 1 μm , but does not match the experimental results after alum pretreatment. The model predictions are sensitive to the assumed clay particle size, and do not agree with observations for the untreated filter if 2 or 3 μm colloid sizes are assumed.

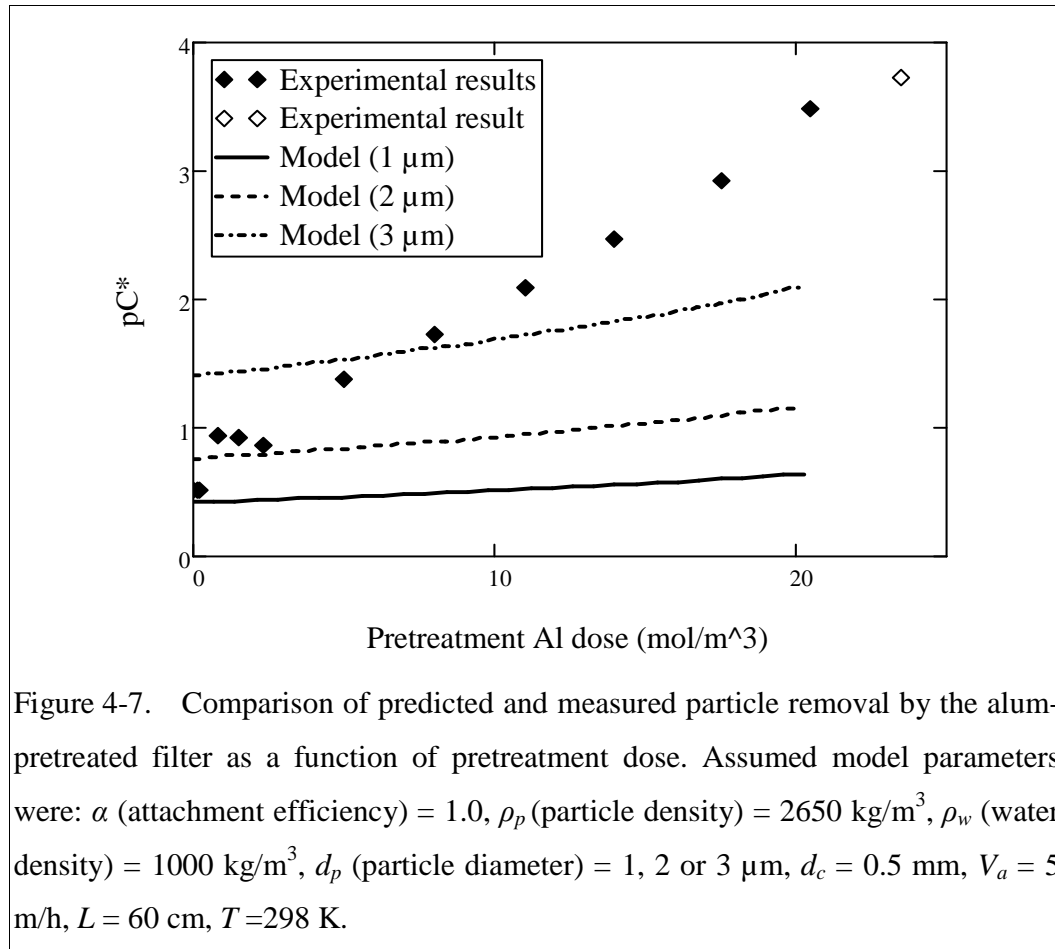


Figure 4-7. Comparison of predicted and measured particle removal by the alum-pretreated filter as a function of pretreatment dose. Assumed model parameters were: α (attachment efficiency) = 1.0, ρ_p (particle density) = 2650 kg/m^3 , ρ_w (water density) = 1000 kg/m^3 , d_p (particle diameter) = 1, 2 or 3 μm , $d_c = 0.5$ mm, $V_a = 5$ m/h, $L = 60$ cm, $T = 298$ K.

4.6.2. Model predictions of head loss and filter performance assuming $\text{Al}(\text{OH})_{3(\text{am})}$ filtration

In this hypothesized mechanism, $\text{Al}(\text{OH})_{3(\text{am})}$ flocs deposited in the pores of the sand filter medium were assumed to act as filters. The total depth of $\text{Al}(\text{OH})_{3(\text{am})}$ filter deposited was calculated by equation 4.9:

$$L_{\text{settled}} = \frac{V_{\text{settled}}}{A_{\text{pore}}} \quad (4.9)$$

where $L_{settled}$ is the total depth that $\text{Al}(\text{OH})_{3(\text{am})}$ deposited in the pores, $V_{settled}$ is settled $\text{Al}(\text{OH})_{3(\text{am})}$ volume that can be obtained from equation 4.1, and A_{pore} is the total area of pores at a filter cross section ($A_{filter}\epsilon_0$).

The experimental head loss data at the Al dose of 20.5 mol Al/m^3 (i.e., 48 cm) was used in the modified Kozeny equation (equation 4.10) to develop a relation between $\text{Al}(\text{OH})_{3(\text{am})}$ floc diameter ($d_{\text{Al}(\text{OH})_3(\text{am})}$) and porosity ($\epsilon_{\text{Al}(\text{OH})_3(\text{am})}$). The modified Kozeny equation used here was separated into two parts which represent head loss through the clean fraction of each pore and $\text{Al}(\text{OH})_{3(\text{am})}$ -deposited fraction of each pore. The breakdown of these two contributions allowed predicting the head loss through two different depths and properties of filter media.

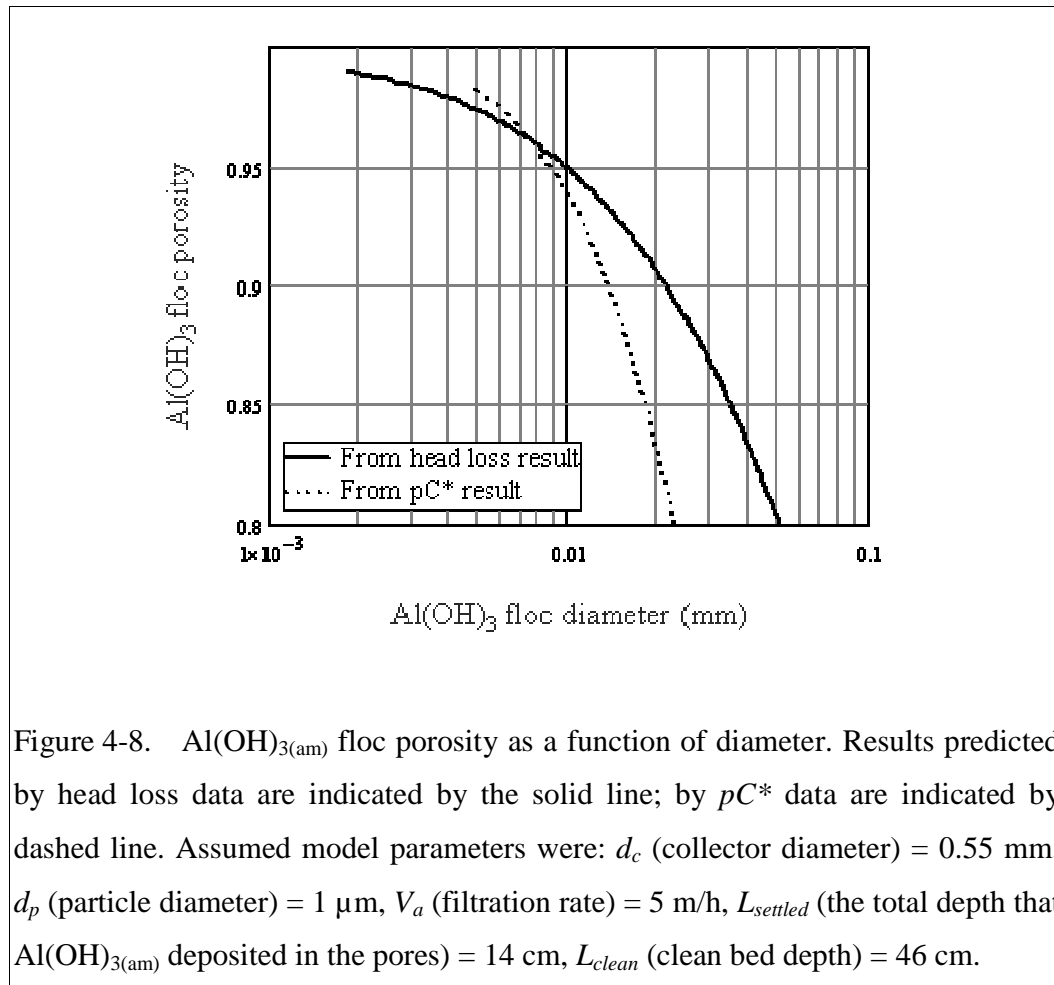
$$h = 36k \frac{(1 - \epsilon_0)^2}{\epsilon_0^3} \frac{\nu V_a}{g d_c^2} L_{clean} + 36k \frac{(1 - \epsilon_{\text{Al}(\text{OH})_3(\text{am})})^2}{\epsilon_{\text{Al}(\text{OH})_3(\text{am})}^3} \frac{\nu V_a}{\epsilon_0 g d_{\text{Al}(\text{OH})_3(\text{am})}^2} L_{settled} \quad (4.10)$$

Where; the clean-bed depth (L_{clean}) is equal total depth (60 cm) minus $L_{settled}$. The paired values of $d_{\text{Al}(\text{OH})_3(\text{am})}$ and $\epsilon_{\text{Al}(\text{OH})_3(\text{am})}$ that combine to predict the observed head loss are indicated by the solid line in Figure 4-8.

For particle removal, the TE filtration model (2004) was modified by creating separate terms for filtration by the clean bed and the $\text{Al}(\text{OH})_{3(\text{am})}$ -deposited bed as shown in equation 4.11. The clean-bed depth (L_{clean}) and porosity (ϵ_0) were used in the $pC^*_{clean-bed}$ term; the total depth that $\text{Al}(\text{OH})_{3(\text{am})}$ deposited in the pores ($L_{settled}$), $\text{Al}(\text{OH})_{3(\text{am})}$ floc diameter ($d_{\text{Al}(\text{OH})_3(\text{am})}$) and porosity ($\epsilon_{\text{Al}(\text{OH})_3(\text{am})}$) were applied in the term $pC^*_{\text{Al}(\text{OH})_3(\text{am})-bed}$. This assumes that particle capture in the $\text{Al}(\text{OH})_{3(\text{am})}$ floc beds is dominated by the flocs and the contribution by the sand covered by the flocs is insignificant.

$$pC^*_{total} = pC^*_{clean-bed} + pC^*_{Al(OH)_3(am)-bed} \quad (4.11)$$

The particle removal data obtained at Al dose of 20.5 mol Al/m³ (i.e., $pC^* = 3.5$) was employed in the modified TE model. The paired values of $d_{Al(OH)_3(am)}$ and $\varepsilon_{Al(OH)_3(am)}$ that combine to predict the observed pC^* are indicated by the dashed line presented in Figure 4-8. The intersection of the two curves in Figure 4-8 represents the Al(OH)_{3(am)} floc diameter and porosity that simultaneously satisfy the model for head loss and pC^* for the Al dose of 20.5 mol Al/m³. The values $d_{Al(OH)_3(am)} = 7.6 \mu\text{m}$ and $\varepsilon_{Al(OH)_3(am)} = 0.96$ result when the assumed clay diameter = 1 μm , $d_{Al(OH)_3(am)} = 18 \mu\text{m}$ and $\varepsilon_{Al(OH)_3(am)} = 0.92$ when the assumed clay diameter = 2 μm , and $d_{Al(OH)_3(am)} = 37 \mu\text{m}$ and $\varepsilon_{Al(OH)_3(am)} = 0.84$ when the assumed clay diameter = 3 μm . These values are used below to predict head loss and particle removal (pC^*) at different alum doses.



4.6.2.1. Head loss

$\text{Al(OH)}_{3(\text{am})}$ floc diameter and porosity determined from Figure 4-8 were used in equation 4.10 to independently predict head loss at other pretreatment Al doses. The line shown in Figure 4-9 is the predicted head loss from the model for the three clay particle diameters. The predicted head losses were proportional to the pretreatment dose, and the trend shows good agreement with the observed head loss.

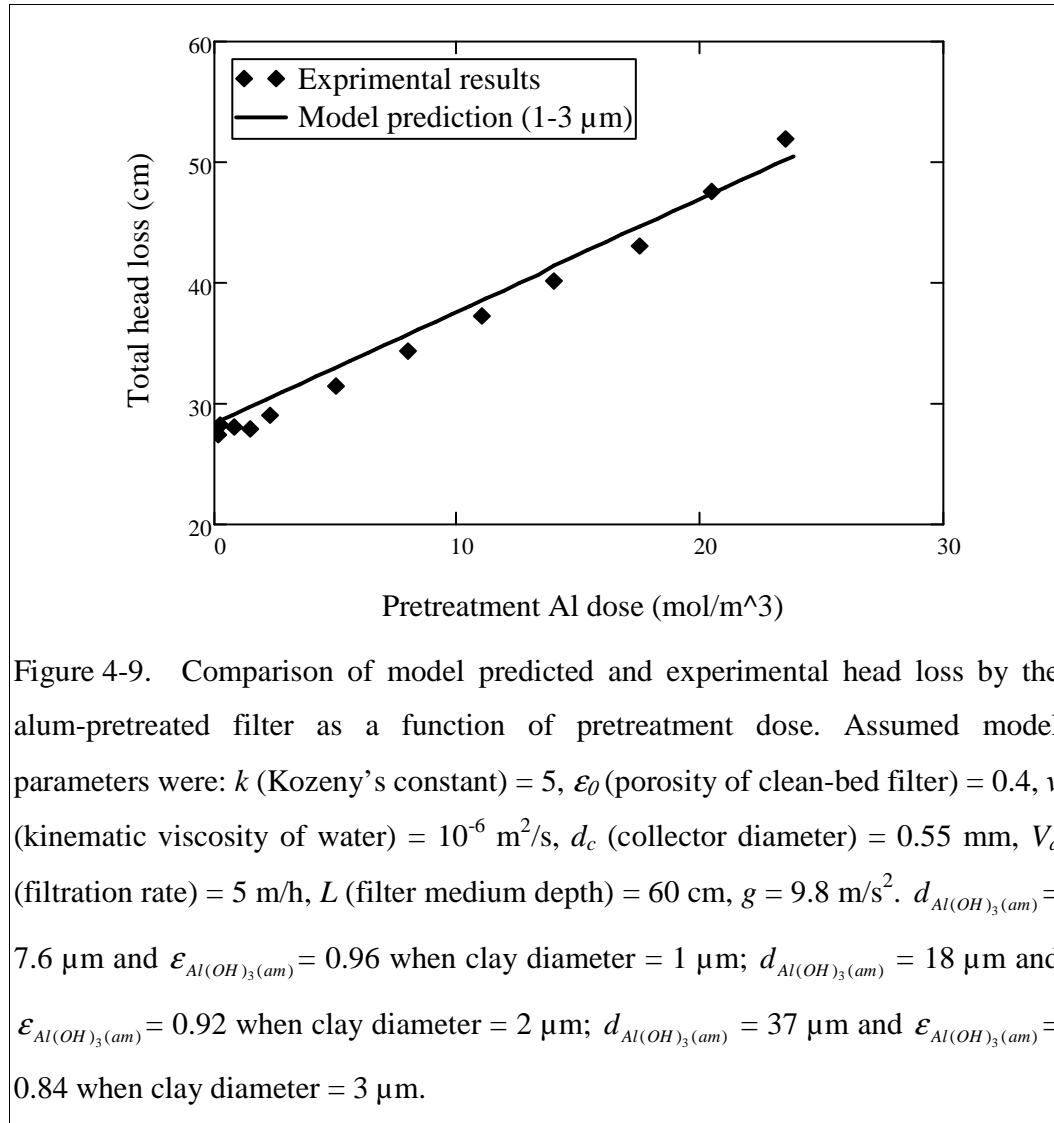


Figure 4-9. Comparison of model predicted and experimental head loss by the alum-pretreated filter as a function of pretreatment dose. Assumed model parameters were: k (Kozeny's constant) = 5, ϵ_0 (porosity of clean-bed filter) = 0.4, ν (kinematic viscosity of water) = 10^{-6} m²/s, d_c (collector diameter) = 0.55 mm, V_a (filtration rate) = 5 m/h, L (filter medium depth) = 60 cm, $g = 9.8$ m/s². $d_{Al(OH)_3(am)} = 7.6$ μ m and $\epsilon_{Al(OH)_3(am)} = 0.96$ when clay diameter = 1 μ m; $d_{Al(OH)_3(am)} = 18$ μ m and $\epsilon_{Al(OH)_3(am)} = 0.92$ when clay diameter = 2 μ m; $d_{Al(OH)_3(am)} = 37$ μ m and $\epsilon_{Al(OH)_3(am)} = 0.84$ when clay diameter = 3 μ m.

4.6.2.2. Particle removal (pC^*)

The porosity and floc diameter of $Al(OH)_3(am)$ obtained from Figure 4-8 were used in equation 4.11, to independently predict pC^* at the other pretreatment Al doses. The predicted pC^* with different particle sizes (1, 2, and 3 μ m) and the observed results are presented in Figure 4-10. The predicted removals agree reasonably well with the measured pC^* assuming the diameters of clay particles were modeled as 1 or 2 μ m. The predicted pC^* for an assumed clay particle diameter of 3 μ m does not match the measured results. These results suggested that clay particles used in this research were

predominantly in the 1 to 2 μm size range. Interestingly, according to the TE model, particle removal by the $\text{Al}(\text{OH})_{3(\text{am})}$ floc filter was dominated by interception as a transport mechanism.

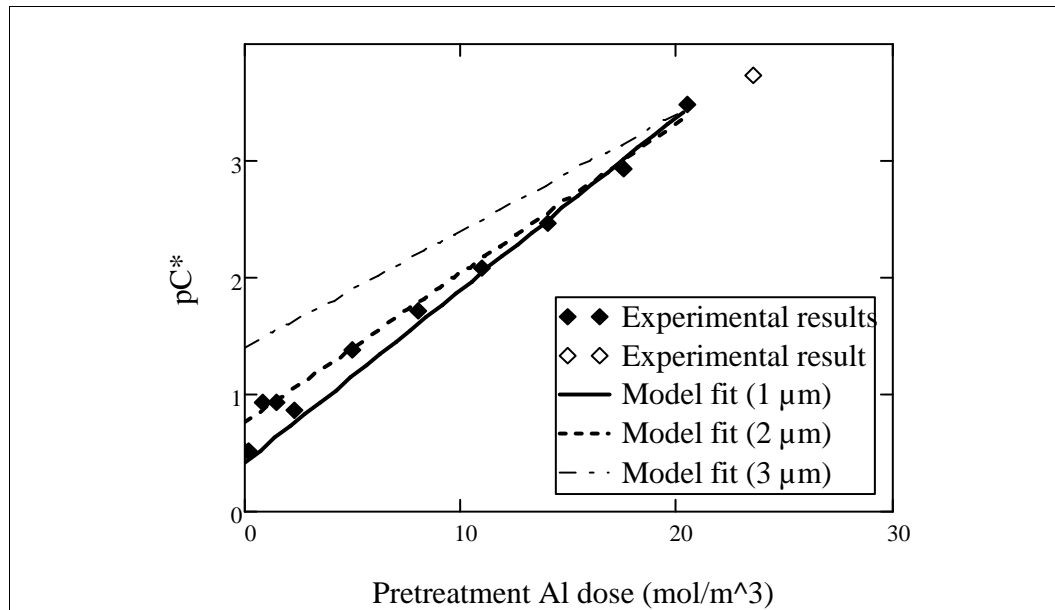


Figure 4-10. Comparison of model predicted and observed particle removal by the alum-pretreated filter as a function of pretreatment dose. The data point at 23.5 mol/m^3 (hollow diamond) was not fit by the predicted curves due to the turbidimeter detection limit. Assumed model parameters were: α (attachment efficiency) = 1.0, ρ_p (particle density) = 2650 kg/m^3 , ρ_w (water density) = 1000 kg/m^3 , d_p (particle diameter) = 1, 2 or 3 μm , $d_c = 0.5$ mm, $V_a = 5$ m/h, $L = 60$ cm, $T = 298$ K. ($d_{\text{Al}(\text{OH})_3(\text{am})} = 7.6$ μm and $\varepsilon_{\text{Al}(\text{OH})_3(\text{am})} = 0.96$ when clay diameter = 1 μm ; $d_{\text{Al}(\text{OH})_3(\text{am})} = 18$ μm and $\varepsilon_{\text{Al}(\text{OH})_3(\text{am})} = 0.92$ when clay diameter = 2 μm ; $d_{\text{Al}(\text{OH})_3(\text{am})} = 37$ μm and $\varepsilon_{\text{Al}(\text{OH})_3(\text{am})} = 0.84$ when clay diameter = 3 μm).

Given that the $\text{Al}(\text{OH})_{3(\text{am})}$ coating model has no adjustable parameters and the $\text{Al}(\text{OH})_{3(\text{am})}$ filtration model has two adjustable parameters ($d_{\text{Al}(\text{OH})_3(\text{am})}$ and $\varepsilon_{\text{Al}(\text{OH})_3(\text{am})}$), it was expected that the $\text{Al}(\text{OH})_{3(\text{am})}$ filtration model would have the better agreement with the experimental results. However, the $\text{Al}(\text{OH})_{3(\text{am})}$ coating model predicted non-

linear relationships between head loss/ pC^* and pretreatment dose and thus could not fit the data even if additional parameters were varied.

4.7 Conclusion

The experimental results presented in this paper confirm that fluidized-bed pretreatment with alum can significantly improve particle removal efficiency at the cost of a modest increase in head loss. The improvement in pC^* and increase in head loss were directly proportional to the pretreatment Al dose. Predictions of head loss and filter performance for two alternative models indicate that the hypothesized mechanism “ $Al(OH)_{3(am)}$ filtration” can best explain the linear improvement in the filter performance and head loss increase with pretreatment Al dose. Although it is possible that $Al(OH)_{3(am)}$ filtration acted in combination with decreased porosity resulting from coating of the sand medium, combination of the two effects is not necessary to explain the observed results. Thus, it is likely that the $Al(OH)_{3(am)}$ flocs that settled in the sand medium pores after pretreatment act as an additional filter and improve the overall filter performance.

4.8 Acknowledgements

The research described in this paper was supported by the U.S. National Science Foundation under Grant CBET-0604566 and by the Sanjuan Foundation.

REFERENCES

- Carman, P. C. (1937). Fluid flow through granular beds. *Chemical Engineering Research and Design* 15, 150-166.
- Elimelech, M. and C. R. O'Melia (1990). Kinetics of deposition of colloidal particles in porous media. *Environ. Sci. Technol.* 24(10), 1528-1536.
- Lin, P.-H., M. L. Weber-Shirk and L. W. Lion (2009). Alum pretreatment of a rapid sand filter to enhance performance. *Water Research*, submitted.
- O'Melia, C. (1980). ES&T Features: Aquasols: the behavior of small particles in aquatic systems. *Environ. Sci. Technol.* 14(9), 1052-1060.
- Tufenkji, N. and M. Elimelech (2004). Correlation equation for predicting single-collector efficiency in physicochemical filtration in saturated porous media. *Environ. Sci. Technol.* 38(2), 529-536.
- Weber-Shirk, M. (2008). An automated method for testing process parameters from <https://confluence.cornell.edu/display/AGUACLARA/Process+Controller>.
- Yao, K.-M., M. T. Habibian and C. R. O'Melia (1971). Water and waste water filtration. Concepts and applications. *Environ. Sci. Technol.* 5(11), 1105-1112.

CHAPTER 5

Conclusions and Recommendations for Future Work

5.1 Conclusions

Pretreatment performed by both downflow and fluidized-bed applications showed that the addition of coagulants such as alum, ferric chloride, or PACl, to a sand filter resulted in greatly enhanced particle removal relative to the untreated sand medium. Although the particle capture efficiency (pC^*) using both pretreatments were similar, the magnitude of head loss accumulation was quite different. Fluidized-bed application resulted in much less head loss (≈ 14 cm head loss at 2.8 mmol Al) than downflow mode (≈ 73 cm head loss at 2.2 mmol Al) because of the more uniform distribution of coagulant in upflow application. The small head loss observed is expected to be compatible with that experienced with application in full-scale conventional water treatment plants.

The results from 48 hour filtration experiments indicated that fluidized-bed alum application eliminated the initial poor performance compared with an otherwise untreated filter in contact filtration. In addition, combining fluidized-bed pretreatment with conventional treatment (i.e., contact filtration) can remove the initial poor effluent quality and provide sustained filtration efficiency (99.8% removal over 14 hours and 96% removal over 30 hours for influent water with ~ 5 NTU turbidity).

pH is a crucial parameter to control Al solubility, hence, the raw water pH consequently affects the Al concentrations in filtered effluent and constrains the applicability of alum fluidized-bed pretreatment. According to theoretical and experimental data, at pH range of 6~7 Al concentrations in the filtered effluent were

below the EPA secondary standard while at pH of 8 Al concentration exceeded the maximum secondary MCL.

The improvement in filter performance and increase in head loss were directly proportional to the upflow pretreatment Al dose. Model predictions compared with experimental results for pC^* and head loss indicate that the mechanism “ $\text{Al(OH)}_{3(\text{am})}$ filtration” can best explain the linear improvement in the particle removal and head loss increase with pretreatment Al dose.

5.2 Future Work

Testing the *in situ* fluidized-bed pretreatment technique in a full-scale filtration plant is needed. However, because of the high pH of raw water ($\text{pH} \geq 8$) coming into the Cornell Water Filtration Plant, pretreatment with alum cannot be performed at this location. Thus, further laboratory experiments utilizing alternative pretreatment coagulant need to be conducted. $\text{Fe(OH)}_{3(\text{am})}$ has a lower solubility than $\text{Al(OH)}_{3(\text{am})}$ at circumneutral pH (i.e., 0.18~0.005 $\mu\text{g/L}$ as soluble Fe at pH of 6~8; the EPA secondary standard for Fe is 300 $\mu\text{g/L}$ as Fe).

Laboratory work that should be conducted before full-scale-plant tests includes: (1) Replace the test filter sand media with sand and anthracite coal which are the media used in Cornell plant. (2) Conduct 48 hour experiments applying fluidized-bed pretreatment (FeCl_3 as a coagulant) combined with contact filtration using polyaluminum chloride to pretreat the raw water. (3) Measure Al and Fe concentrations in filtered effluent during filter runs. Repetitive filter runs with conventional backwash (i.e., excluding use of an acid wash step) should be performed to ensure accumulation of iron does not occur in a way that impairs filter performance.

In the full-scale plant tests, a critical task will be to measure the Fe and Al concentrations in the filtered effluent during filter operation to ensure concentrations of both metals are below the secondary MCL. Head loss development, effluent turbidity, total organic carbon and alkalinity should be monitored to compare with the data obtained by filters that have not been pretreated.

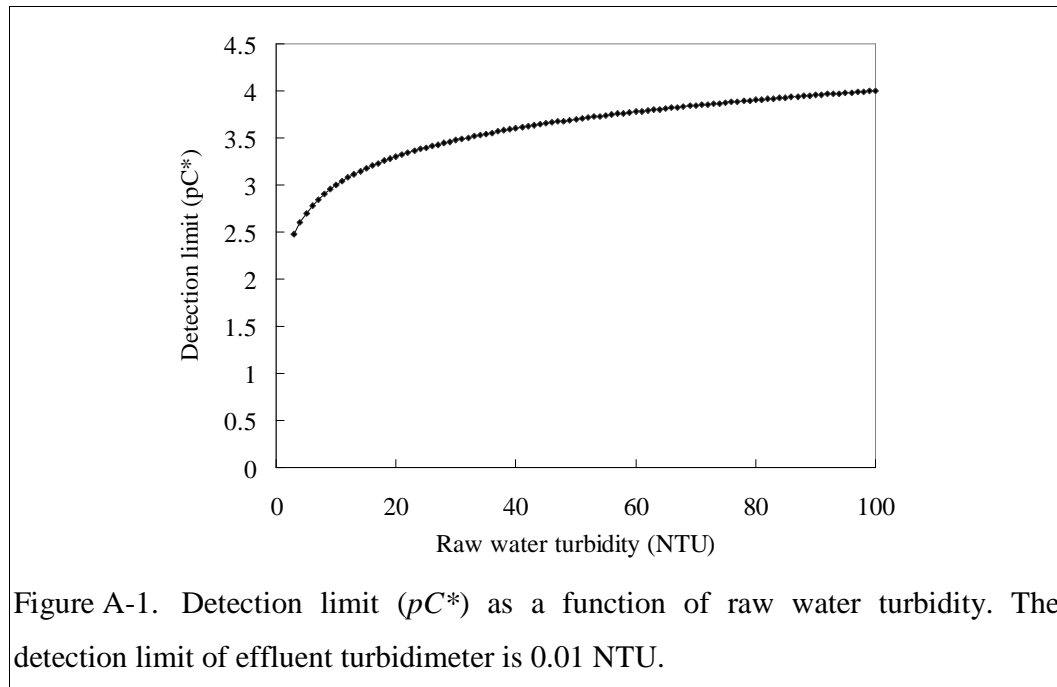
APPENDIX A

A.1 Calculation of the detection limit of particle capture efficiency

In this research particle capture efficiency is expressed as pC^* where C^* is the turbidity of the effluent water in Nephelometric Turbidity Units (NTU) normalized by the turbidity of the influent water, and p is the negative logarithm (base 10) (i.e., $pC^* = -\log(C_{\text{effluent}}/C_{\text{influent}})$). The detection limit of capture efficiency (pC^*) is calculated in equation 1 using the detection limit of the effluent turbidimeter of 0.01 NTU.

$$pC^* = -\log\left(\frac{0.01}{C_{\text{influent}}}\right) \quad (1)$$

The detection limit of capture efficiency (pC^*) is plotted in Figure A-1 as a function of raw water turbidity (i.e., C_{influent}). These values correspond to the maximum pC^* that can be observed with different influent raw water turbidities.



A.2 Comparison of FeCl₃ and alum in long term experiments

A.2.1 Introduction

In experiments lasting 24 hours, alum and ferric chloride (FeCl₃) were used respectively to pretreat the sand column (7.5 cm of sand bed; ≈ 0.5 mm in diameter of sand grain). Pretreatment was performed by downflow application of the filter aids to the top of the filter medium. A clay suspension with 7~9 NTU kaolin and 0.5 mg/L of humic acid (HA) was used as the raw water. Four experiments were conducted: (1) Clean-bed filtration (control); (2) Downflow pretreatment with 100 mmol Al/m²; (3) Contact filtration of alum treated clay by a clean bed. Filtration of alum treated clay by filter media that has not been pretreated with alum or FeCl₃ is what is typically practiced in conventional water treatment. For this case, alum (3.3 mg/L as alum during coagulation) was mixed with the raw water prior to filtration. The total alum applied during the 24 hour experiment was 1190 mmol Al/m². It should be noted that 3.3 mg/L as alum was not the optimal dose for contact filtration. (4) Combination of pretreatment and contact filtration (total Al surface loading applied was 1290 mmol/m²).

A.2.2 Results

Figure A-2 shows particle removal over 24 hours by the filter using alum for the pretreatment and by contact filtration. pC^* of the control experiment (i.e., no alum used, gray dashed line) was ~ 0.1 (20% removal) and provides a baseline for clean-bed filtration. The performance of alum-pretreated filter (black dashed line) started at $pC^* \approx 0.7$ and then deteriorated. However, the pC^* was better than that of the control. For example, at the 12th hour the removal efficiency of the pretreatment experiment was 44% versus 20% in the control. In contact filtration of alum treated clay (black solid line) the removal efficiency started at 60%, increased to 90% after 4 hours, and then declined. Comparing these two experiments, the pretreatment experiment had a better

particle removal during the first 20 minutes of operation than contact filtration. The result indicates that downflow alum pretreatment can eliminate the poor performance during the ripening period in contact filtration. Combining pretreatment with contact filtration (gray solid line) the particle removal was better than that obtained by conventional contact filtration over the initial two hours of operation. This result demonstrates that combining downflow pretreatment with contact filtration can remove the ripening period usually observed in conventional treatment.

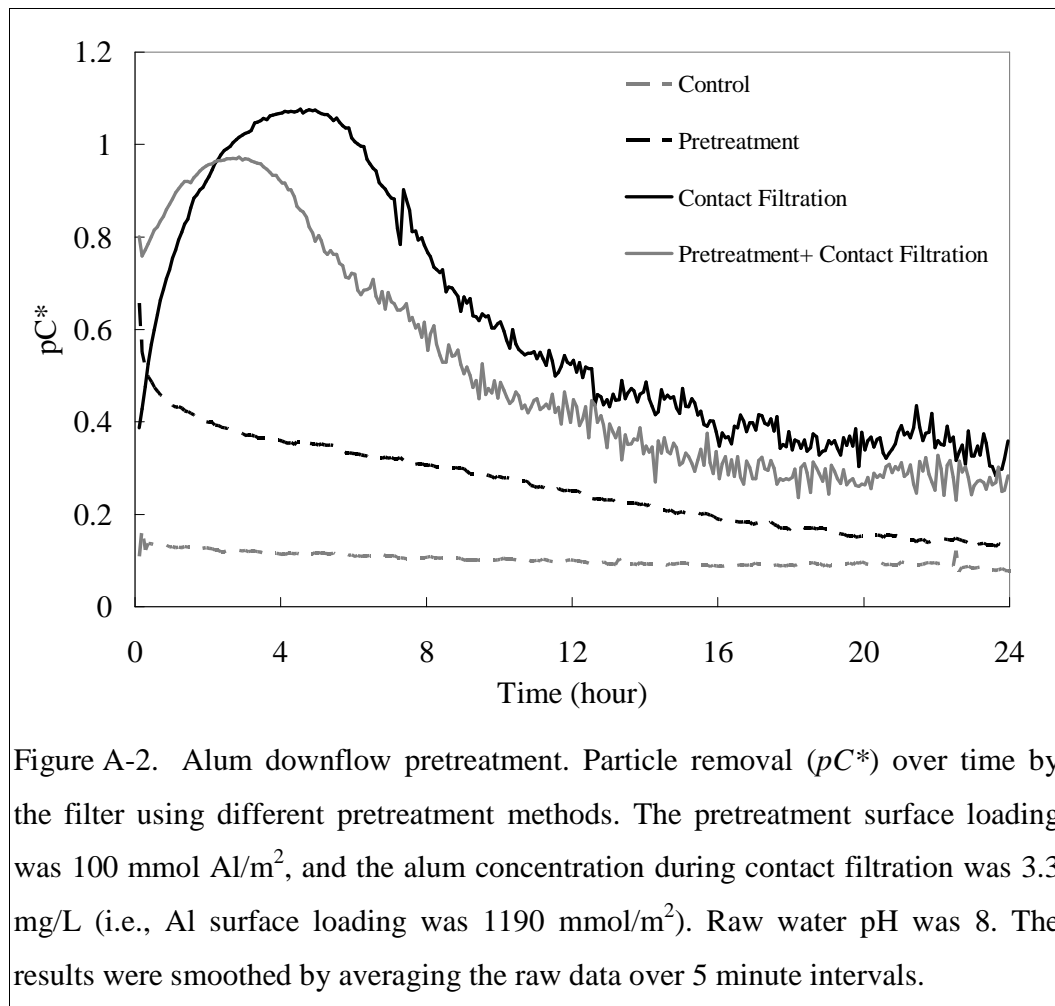


Figure A-3 presents pC^* over a 24 hour experiment when applying FeCl_3 for pretreatment and contact filtration. The trends were similar to those obtained using

alum (see Figure A-2). Particle removal in the combined experiments was better than that obtained by contact filtration during the first 3 hours of operation. The results also indicate that downflow pretreatment with FeCl_3 can improve filter performance relative to that obtained with an untreated filter. In addition, combining pretreatment with conventional treatment helped eliminate the poor performance during the ripening period.

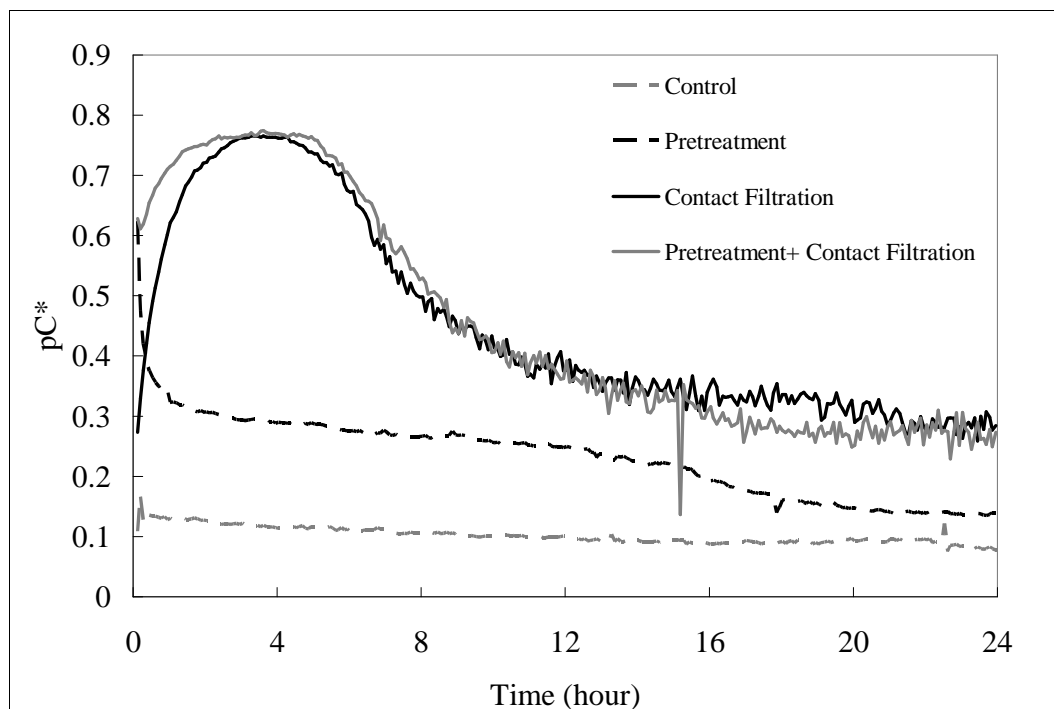


Figure A-3. FeCl_3 downflow pretreatment. Particle removal (pC^*) over time by the filter using different pretreatment methods. The pretreatment surface loading was 100 mmol Fe/m^2 , and the FeCl_3 concentration during contact filtration was 3.0 mg/L (i.e., Fe surface loading was 1190 mmol/m^2). Raw water pH was 8. The results were smoothed by averaging the raw data over 5 minute intervals.

Alum and FeCl_3 are both common coagulants used in water treatment. Previous experimental results (see Chapter 2) have shown that at lower surface loading ($\leq 550 \text{ mmol/m}^2$) downflow application of alum and FeCl_3 resulted in similar clay removal

efficiencies in the absence of HA. However, comparison of results of the combined experiments with alum to those with FeCl_3 (see Figure A-4) indicates that alum results in a better removal than FeCl_3 during the first 5 hours of operation when the raw water contains HA. Moreover, the data from pretreatment and contact filtration experiments also yielded consistent results (data not shown). Thus, alum as a filter aid has a better ability to remove colloidal clay when the influent contains humic acid than does FeCl_3 .

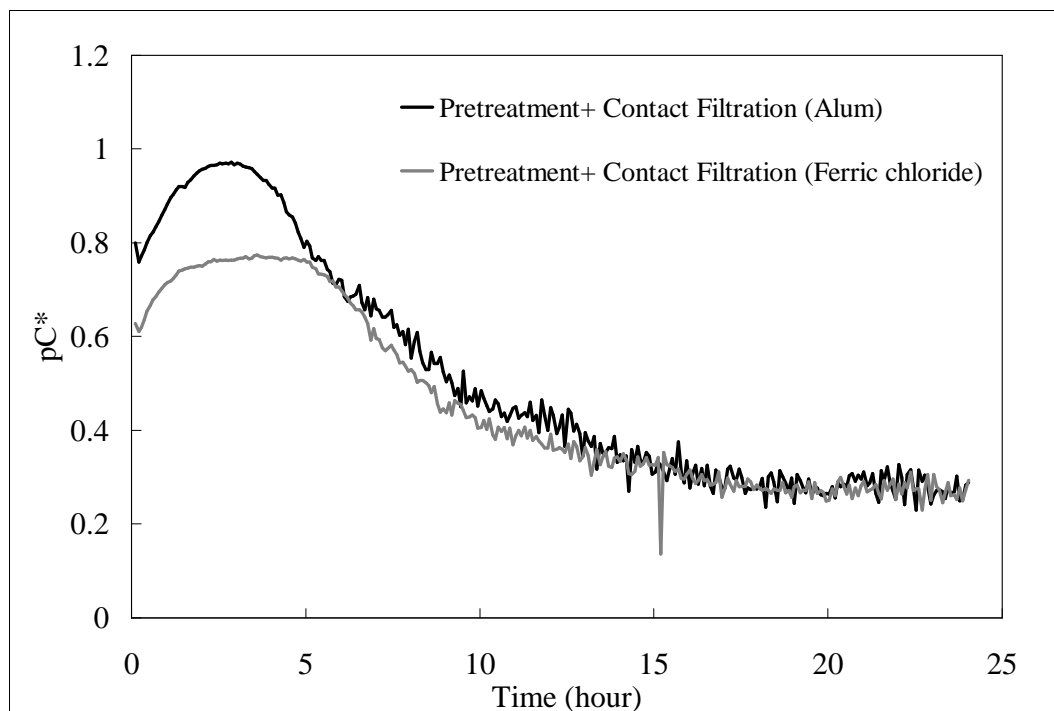


Figure A-4. Comparison of using alum and FeCl_3 for combining pretreatment and contact filtration.

A.3 Distribution of aluminum in the filter column

A.3.1 Aluminum distribution in short (7.5 cm) sand column

A filter column equipped with multiple pressure sensors (Figure A-5 (a)) was utilized to monitor pressure drop as a function of depth. Pressure drop was used as a diagnostic tool to evaluate the distribution of alum applied during downflow

pretreatment. The sand size used in this series of experiments was about 0.5 mm in diameter.

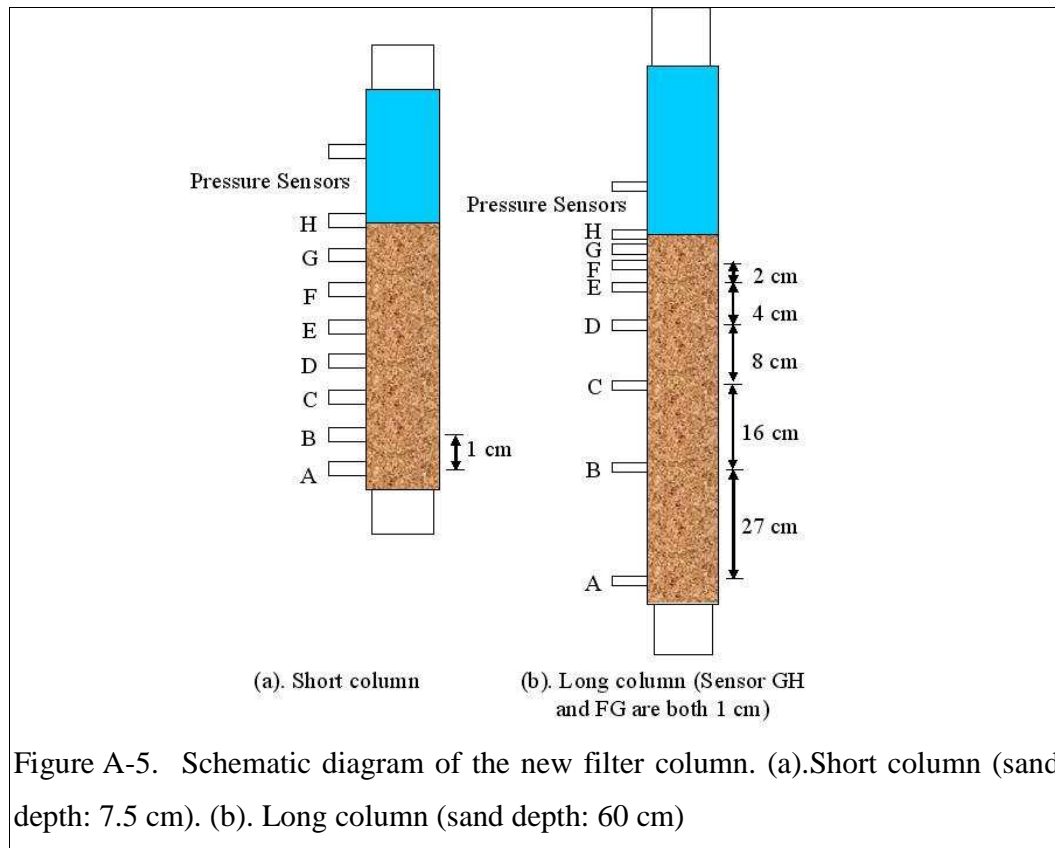
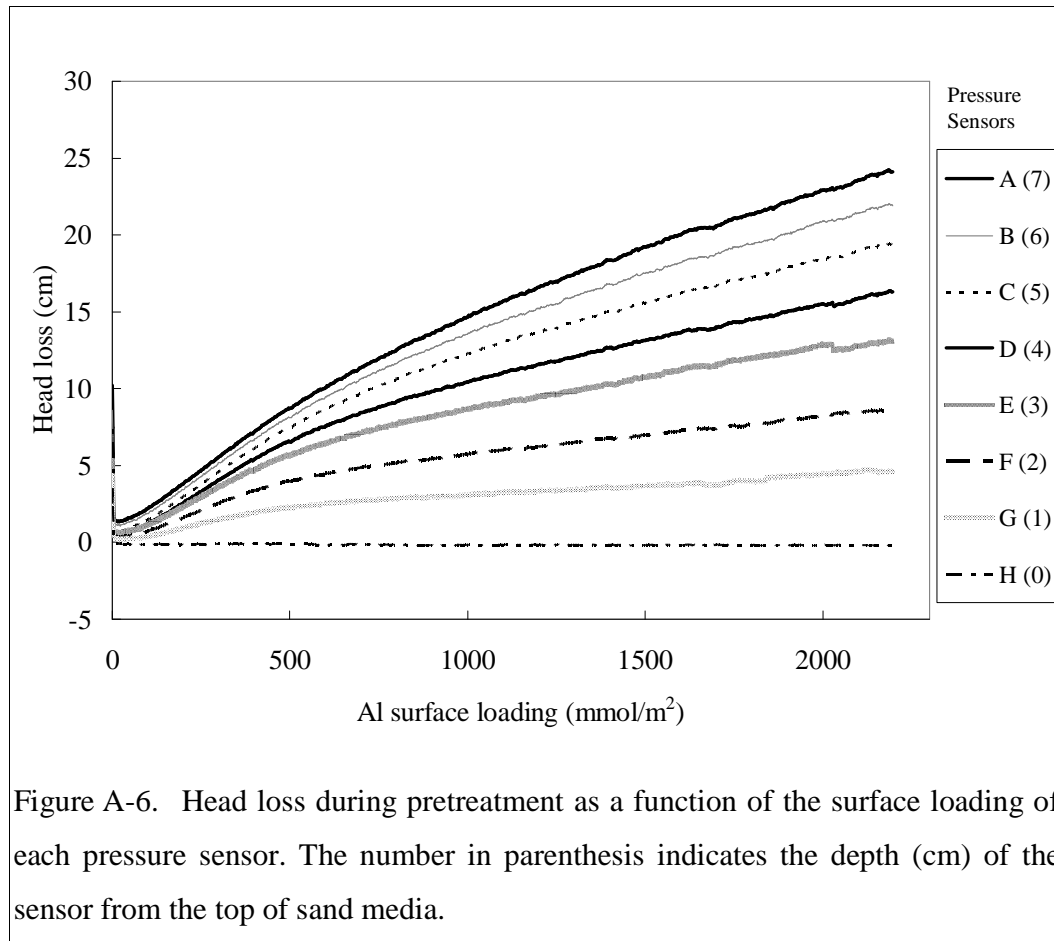
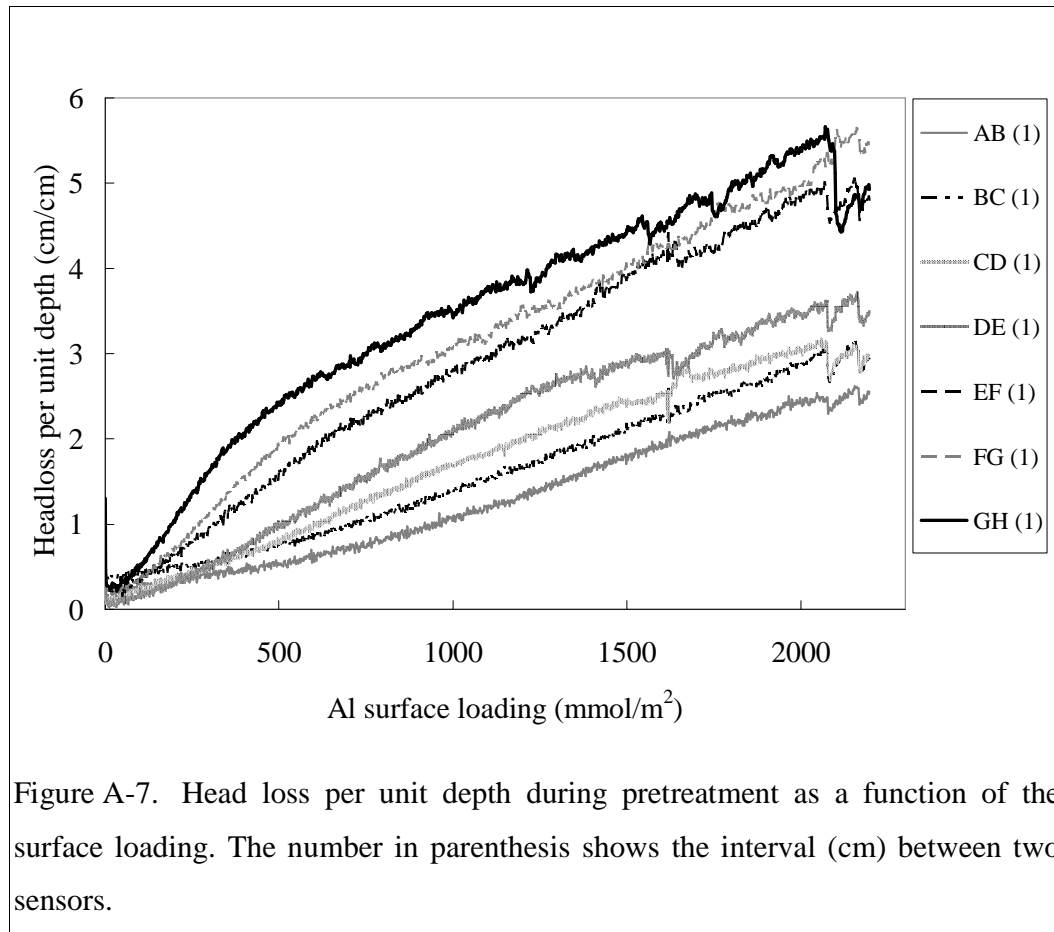


Figure A-6 presents head loss as a function of surface loading of alum. The total surface loading was 2200 mmol Al/m². Each line shows the head loss trend at different depths in the filter (locations are relative to Figure A-5(a)).



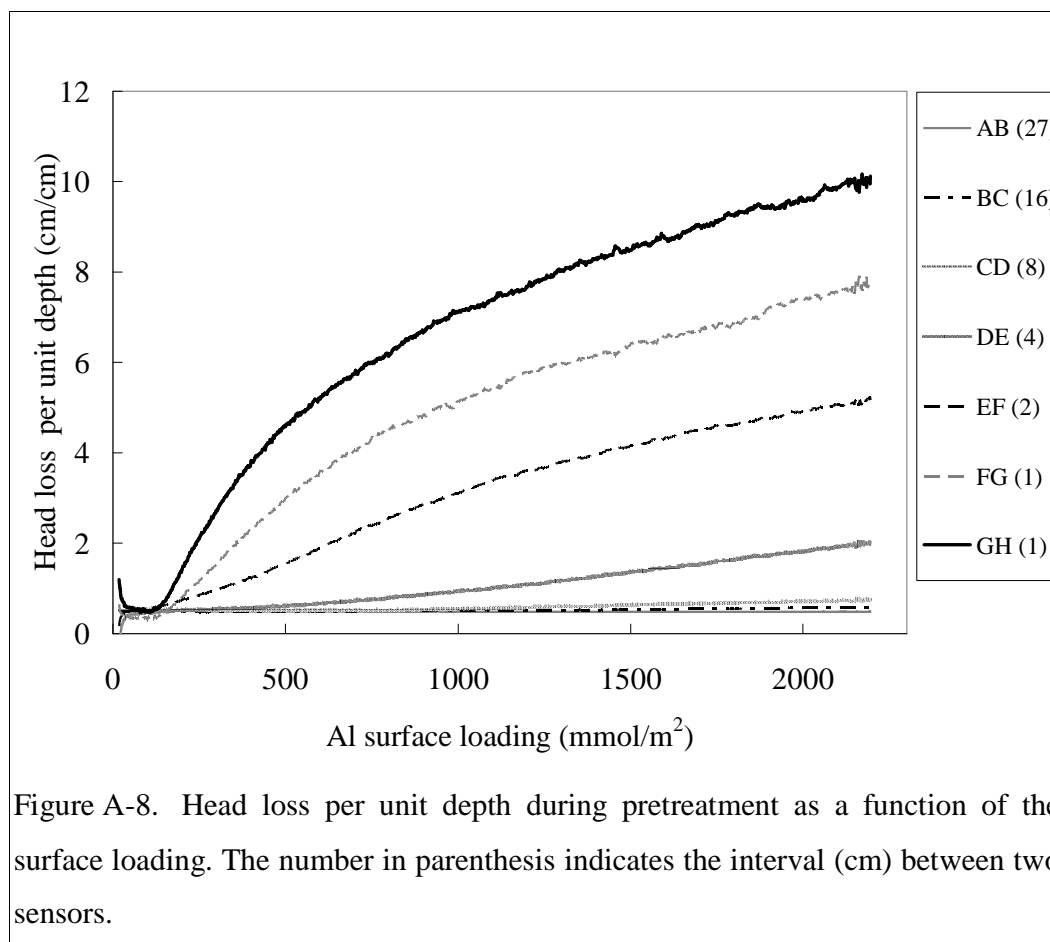
Head loss per unit depth can be obtained by calculating the difference of head loss of two adjacent sensors and then dividing by the distance between these two sensors. Figure A-7 shows head loss per unit depth calculated from Figure A-6 as a function of the surface loading. The head loss per unit depth in the superficial GH layer was the highest, and followed by FG and EF layers. These results indicate that most aluminum hydroxide deposited in the first 3 cm of the filter. In addition, some head loss was generated between sensors A and B which indicated that some aluminum hydroxide was also deposited over the entire column.



A.3.2 Aluminum distribution in long (60 cm) sand column

A longer (60 cm of sand depth) filter column equipped with pressure sensors was built to simulate the filter depth used in water treatment practice. A schematic diagram of the column is shown in Figure A-5(b). The same surface loading of alum (2200 mmol Al/m²) used in the short filter column was applied to this long column, and the head loss per unit depth during pretreatment versus Al surface loading is presented in Figure A-8. These results were similar to the results from the short column, most aluminum deposited in the first 4 cm region (between sensor H and E). Moreover, only 8 cm of sand media (between sensor H to D) was pretreated with alum in the long column which was consistent with the results from aluminum concentration in the

effluent from the short column (i.e., 96% of Al was retained in the 7.5 cm from the top of the filter column when pretreating with 2200 mmol Al/m²).



A.4 Deterioration of performance in pretreated filters

A.4.1 Colloid capacity

A finite surface capacity may be one of the important factors expected to result in deterioration of filter performance. The pretreatment technique conducted here was fluidized-bed pretreatment. Two different clay concentrations (~5 and ~55 NTU) with 0.5 mg/L of humic acid (HA) were used to challenge the alum-pretreated filter (i.e., 23 mol Al/m³ of pore volume) for 12 hours. Figure A-9 shows particle removal (pC^*) over time as a function of clay concentration. The effluent turbidity was below

detection limit (i.e., ≤ 0.01 NTU) during the first 1.5 and 4 hours for 55 and 5 NTU experiment, respectively. A turbidity of 0.01 NTU was assumed for purpose of calculating pC^* when the effluent was below the detection limit. The trend of pC^* was similar after 5 hours. The disparity of pC^* during the first 5 hours could result from different initial influent turbidity.

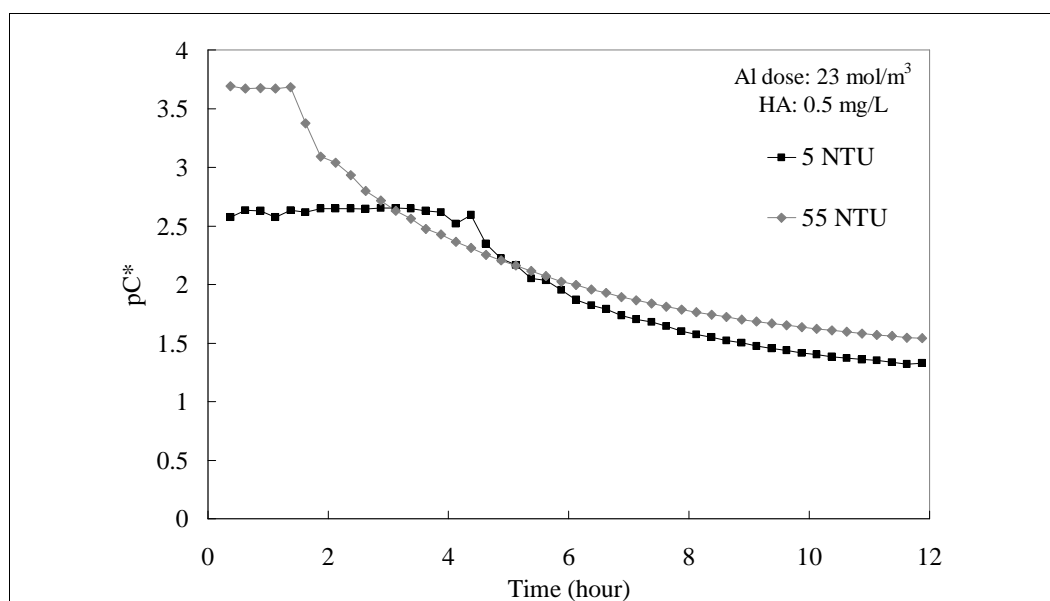


Figure A-9. Alum fluidized-bed pretreatment. Particle removal (pC^*) over time by a sand filter as a function of the clay concentration. Raw water pH was 7. The results were smoothed by averaging the raw data over 15 min intervals.

Particle removal (pC^*) for the above results as a function of cumulative removed clay (in NTU units) over 12 hours is shown in Figure A-10. The difference in the initial pC^* is due to the detection limit of the effluent turbidimeter. When cumulative removed clay is 38000 NTU (vertical black line), the pC^* of 55 NTU is significantly better than that obtained using 5 NTU raw water. The divergence of two curves shows that colloid retention capacity is not a significant contribution to deterioration of the filter performance.

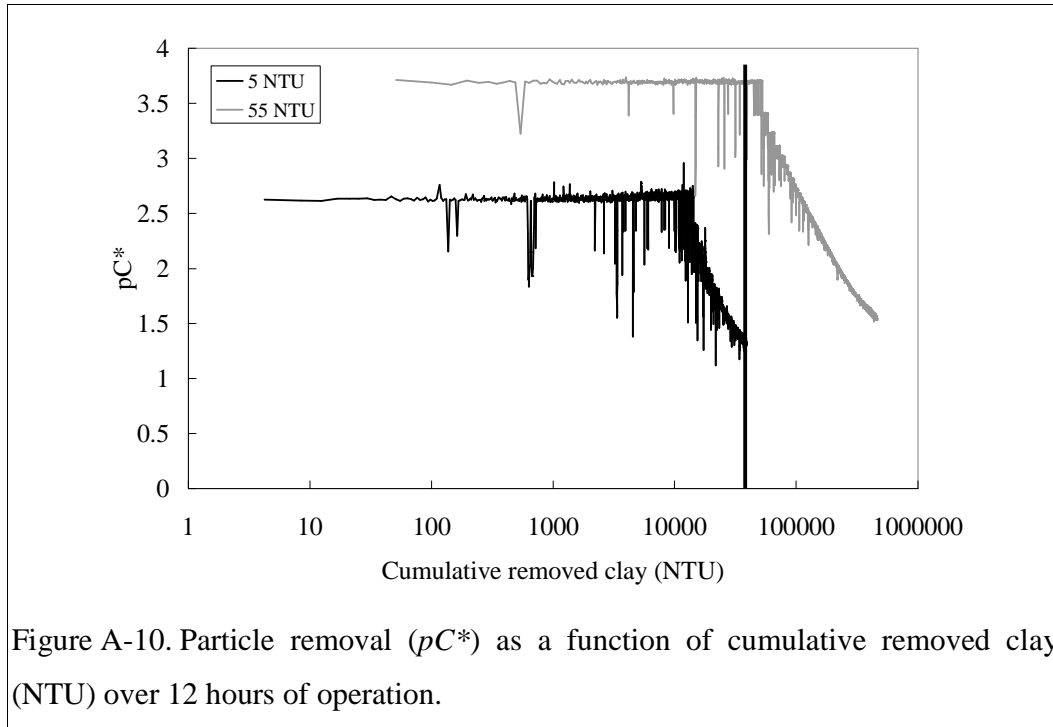
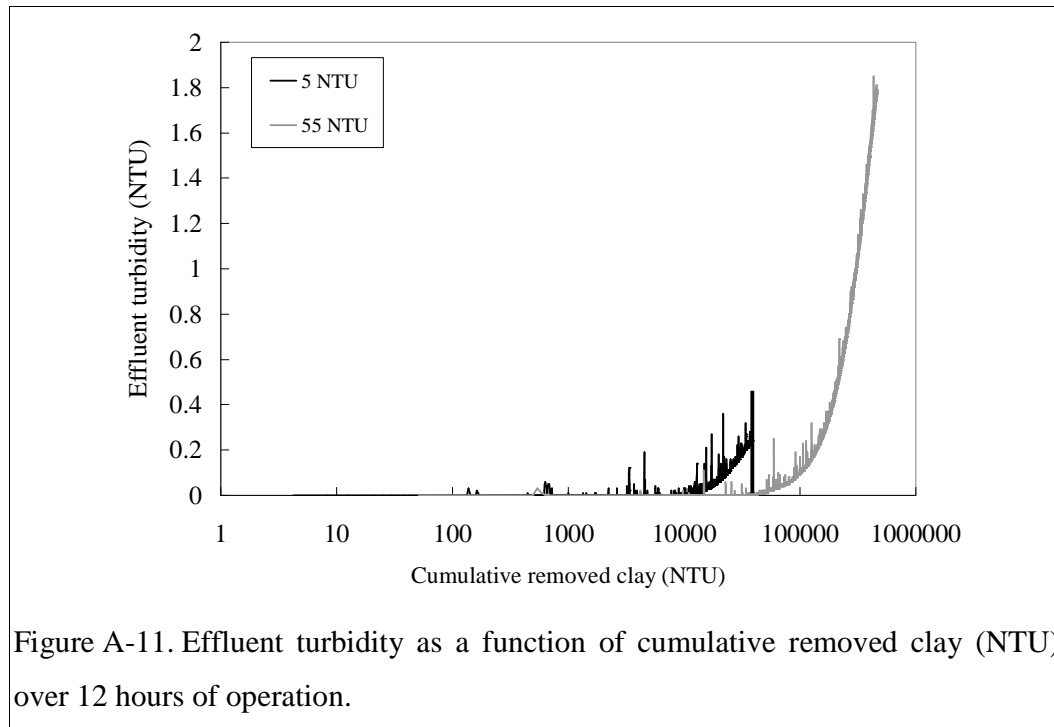


Figure A-11, effluent turbidity as a function of cumulative removed clay over 12 hours, provides another insight to illustrate that colloid capture capacity does not cause filter deterioration of performance. At the cumulative removed clay of 38000 NTU (vertical black line), the effluent turbidity using 5 NTU clay as raw water is 0.3 NTU while the turbidity of using 55 NTU is 0.01 NTU. These two graphs clearly indicate that colloid retention capacity is not a significant mechanism that causes deterioration of the filter performance.



A.4.2 Negative charge capacity

Aquatic humic substances, which are negatively charged macromolecules because of the ionization of acidic functional groups, can adsorb onto the surface of clay and other natural particles, further increasing their negative charge (Pernitsky & Edzwald 2006). In this experiment, HA was selected as a surrogate of natural organic matter. ~55 NTU of clay suspension with three concentrations of HA (0, 0.5, and 5 mg/L) were used to challenge the alum-pretreated filter (i.e., 23 mol Al/m³) for 12 hours, and the results are presented in Figure A-12. The effluent turbidity during the entire experiment was below detection limit when the clay suspension contained no HA. For the experiment containing 0.5 mg/L of HA the effluent turbidity was below detection limit during the first 1.5 hours. This graph clearly illustrates that HA causes deterioration of the performance. In addition, the higher the HA concentration, the worse the particle removal. This result indicates that the capacity of the pretreated

filter to neutralize applied negative charge is one of the factors that controls filter performance.

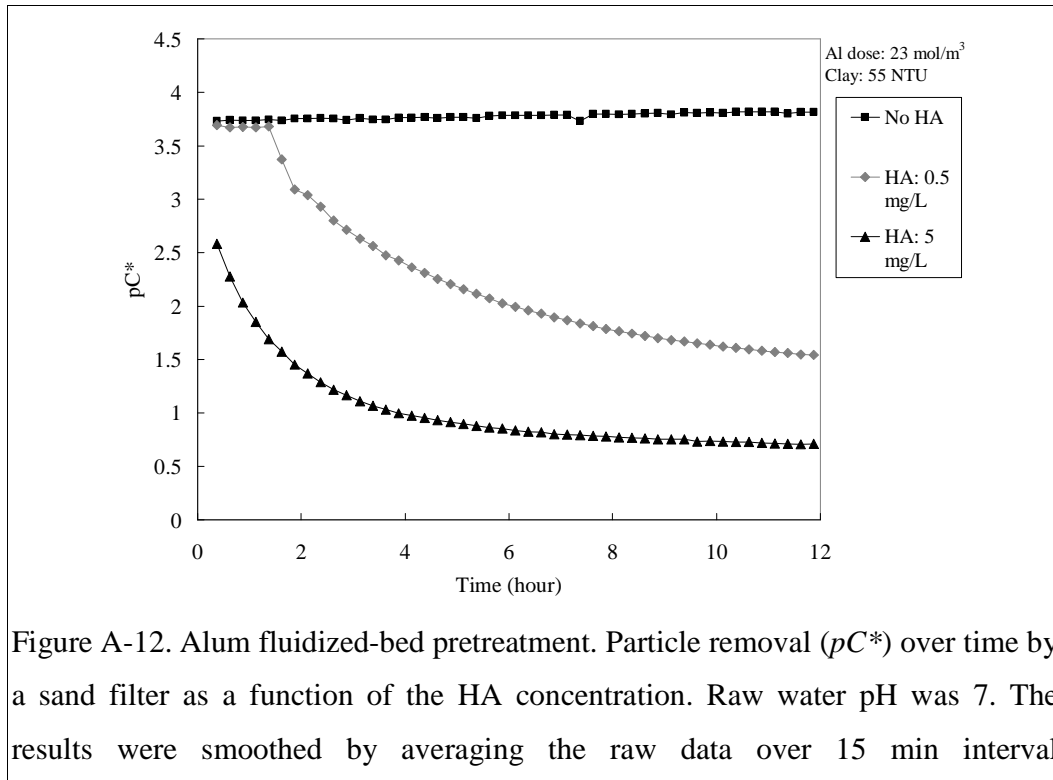


Figure A-12. Alum fluidized-bed pretreatment. Particle removal (pC^*) over time by a sand filter as a function of the HA concentration. Raw water pH was 7. The results were smoothed by averaging the raw data over 15 min interval